Charles University in Prague

Department of Physiology

and

Institute of Physiology AS CR, Prague

Biochemistry of Membrane Receptors

Postnatal development of $GABA_B$–receptors in the frontal rat brain cortex

Mgr. Dmytro Kagan

PhD Thesis

2014

Supervisor:

Doc. RNDr. Petr Svoboda, DrSc.

Institute of Physiology AS CR, Prague

Biochemistry of Membrane Receptors

Declaration by candidate.

I hereby declare that this thesis is my own work and it has not been submitted anywhere for any award. Where the sources of information have been used, they have been acknowledged.

In Prague, August 10, 2014 ……

Mgr. Dmytro Kagan

Acknowledgements.

First and foremost I would like to express my sincere gratitude to my advisor Doc. RNDr. Petr Svoboda, DrSc. for his continuous support of my Ph.D. study and research.

I am also very grateful to my colleagues from the Department who contributed immensely to my professional and personal time at the Institute of Physiology.

Lastly, I would like to thank my family for all their love and encouragement.

ABSTRACT

In this work, the detailed analysis of $GABA_B$–R/G protein coupling in the course of pre– and postnatal development of rat brain cortex indicated the significant intrinsic efficacy of $GABA_B$–receptors already shortly after the birth: at postnatal day 1 and 2. Subsequently, both baclofen and SKF97541–stimulated G protein activity, measured as the high–affinity [^{35}S]GTPγS binding, was increased. The highest level of agonist–stimulated [^{35}S]GTPγS binding was detected at postnatal days 14 and 15. In older rats, the efficacy, i.e. the maximum response of baclofen– and SKF97541–stimulated [^{35}S]GTPγS binding was continuously decreased so, that the level in adult, 90–days old rats was not different from that in newborn animals.

The potency of G protein response to baclofen stimulation, characterized by EC_{50} values, was also high at birth but unchanged by further development. The individual variance among the agonists was observed in this respect, as the potency of SKF97541 response was decreased when compared in 2–days old and adult rats.

The highest plasma membrane density of $GABA_B$–R, determined by saturation binding assay with specific antagonist [^{3}H]CGP54626A, was observed in 1–day old animals. The further development was reflected in *decrease* of receptor number. The adult level was ≈3–fold lower than in new born rats.

The ontogenetic development of Na^+/K^+–ATPase, which was used as marker of the overall brain development, was completely different from that observed in the study of $GABA_B$–R–signaling cascade: plasma membrane density of Na^+/K^+–ATPase was continuously increased in the course of the whole postnatal period; the adult level was ≈3–fold higher than in new born (1–day–old) rats.

The high level of lipofuscin like pigments (LFP) was generated in rat brain cortex during the first 5 days of postnatal life. Maximum level of LFP was detected on the postnatal day 2. Starting from the postnatal day 10, LFP concentration returned down to the prenatal level. A new rise in LFP concentration was observed in 90-days old animals. This second increase of LFP may indicate the beginning of the aging process in rat brain cortex.

ABSTRAKT

Byla provedena detailní analýza spřažení $GABA_B$-R s G proteinem během prenatálního a postnatálního vývoje mozkové kůry potkana, která ukázala významnou vnitřní účinnost $GABA_B$-R hned po narození (1. a 2. den). Následně byla zjištěna stimulovaná funkční aktivita G proteinů baklofenem i SKF97541 (agonisté $GABA_B$-R), která byla měřena pomocí vazby [^{35}S] GTPγS, jejíž nejvyšší hodnota byla detekována během 14. a 15. dne postnatálního vývoje. Účinnost, tj. maximální odpověď baklofenem a SKF97541 stimulované vazby [^{35}S] GTPγS, se u starších potkanů stále snižovala tak, že její hodnota měřená u devadesátidenních potkanů se nelišila od hodnot u novorozených zvířat.

Velikost odpovědi G proteinů na stimulaci baklofenem (vyjádřena jako EC_{50}) byla také zvýšena po narození a během dalšího vývoje se neměnila. Na rozdíl od baklofenu se síla odpovědi SKF97541 zmenšovala (při porovnání dvoudenních mláďat a dospělých potkanů).

Nejvyšší zastoupení $GABA_B$-R v plazmatické membráně stanovené pomocí saturačních vazebných pokusů s použitím specifického antagonisty [^{3}H] CGP54626A bylo detekováno u jednodenních zvířat. Další vývoj byl charakterizován *snížením* počtu receptorů. Ve srovnání s novorozenými potkany byla hladina u dospělých jedinců 3x nižší.

Ontogenetický vývoj Na^+/K^+-ATPázy (která slouží jako standard celkového vývoje mozku) se zcela lišil ve srovnání s vývojem signalizační kaskády $GABA_B$-R: množství Na^+/K^+-ATPázy ve frakcích plazmatických membrán se neustále zvyšovalo v průběhu celé ontogeneze; hladina u dospělých zvířat byla až 3x vyšší než u mláďat.

V mozkové kůře se vytvářela vysoká hladina lipofuscinových pigmentů (LFP) během prvních pěti dnů od narození. Maximální množství LFP bylo detekováno u dvoudenních zvířat. Po 10 dnech se koncentrace LFP vrátila na prenatální hodnotu. Nový vzestup LFP byl zaznamenán u devadesátidenních potkanů. Toto další zvýšení obsahu LFP může představovat začátek procesu stárnutí mozkové kůry potkana.

CONTENTS

1. LIST OF AUTHOR'S PUBLICATIONS

1. Bourova, L., Vosahlikova, M., **Kagan, D.**, Dlouha, K., Novotny, J. and Svoboda, P. (2010): Long–term adaptation to high doses of morphine causes desensitization of mu–OR– and delta–OR–stimulated G protein response in forebrain cortex but does not decrease the amount of G protein alpha subunits. Medical Science Monitor 16, BR260–270 (IF = 1.543).

2. Ujcikova, H., Dlouha, K., Roubalova, L., Vosahlikova, M., **Kagan, D.** and Svoboda P. (2011): Up–regulation of adenylylcyclases I and II induced by long–term adaptation of rats to morphine fades away 20 days after morphine withdrawal. Biochimica et Biophysica Acta 1810, 1220–1229 (IF = 3.990).

3. Wilhelm, J., Ivica, J., **Kagan, D.** and Svoboda P. (2011) Early postnatal development of rat brain is accompanied by generation of lipofuscin–like pigments. Molecular and Cellular Biochemistry 347, 157–162 (IF = 2.168).

4. **Kagan, D.**, Dlouhá, K., Roubalová, L. and Svoboda, P. (2012): Ontogenetic development of GABA(B)–receptor signaling cascade in plasma membranes isolated from rat brain cortex; the number of GABA(B)–receptors is high already shortly after the birth. Physiological Research 61, 629–635 (IF = 1.531).

5. Dlouhá, K., **Kagan, D.**, Roubalová, L., Ujčíková, H. and Svoboda, P. (2013) Plasma membrane density of GABAB–R1a, GABAB–R1b, GABA–R2 and trimeric G proteins in the course of postnatal development of rat brain cortex. Physiological Research 62, 547–559 (IF = 1.555).

6. Ujčíková H., Brejchová J., Vošahlíková M., **Kagan D.**, Dlouhá K., Sýkora J., Merta L., Drastichová Z., Novotný J., Ostašov P., Roubalová L., Hof M. and Svoboda P. (2014): Opioid–Receptor (OR) Signaling Cascades in Rat Cerebral Cortex and Model Cell Lines: the Role of Plasma Membrane Structure. Physiological Research, 63, Suppl. 1, 165–176 (IF = 1.555).

7. Ujcikova, H., Eckhardt, A., **Kagan, D.**, Roubalova, L. and Svoboda, P. (2014): Proteomic analysis of post–nuclear supernatant fraction and Percoll–purified membranes prepared from brain cortex of rats exposed to increasing doses of morphine. Proteome Science, 12:11 (IF = 1.88).

2. ABBREVIATIONS

BPM – bulk of plasma membranes

DRM – detergent–resistant membrane domain

cAMP – cyclic adenosine monophosphate

EDTA – Ethylenediaminetetraacetic acid

GABA– γ–aminobutyric acid

$GABA_B$–R – $GABA_B$ receptors

GDP – guanozine diphosphate

GPCR – G protein coupled receptor

α–GPDH – α–glycerolphosphate

GSH/GSSG – reduced glutathione/oxidised glutathione

GTP – guanozine triphosphate

IP_3 – inositol triphosphate

HEK293 – human embryonal kidney cells

HEPES – 4–(2–hydroxyethyl)–1–piperazineethanesulfonic acid

HPLC – high performance liquid chromatography

mGluR – metabotropic glutamate receptor

nAChR – nicotinic acetylcholine receptor

LPM – low density membrane fragments

LFP – lipofuscin–like pigments

MDCK – Madin–Darby canine kidney cells

PM – plasma membranes

rpm – rounds per minute

ROS – reactive oxygen species

SKF – 1–[2–(4–Methoxyphenyl)–2–[3–(4–methoxyphenyl)propoxy]ethyl]imidazole

SDH – succinate dehydrogenase

TM – transmembrane

Tris – tris–(hydromethyl)–aminomethan

VIP–PACAP – Vasoactive intestinal peptide – Pituitary adenylate cyclase–activating polypeptide

3. AIMS OF THE THESIS

1) ***The first aim*** of my work was to improve and refine the method for isolation of plasma membrane fraction (PM) from frontal brain cortex. The main problem in the past was to find an optimum compromise between the amount of protein applied per density gradient and the purity of PM preparation. Application of the high amount of protein in post–nuclear fraction (PNS) resulted in PM contaminated to the higher or lower degree by mitochondrial fragments. Furthermore, the recovery of PM protein, when compared with the starting homogenate or post–nuclear fraction, was not always reproducible and standard. The improved method was subsequently used for studies of opioid– and $GABA_B$–receptor signaling in frontal brain cortex (Bourova *et al.*, 2010; Ujcikova *et al.*, 2011, Ujcikova *et al.*, 2014).

I have also participated in testing the effect of non–ionic detergents Triton–X100 and Brij58 on brain cortex PM and compared flotation of Percoll–purified PM in the presence or absence of low–concentrations of these detergents. This procedure has been introduced in our laboratory by Drs. V. Lisy, L. Rudajev and J. Stohr and at present time, it may be used for preparation of membrane domains/ rafts with unchanged or even higher efficacy of coupling between $GABA_B$–R and the cognate G protein of Gi/Go family, than the original, detergent–untreated domains (**Figs. 22–25**).

2) ***The second aim*** of my work was to introduce the new method for determination of the number of $GABA_B$–R in PM prepared form the frontal rat brain cortex. This can not be done by radiolabelled GABA itself because of the low–affinity of GABA for these receptors. Therefore, I have introduced the two radioligands, agonist [^{3}H]baclofen and antagonist [^{3}H]CGP54626A, carried out the direct saturation binding assays with increasing concentrations of these specific and highly radioactive ligands and determined the maximum number (Bmax) and dissociation constant (Kd) of their binding sites in various PM preparations (Kagan *et al.*, 2012). The Bmax values of [^{3}H]baclofen– and [^{3}H]CGP54626A–binding in PM were determined in parallel with [^{3}H]ouabain binding, which was used as an estimate of PM density of prototypical PM marker, Na^+/K^+–ATPase (Dlouha *et al.*, 2012). PM content of Na^+/K^+–ATPase was also used as a general marker of forebrain cortex development and maturation of PM protein composition.

3) Determination of the number of $GABA_B$–receptors at different stages of ontogenetic development is not sufficient to characterize the function of $GABA_B$–R signaling cascade as the primary signal represented by binding of GABA to receptor sites oriented at the extracellular side of plasma membrane is transmitted into the cell interior by trimeric G proteins. These proteins transmit the signal further down–stream but also terminate and regulate the functioning of $GABA_B$–R pathway. For ***this third aim*** of my work I used the high–affinity [^{35}S]GTPγS binding assay adapted to analysis of the brain tissue. This methodological improvement was based on the usage of relatively high GDP concentrations (20–30 μM) which suppressed the high basal level of [^{35}S]GTPγS binding (Roubalova *et al.*, 2010; Kagan *et al.*, 2012).

4) Potent $GABA_B$–R agonist SKF97541 was described as a useful agent in treatment of at least some forms of epileptic seizures. Therefore, I have compared the ontogenetic profile of baclofen– and SKF–stimulated [^{35}S]GTPγS binding with the aim to define even the small difference between these two agents when stimulating the cognate G proteins. The maximum of baclofen–stimulated [^{35}S]GTPγS binding was detected at postnatal day 10, while the maximum of SKF–stimulated [^{35}S]GTPγS binding was measured at postnatal day 15. Thus, the effect of these two agonists on functional activity of $GABA_B$–R in the course of postnatal period was not the same (Kagan *et al.*, 2012).

5) Finally, I have participated in studies of formation of lipofuscin–like pigments (LFP) in frontal rat brain cortex in the neonatal period and during the early postnatal period. The generation of LFP represents an important test/ marker of oxidative damage of the brain tissue by free oxygen radicals. Analysis of LFP was made first in the whole tissue homogenates (Wilhelm at al., 2011), subsequently, LFP were determined in different subcellular membrane fractions: nuclear sediment, post–nuclear supernatant, mitochondria, microsomes, crude plasma membranes and cytosol (**Fig. 35**). Our results indicate that the highest accumulation of oxidative products takes place immediately after the birth; our results also indicate that brain LFP constitute a complex mixture of many chemical compounds whose composition is changing during development.

4. INTRODUCTION

4.1. G protein coupled receptors

The extracellular signals such as the light, hormones, neurotransmitters, pheromones, odorants and also Ca^{2+} cations interact with and bind to the large family of the plasma membrane receptors which are functionally coupled with guanine–nucleotide binding regulatory proteins (G proteins), G protein–coupled receptors.

Hormones and neurotransmitters bind primarily to the stereo–specific site of the receptor molecule which is located at the cell surface and exposed to extracellular side of plasma membrane and a surrounding water space. The binding reaction represents the first step in complicated sequence of molecular events transmitting the signal from the extracellular side of plasma membrane into the cell interior. Therefore, the final physiological response of a given cell type is initiated and regulated by the primary molecular events proceeding in plasma membrane at receptor level. In *all* GPCR–initiated signaling cascades, the hormone or neurotransmitter binding induces conformational change of receptor molecule, which is transmitted to G protein and induces dissociation of trimeric G protein–complex (non–active) into the free (active) Gα and Gβγ subunits. Subsequently, both Gα and Gβγ activate a numerous enzyme activities (effectors) or ionic channels which then regulate the intracellular concentrations of secondary messengers such as cAMP, cGMP, IP_3, diacylglycerol (DAG), arachidonic acid, sodium, potassium or calcium cations **(Fig. 1**).

Fig. 1 Structural and functional organization of G protein–coupled receptors (GPCRs) in plasma membrane

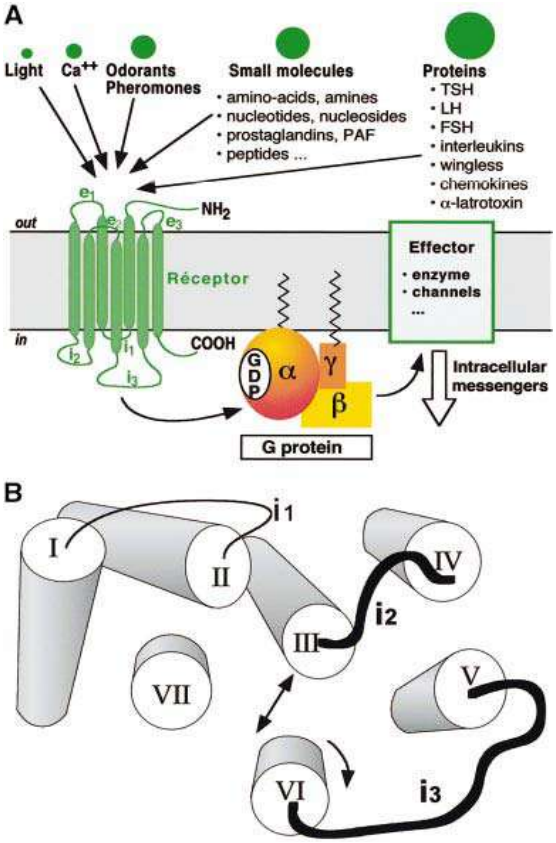

From Bockaert, J., Pin J. P. (1999) Molecular tinkering of G protein–coupled receptors: an evolutionary success. The EMBO Journal 18, 1723–1729

(**A**) GPCRs have a central common core made of seven transmembrane helices (TM1–TM7) connected by three intracellular (i1, i2, i3) and three extracellular (e1, e2, e3) loops. The diversity of messages which activate these receptors is an illustration of their evolutionary success.

(**B**) Illustration of the central core of rhodopsin. The core is viewed from the cytoplasm. The length and orientation of the TMs are deduced from the two–dimensional crystal of bovine and frog rhodopsin. The N– and C–terminal and i3 are included in TM3 and TM6. The core is represented in its *active conformation*. The TM6 and TM7 lean out of the structure, the TM7 turn by 30% on its axis (clockwise as viewed from the cytoplasm). This opens a cleft in the central core in which G proteins can find their way. The i2 and i3 loops are the two main loops engaged in G protein recognition and activation.

4.2. Classification and diversity of GPCRs

Three main families of GPCRs were recognized by comparison of amino–acid sequences of individual receptor proteins. Receptors from different families share no sequence similarity. This indicates a remarkable example of molecular convergence in the course of evolution (**Fig. 2**).

Family 1 contains most GPCRs including receptors for odorants. **Group 1a** contains GPCRs for small ligands including rhodopsin and β–adrenergic receptors. The binding site is localized within the seven TMs. **Group 1b** contains receptors for peptides whose binding site includes the N–terminal, the extracellular loops and the superior parts of TMs. **Group 1c** contains GPCRs for glycoprotein hormones. It is characterized by a large extracellular domain and a binding site which is mostly extracellular but at least with contact with extracellular loops e1 and e3.

Family 2 GPCRs have a similar morphology to group Ic GPCRs, but they do not share any sequence homology. Their ligands include high molecular weight hormones such as glucagon, secretine, VIP–PACAP and the Black widow spider toxin, α–latrotoxin (Krasnoperov *et al.*, 1997; Davletov *et al.*, 1998).

Family 3 contains mGluRs, Ca^{2+}–sensing receptors, $GABA_B$–receptors and a group of putative pheromone receptors coupled to the G protein Go (termed VRs and Go–VN) became new members of this family.

Family 4 comprises pheromone receptors (VNs) associated with Gi.

Family 5 includes the ‘frizzled’ and the ‘smoothened’ (Smo) receptors involved in embryonic development and in particular in cell polarity and segmentation. The cAMP receptors (cAR) have only been found in *D. discoıdeum* but its possible expression in vertebrate has not yet been reported.

Fig. 2 **Classification and diversity of GPCRs**

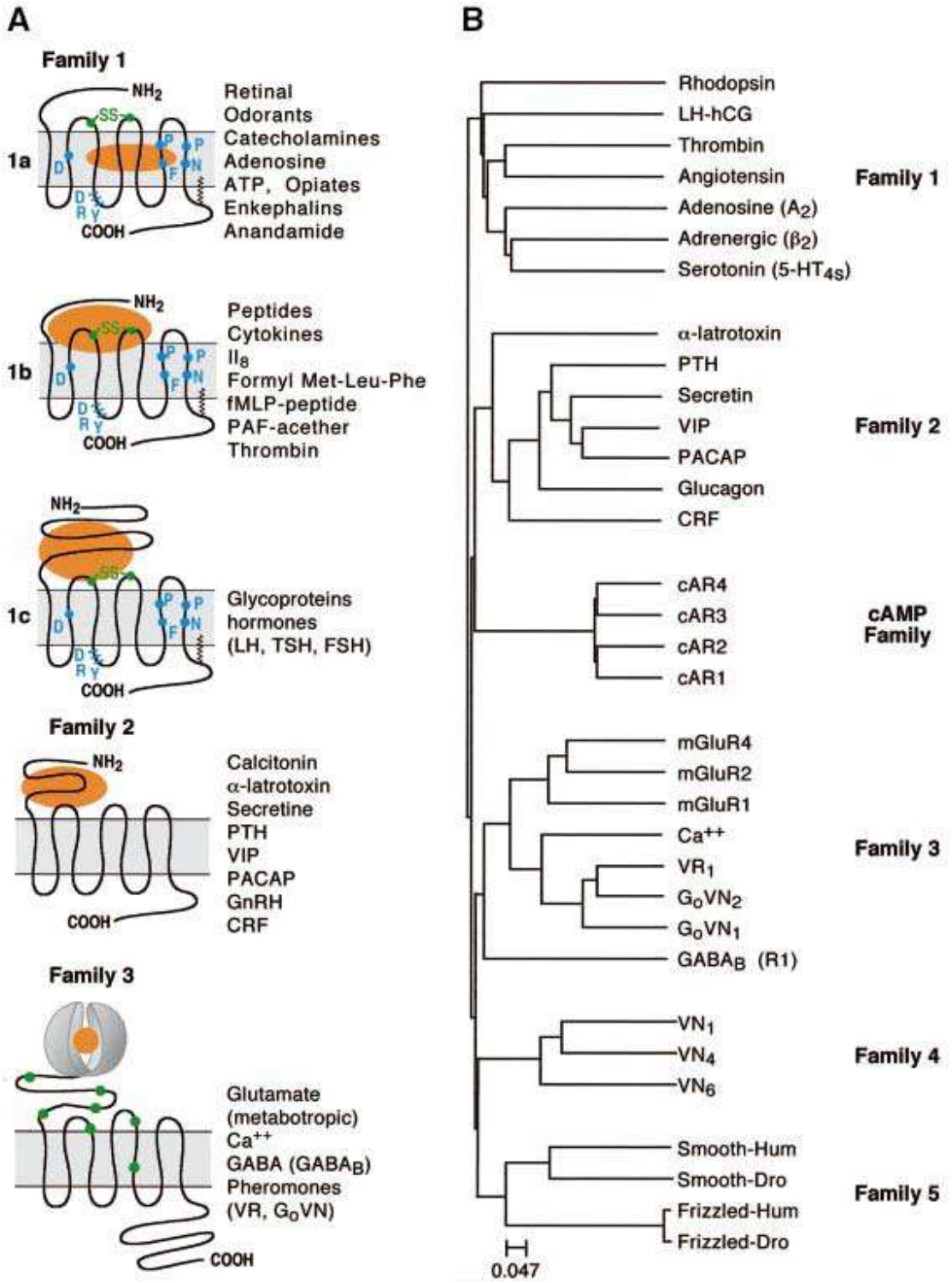

From Bockaert J., Pin, J.P. (1999) Molecular tinkering of G protein–coupled receptors: an evolutionary success. The EMBO Journal 18, 1723–1729

4.3. Receptors for γ–aminobutric acid (GABA)

The main inhibitory system in the brain uses γ–aminobutyric acid (GABA) as a transmitter. γ–aminobutyric binds to three types of receptors – $GABA_A$ (Olsen and Venter, 1986), $GABA_B$ (Bowery *et al.* 1989, 1991, 1993) and $GABA_C$ (Bormann and Feigenspan 1995). *$GABA_A$ receptor* is a part of supra–molecular complex $GABA_A$ chloride ionophore and a consequence of its activation is opening of chloride channel and hyperpolarization of membrane potential (Olsen and Venter, 1986). The subunit composition of $GABA_A$ receptor has sequence homology with the neural type of nicotinic acetylcholine receptor (nACh–R). It is organized as a pentamer of five different subunits (α, β, γ, δ and ε). Each subunit group has different subtypes, e.g. six different α, four β, four γ and two δ were identified. Like neuronal nACh–R, these subunits mix in a heterogeneous fashion to produce a wide array of $GABA_A$ receptors with different pharmacological and electrophysiological properties (Vicini, 1991).

Historically, *$GABA_B$ receptors* were pharmacologically distinguished from $GABA_A$ receptors as bicuculine–insensitive sites for GABA for which specific agonist is (–)–baclofen (Hill and Bowery (1981); Bowery *et al.* (1983, 1984, 1985, 1987); Hill (1985)). After discovery of specific antagonists, $GABA_B$ receptors were defined as a class of bicuculine–insensitive GABA receptors for which (–)–baclofen is a specific agonist and phaclofen and 2–hydrox–saclofen specific antagonist (Kerr and Ong, 1995). These receptors are not physically bound to an ionic channel and belong to the family of G protein coupled receptors, GPCR (Bowery *et al.* 1989, 1991, 1993; Kerr and Ong, 1995). Thus, the signal initiated by binding of GABA to $GABA_B$–R is transmitted further down–stream by trimeric G proteins. Increased concentrations of GTP favor the dissociation of activated G proteins from the high affinity state of the receptor driving it towards lower affinity state what results in a reduction of $GABA_B$ receptor binding (Hill *et al.*, 1981, 1984). This result provided the first evidence that $GABA_B$ receptors are linked to G proteins.

The functional $GABA_B$ receptor is a hetero–dimer formed by a GABA B1 and B2 subunit (**Fig. 3**). Each of the subunits possesses extracellular N–termini, seven–transmembrane domains, and intracellular C–termini. The functional receptors heterodimerize via a C–terminal coiled–coil domain that shields an ER retention motif on B1, promoting cell surface expression. Two splice variants of the B1 subunit (1A and 1B) exist, differing by the presence of two “sushi” axonal targeting domains in the 1a subunit. Activation of the receptor

occurs when ligand (GABA or baclofen) binds to the N–termini of the B1 subunit in a venus flytrap mode of ligand binding (zoom panel). Essential ligand–binding amino acids have been highlighted. The B2 subunit then confers functional activity coupling to Gi/o G proteins via its intracellular loops.

Fig. 3 **$GABA_B$–receptor structure**

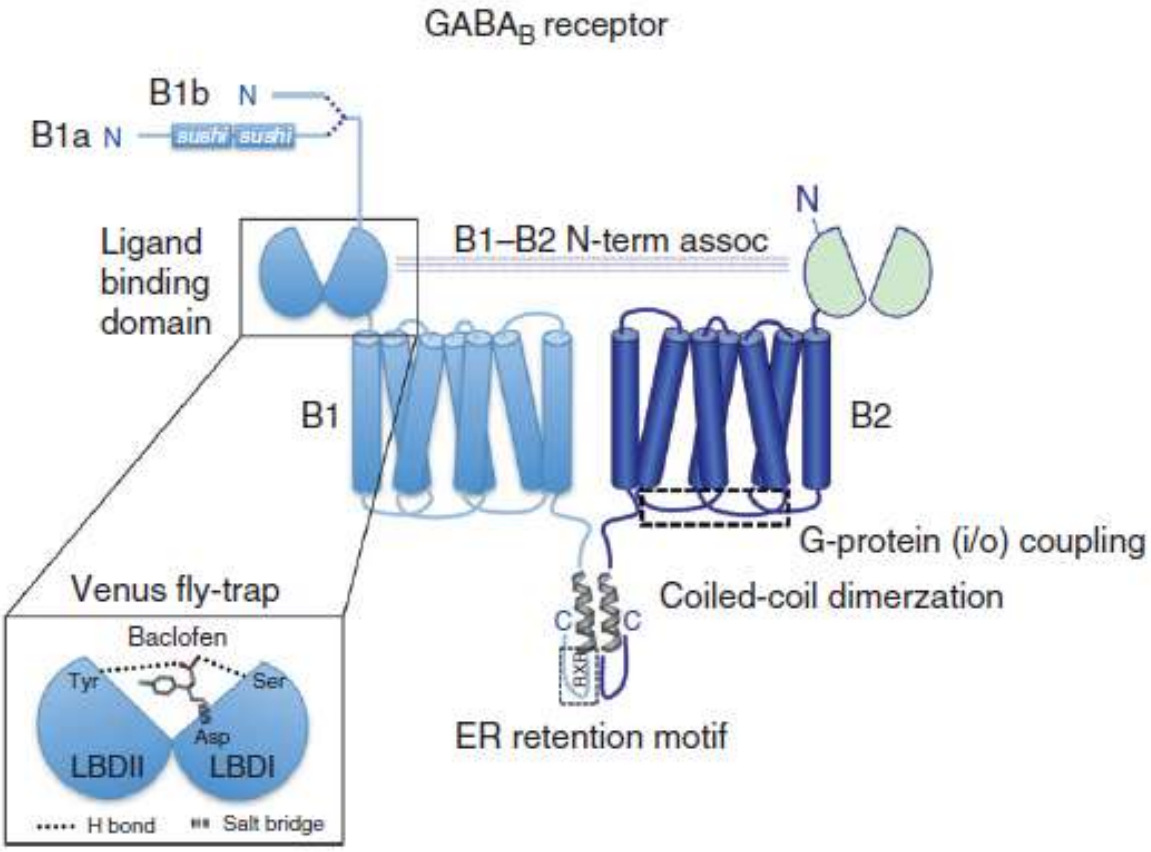

From Pagnet and Slezinger (2010) $GABA_B$ receptor coupling to G proteins and Ion channels. Advances in Pharmacology 58, 123–147

4.4. Trimeric G proteins and GDP/GTP exchange in guanine–nucleotide binding site of Gα subunits (G protein cycle)

From the structural point of view, trimeric G proteins are composed from three subunits, Gα and Gβγ (Rodbell, 1980; Gilman, 1987; Birnbaumer, 1990; Birnbaumer at al., 1990; Kaziro *et al.*, 1991; Helmreich and Hofman, 1996). Binding of an agonist to receptor molecule induces an exchange of GDP (which is in the resting state tightly bound to the Gα) for GTP. G protein complex containing Gα–GTP dissociates quickly into free Gα–GTP and Gβγ subunits. Both Gα–GTP and Gβγ subsequently stimulate or inhibit numerous enzymes and ionic channels at intracellular side of plasma membrane. Shortly after the dissociation of G protein complex Gαβγ into the free Gα–GTP and Gβγ, an endogenous GTPase activity of Gα subunit is activated and Gα–GTP is hydrolyzed to Gα–GDP. Gα subunits in GDP–liganded state (Gα–GDP) exhibit high–affinity towards free Gβγ. Therefore, Gα–GDP bind Gβγ and the non–active, trimeric G protein complex Gαβγ is formed again and the whole cycle may start again after encounter with activated, i.e. an agonist–bound receptor, **Fig. 4** (Gilman, 1987; Kaziro *et al.*, 1991; Helmreich and Hofman, 1996).

Fig. 4 **Trimeric G protein cycle; the general scheme**

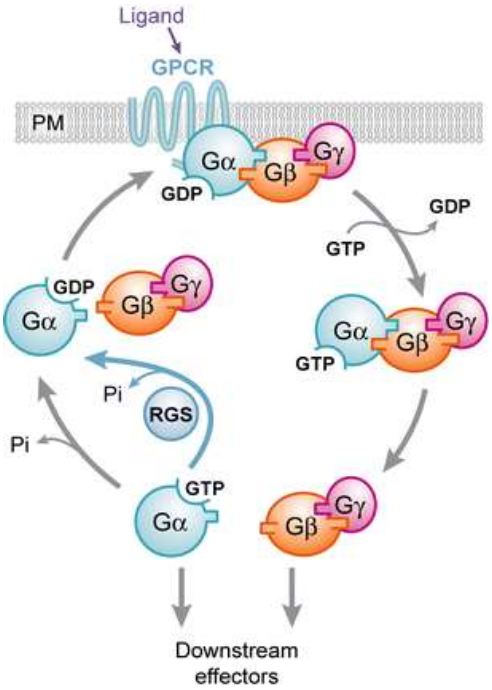

From Li L, Wright SJ, Krystofova S, Park G, Borkovich KA (2007) Heterotrimeric G protein signalling in filamentous fungi. Annual Rev Microbiol 61, 423–452

4.5. Classification and function of G proteins

G protein classification is based on similarity of amino acid sequence/ structure of Gα subunits (Kaziro *et al.*, 1991). The four major families of Gα subunits were identified.

1) G_s/G_{olf} family (four splice variants of $G_s\alpha$ and Gα protein of olfactory bulb, $G_{olf}\alpha$); Gα subunits of G_s/G_{olf} family stimulate adenylyl cyclase (AC) activity in cholera–toxin sensitive manner.

2) G_i/G_o family [$G_i1\alpha$, $G_i2\alpha$, $G_i3\alpha$, $G_o1\alpha$, $G_o2\alpha$, $G_t1\alpha$ (R) in retinal rodes, $G_t2\alpha$ (C) in retinal cones, $G_q\alpha$ (gustducin), $G_z\alpha$]. Gα subunits of G_i/G_o family inhibit adenylyl cyclase, stimulate phospholipase Cβ3 or affect ionic channels in pertussis–toxin (PTX) sensitive manner.

3) $G_q/G_{11}\alpha$ family ($G_q\alpha$, $G_{11}\alpha$, $G_{14}\alpha$, $G_{15}\alpha$, $G_{16}\alpha$). Gα subunits of $G_q/G_{11}\alpha$ family proteins inhibit adenylyl cyclase or stimulate phospholipase Cβ3 in PTX–insensitive manner,

4) $G_{12}\alpha/G_{13}\alpha$ family. Gα subunits of $G_{12}\alpha/G_{13}\alpha$ family activate small, monomeric G proteins of Rho family and regulate intracellular membrane traffic (Riobo and Manning, 2005).

4.6. $GABA_B$–receptors and PTX–sensitive G proteins of Gi/Go family

Pertussis–toxin (PTX), exotoxin produced by Bordetella Pertussis, ADP–ribosylates and uncouples the Gi and Go proteins from G protein coupled receptors, which revert to low–affinity state, by catalyzing the ADP–ribosylation of the Galpha–subunits (Katada and Ui, 1982). This covalent modification, proceeding at the C–terminus cystein –4 of the alpha–subunit of Gi/Go proteins, blocks the interaction with the activated receptor (occupied by an agonist) so, that the alpha–subunit remains in non–active, GDP–liganded state and it is unable to enter the GTP–GDP cycle initiated by GDP–GTP exchange reaction. High–affinity [^{3}H]GABA binding to $GABA_B$ sites is reduced and low–affinity binding is increased by treatment of brain membranes with PTX, whilst PTX and N–ethylmaleinimide uncouple $GABA_B$ receptors from G proteins, an effect which is reversed by the addition of purified Gi–proteins (Asano a spol., 1985; Asano a Ogasavara, 1986).

Increased concentration of GTP favors the dissociation of activated G proteins from the high affinity state of the receptor. Receptors are driven to the low–affinity state what results in a reduction of agonist binding to $GABA_B$–R (Hill *et al.*, 1981, 1984). This result provided the *first evidence* that $GABA_B$–R are linked to G proteins. $GABA_B$–agonist stimulation of high–

affinity [^{32}P]GTPase was the *second experimental evidence* supporting the idea, that the effect of $GABA_B$ agonists was mediated via trimeric G proteins (Bowery *et al.*, 1987) and close correlation between baclofen–stimulated GTPase and regional distribution of $GABA_B$–R in the brain also supported this idea. Baclofen–stimulated GTPase activity in vitro was significantly inhibited by pertussis toxin (PTX) and also by specific antipeptide antisera oriented against $G_i\alpha$ subunit proteins (Sweeney and Dolphin, 1992). The electrophysiological analysis using the specific antisera indicated that both PTX–sensitive $G_i\alpha$ and $G_o\alpha$ proteins were effected by $GABA_B$–R agonists (Dolphine, 1990, 1991).

4.7. G protein turnover affects $GABA_B$–receptor function

Agonist activation of $GABA_B$ receptor ($GABA_{B1/B2}$–R) leads to GTP exchange for GDP on $G_{i/o}\alpha$. The activated heterotrimeric complex ($G_{i/o}\alpha$–GTP$\beta\gamma$) then signals to different effectors (e.g., adenylyl cyclase, GIRK, and CaV). The intrinsic GTPase activity of $G_{i/o}\alpha$ hydrolyzes GTP to GDP, allowing the inactive heterotrimer ($G_{i/o}\alpha$–GDP–G$\beta\gamma$) to reform. The presence of RGS accelerates the GTPase activity of $G_{i/o}\alpha$, leading to less $G_{i/o}\alpha$–GTP–G$\beta\gamma$ and G$\beta\gamma$, leading to desensitization of GIRK and CaV currents, and shift in the GABAB coupling efficiency to higher concentrations (**Fig. 5**).

Fig. 5 G protein turnover affects $GABA_B$–receptor function

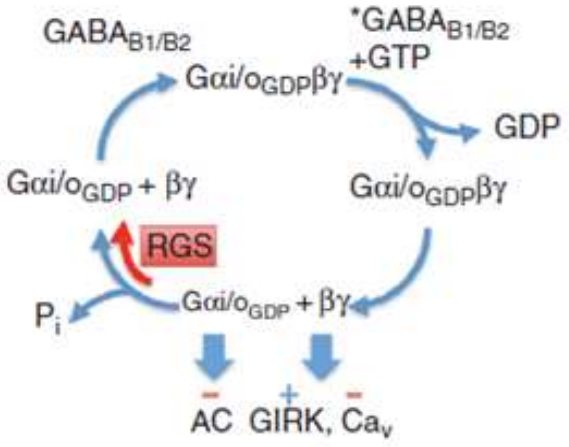

From Padgett and Slezinger (2010) $GABA_B$ receptor coupling to G proteins and Ion channels. Advances in Pharmacology 58, 123–147

4.8. Effectors and physiological functions of $GABA_B$–receptors

As described in the previous paragraphs, $GABA_B$–receptors modulate their effectors via the activated free Gα and Gβγ subunits released from trimeric Gαβγ complex. The first $GABA_B$–R effector characterized was *adenylcyclase* whose activity was shown to be inhibited by free Gα subunits of G_i/G_o family (Xu and Wojcik, 1986). The physiological significance of AC inhibition in brain, however, is difficult to outline in uneqivocal way because the numerous different AC isoforms I–X were discovered (**Fig. 6**) and shown to exhibit widely different responsiveness to individual Gα or Gβ subunit proteins (**Figs. 7 and 8**) (Simonds, 1999; Sunahara and Taussig, 2002). Even at present time, the physiological consequences of inhibition of AC activity are poorly understood and include effects on transcription factors, kinases and intracellular Ca^{2+} signaling (Couve *et al.*, 2002; New *et al.*, 2006; Ren and Mody, 2003; Steiger *et al.*, 2004).

Fig. 6 **Structure and membrane topology of adenylcyclase**

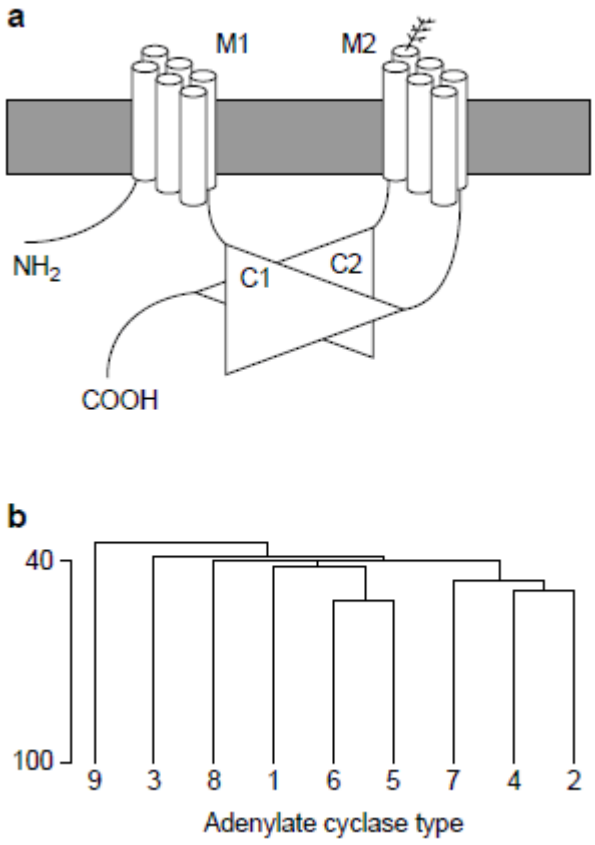

Legend to Fig. 6

a) Schematic diagram of the proposed membrane topology of the adenylyl cyclases (AC) based on hydropathy analysis and the terminology of $G_o\alpha$ by A. G. Gilman. The grey rectangle represents the plasma membrane into which the clusters M1 and M2 of six transmembrane spanning α–helical segments anchor the enzyme. The cytosolic domains include the N–terminal region, the homologous ~25 kDa catalytic domains C1 and C2 interacting in a head–to–tail manner and the C–terminus. The cDNAs for all nine principal cyclase isoforms predict sites of N–linked glycosylation in M2 (branching tuft) and the glycoprotein nature of several AC isoforms has been proven by glycohydrolytic analysis.

b) Sequence relationships among the nine AC isoforms are represented in a dendrogram generated by the program PILEUP in which the vertical distance is proportional to the similarity between sequences. A scale approximating the percent sequence similarity is provided on the left, in which the similarity between AC9 and AC3 determined by the program GAP is indicated as 40%.

Fig. 7 **Distribution in AC isoforms in mammalian tissues**

Table 1. Mammalian isforms of adenylate cyclase

Adenylate cyclase (AC) type	Size (no. of amino acids)	mRNA expression	Refs
AC1	1134	Brain, retina, adrenal medulla	5, 6
AC2	1090	Brain; olfactory bulb > lung	6, 7
AC3	1144	Olfactory neurones, brain, retina, aorta, lung, testis	8–10
AC4	1064	Kidney, brain, heart, liver, lung	11
AC5	1184	Heart > brain > kidney	12, 13
AC6	1165	Heart, brain > kidney, testis, spleen, liver	13–16
AC7	1099	Lung, heart, spleen, kidney, brain	17, 18
AC8	1248	Brain[a]	14, 19
AC9	1353	Skeletal muscle, brain > kidney lung, liver, heart	20, 21

[a]Northern blotting[19], demonstrated the expression of AC8 message in brain, while reverse transcriptase (RT)–PCR identified AC8 mRNA in brain, but not in heart, liver, kidney, testis or skeletal muscle[14].

Fig. 8 Functional responsiveness of different AC isoforms to G protein activation

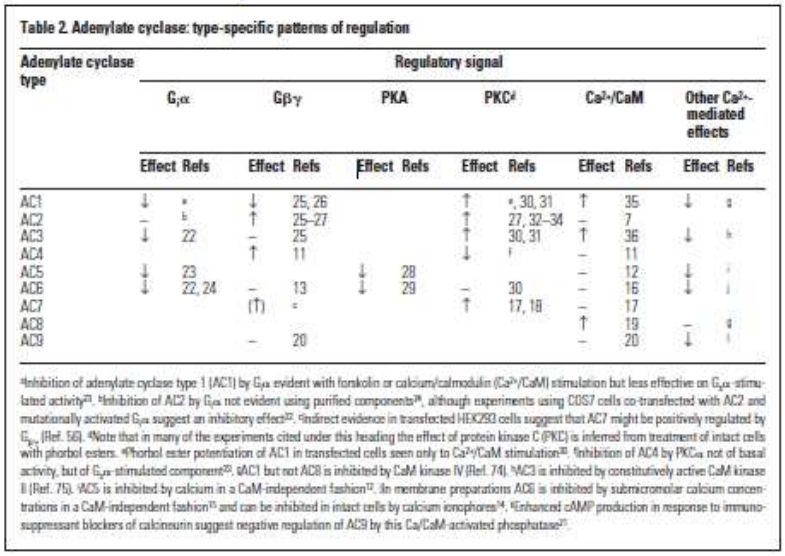

Table 2. Adenylate cyclase: type-specific patterns of regulation

Adenylate cyclase type	Regulatory signal											
	$G_i\alpha$		$G\beta\gamma$		PKA		PKC[d]		Ca^{2+}/CaM		Other Ca^{2+}-mediated effects	
	Effect	Refs	Effect	Refs	Effect	Refs	Effect	Refs	Effect	Refs	Effect	Refs
AC1	↓	[a]	↓	25, 26			↑	[a], 30, 31	↑	35	↓	[a]
AC2	–	[b]	↑	25–27			↑	27, 32–34	–	7		
AC3	↓	22	–	25			↑	30, 31	↑	36	↓	[b]
AC4			↑	11			↓	[f]	–	11		
AC5	↓	23			↓	28			–	12	↓	[i]
AC6	↓	22, 24	–	13	↓	29	–	30	–	16	↓	[j]
AC7			(↑)	[c]			↑	17, 18	–	17		
AC8									↑	19	–	[g]
AC9			–	20					–	20	↓	[k]

[a]Inhibition of adenylate cyclase type 1 (AC1) by $G_{i}\alpha$ evident with forskolin or calcium/calmodulin (Ca^{2+}/CaM) stimulation but less effective on $G_{s}\alpha$-stimulated activity[27]. [b]Inhibition of AC2 by $G_{i}\alpha$ not evident using purified components[28], although experiments using COS7 cells co-transfected with AC2 and mutationally activated $G_{i}\alpha$ suggest an inhibitory effect[32]. [c]Indirect evidence in transfected HEK293 cells suggest that AC7 might be positively regulated by $G_{\beta\gamma}$ (Ref. 56). [d]Note that in many of the experiments cited under this heading the effect of protein kinase C (PKC) is inferred from treatment of intact cells with phorbol esters. [e]Phorbol ester potentiation of AC1 in transfected cells seen only to Ca^{2+}/CaM stimulation[30]. [f]Inhibition of AC4 by PKC_{α} not of basal activity, but of $G_{s}\alpha$-stimulated component[33]. [g]AC1 but not AC8 is inhibited by CaM kinase IV (Ref. 74). [h]AC3 is inhibited by constitutively active CaM kinase II (Ref. 75). [i]AC5 is inhibited by calcium in a CaM-independent fashion[12]. [j]In membrane preparations AC6 is inhibited by submicromolar calcium concentrations in a CaM-independent fashion[15] and can be inhibited in intact cells by calcium ionophores[34]. [k]Enhanced cAMP production in response to immunosuppressant blockers of calcineurin suggest negative regulation of AC9 by this Ca/CaM-activated phosphatase[21].

In comparison to Gα–mediated signaling, Gβγ–mediated signaling is much better understood. The main Gβγ–dependent effectors of presynaptic $GABA_B$ receptors are *P/Q–and N–type voltage–dependent Ca^{2+} channels* (Barral *et al.*, 2000; Bussieres and El Manira, 1999; Chen and van den Pol, 1998). $GABA_B$ receptors inhibit these Ca^{2+} channels at excitatory and inhibitory terminals, thereby restricting neurotransmitter release. By definition, $GABA_B$ *autoreceptors* inhibit GABA release while $GABA_B$ *heteroreceptors* decrease the release of other neurotransmitters, including, for example, glutamate, dopamine, adrenaline, or serotonin. Depending on whether the terminal releases an inhibitory or excitatory neurotransmitter, presynaptic $GABA_B$ receptors increase or decrease the excitability of the postsynaptic neuron.

Presynaptic $GABA_B$–receptors restrict the neurotransmitter release not only by inhibiting $Ca2^+$ channels but also by retarding the recruitment of synaptic vesicles (Sakaba and Neher, 2003). Recent evidence also suggests that presynaptic $GABA_B$ receptors couple to inwardly rectifying Kir3–type K^+ channels (also designated GIRK channels) to inhibit glutamate release (Fernandez–Alacid *et al.*, 2009; Ladera *et al.*, 2008). However, Kir3 channels are generally considered as the main effectors of postsynaptic $GABA_B$ receptors (Luscher *et al.*, 1997; Wagner and Dekin, 1993). $GABA_B$–mediated activation of Kir3 channels produces slow inhibitory postsynaptic potentials (IPSPs) by inducing K^+ efflux, which hyperpolarizes the membrane and shunts excitatory currents. Postsynaptic $GABA_B$ receptors also down–regulate Ca^{2+} channels, which inhibit dendritic $Ca2^+$–spike propagation (Perez–Garci *et al.*, 2006). The alteration of membrane potential by activated $GABA_B$–R by means of opening

the Ca^{2+} or K^+ channels is explained in details in **Fig. 9.**

Activation of the G protein coupled $GABA_B$–receptor stimulates GTP–dependent G protein (Gi/o) dissociation of the Gα and Gβγ dimer. The Gα i/o subunit has been shown to inhibit adenylyl cyclase while the Gβγ dimer is capable of modulating voltage–gated Ca^{2+} (v) or G protein–gated inwardly rectifying K^+ (GIRK) channels, resulting in potent neuronal inhibition. Effector specificity may be regulated by hetero–complex formation, guided by targeting protein partners and subcellular localization.

Fig. 9 $GABA_B$–R signaling via K^+ (GIRKs) and $Ca2^+$ (v) channels

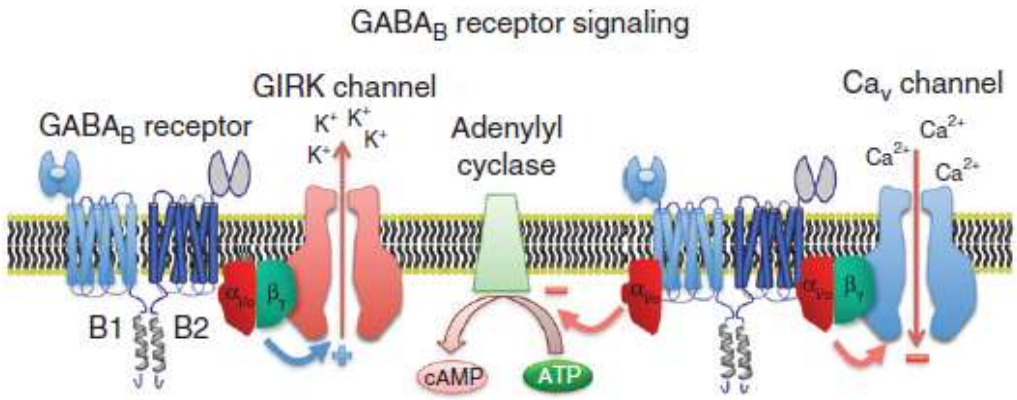

From Padgett and Slezinger (2010) $GABA_B$ receptor coupling to G proteins and Ion channels. Advances in Pharmacology 58, 123–147

The cell interior is negatively charged in comparison with the extracellular space. The **Ca^{2+} (v) channels** (voltage–dependent calcium channels) are activated (opened) in the course of depolarization of cell membrane. Opening of Ca_V channels causes *depolarization* of the membrane. Calcium cations enter intracellular compartment (pre–synaptic part) and induce fusion of neurotransmitter containing vesicles with plasma membrane and release of neurotransmitter into synaptic cleft. $GABA_B$–R via Gβ block the opening of **Ca^{2+} (v) channels** and in this way inhibit the neurotransmitter release.

Transport of potassium cations by G protein gated inwardly rectifying **K^+ channels (GIRKs)** out from the cell interior induces *hyperpolarization* of cell membrane, generates "slow inhibitory postsynaptic potentials (IPSPs) and shunts the excitatory currents. In this

way it inhibits excitation. Post–synaptic $GABA_B$–R open GIRKs channels, again via Gβ subunits, and in this way decrease the excitability at post–synaptic level. $GABA_B$–auto–receptors inhibit release of its own neurotransmitter, i.e. GABA. $GABA_B$–heteroreceptors inhibit release of other neurotransmitters such as glutamate or serotonine.

The present state of knowledge about the plasma membrane part of $GABA_B$–receptor signaling cascade may be therefore described as a mutually interrelated regulatory network of receptors, G proteins, AC isoforms and ionic channels proceeding as positive or negative feed–back regulatory loops (Pinard *et al.*, 2010). The final out–come of these regulatory circuits depends on expression level and activity of individual proteins in a given cell population present in a given brain area. *Therefore, when considering GABA as the main inhibitory neurotransmitter of mammalian brain, activation of pertussis–toxin sensitive G proteins of G_i/G_o family by $GABA_B$–receptors represents the crucial primary regulatory mechanism for an optimum of function of the brain.*

4.9. Subcellular fractionation of the frontal rat brain cortex and isolation of plasma membranes from mammalian cells; *historical perspective*

The original methods for subcellular fractionation of the rat brain tissue and isolation of plasma membrane fragments in density gradients were using the highly hypertonic solutions of sucrose (De Robertis at al., 1962a, b; Whittacker *et al.*, 1964; Lisy *et al.*, 1971). A synthetic polymer of sucrose Ficoll (Amersham Pharmacia Biotech, Uppsala, Sweden) was subsequently introduced to overcome the problem of the high osmotic pressure (Holter and Moller, 1958; Pertoft, 1966). This has been successfully made and Ficoll is used up to now for isolation of lymphocytes, other blood cells and separation of different cell populations in general, but is unappropriate for fractionation of subcellular membrane particles because of the very high viscosity of its aqueous solutions (Pertoft, 2000).

The more advanced methods (De Pierre and Karkowsky, 1973; Whittacker, 1984; Rickwood, 1984, Hollingsworth *et al.*, 1985; Fisher *et al.*, 1986; Dunkley *et al.*, 1986; Maloteaux *et al.*, 1995; Luabeya *et al.*, 1997; Pertoft, 2000) were using aqueous solutions of Percoll and Iodixanol (OptiPrep). These organic macromolecules, when diluted to proper concentration and supported by salts, represented much less damaging environment for isolation of the whole cells or subcellular membrane fragments/ vesicles. The rather complicated and sophisticated isolation of small synaptosomal vesicles enriched in trimeric G proteins (Ahnert–Hilger at al., 1993) as well as existence of aggregated forms of trimeric G

proteins isolated in the presence of mild detergents such as digitonin or Lubrol PX (Jahangeer and Rodbell, 1993) should be also noticed. The difficulties of how to overcome the toxicity, osmotic pressure changes and penetration of density gradient media into the particles have been discussed by Rickwood (1984). The detailed methodological advices of how to use OptiPrep were presented by Graham (2002).

4.10. Isoosmotic density gradient media

Various density gradient media were developed for specific applications of centrifugational techniques. These media, if possible, should not alter the cells or particles to be separated and should provide a proper density range for separation of one type of cells (or subcellular) membrane particles from another. The difficulties which have to be overcomed when viewed from the general point of view are represented by toxicity, osmotic pressure changes and penetration of a given chemical used for preparation density gradient medium into the particles which are being isolated or separated form each other (Rickwood, 1984).

Sucrose

The main disadvantages of sucrose solutions are some of their physico–chemical properties. Sucrose solutions in high concentration range have a high osmolarity and are also highly viscous. Cells and subcellular particles, which are osmotically sensitive, will band at a density which differ from their physiological density. Furthermore, due to the low molecular weight, the sucrose may penetrate into the cells and an to envelope the intracellar particles.

Polysucrose

A synthetic polymer of sucrose (Ficoll; Amersham Pharmacia Biotech, Uppsala, Sweden) was introduced early to overcome the problem of high osmotic pressure inherently combined with usage of sucrose itself (Holter and Moller, 1958). However, Ficoll of molecular weight 400,000 also gives measurable osmotic effects at high concentrations; this problem had to be compensated by addition of salts into the density gradient media with the aim to to keep iso–osmotic conditions throughout the centrifuge tube (Pertoft, 2000).

Iodinated compounds

Iodinated compounds are widely used as centrifugation media (Iodixanol, Optiprep^{TM}) (Graham, 2002). In Optiprep^{TM} solutions, the cells band isopycnically without being subject to the high osmotic stress existing in sucrose gadients (Rickwood, 1984).

Colloidal silica

The use of colloidal silica was first reported by Mateyko and Kopac (1995). They

reported the osmotic pressure effects, the ability to separate cells, permeation into the particles and solubility in aqueous solutions used for preparation of density gradient media. Of all substances tested, none came closer to providing all the desired characteristics than colloidal silica. However, it was found that a pure silica sol was toxic to cells and caused hemolysis of red blood cells. At the time when polysaccharides were introduced to stabilize colloidal silca gradients they were also found to inhibit toxic effects of the silica (Pertoft, 1966). The introduction of absorbed polymers to silica particles to obtain iso–osmotic, pH–neutral and high density solutions led to introduction of Percoll in 1977 (Amersham Pharmacia Biotech, Uppsala, Sweden).

It follows that Percoll has proved to be the density gradient medium of choice since it fulfils almost all criteria for an ideal density gradient medium. Therefore, Percoll was used by us for subcellular fractionation of the brain tissue as well as cell homogenates prepared from HEK293 cell lines.

4.11. Structural organization of trimeric G proteins in plasma membrane*; membrane domains and multimeric structures of G proteins*

The multimeric structures of trimeric G proteins in brain membranes have been originally described by Jahangeer and Rodbell (1993). The functional evidence for the existence of non–uniformly or non–randomly organized, clustered forms of signaling units containing G proteins has been originally formulated by Neubig (1994). This early idea had subsequently induced a large experimental attention which was oriented to the detailed biochemical analysis of plasma membrane preparations isolated from stably transfected cell lines (specifically expressing the given type of GPCR), primary tissue culture cells or natural tissues. Subsequently, a large number of reports dealing with the plasma membrane sub–compartments denominated as *membrane domains or rafts* was published (Jacobson and Dietrich, 1999; Smart *et al.*, 1999; Simons and Tomre, 2000; Brown and London, 2000, Babichuk and Draeger, 2006; Allen *et al.*, 2007). The biochemical preparations of membrane domains were found to be enriched in cholesterol, glycolipids, sphingolipids and trimeric G proteins (for general reviews see Jacobson and Dietrich, 1999; Smart *et al.*, 1999; Simons and Tomre, 2000; Brown and London, 2000, Babichuk and Draeger, 2006; Allen *et al.*, 2007). The content of GPCR in membrane domains was relatively low (Moravcova *et al.*, 2004; Svoboda *et al.*, 2004; Rudajev *et al.*, 2005).

However, these studies were performed under the widely different methodological conditions. The usage of high detergent concentrations for preparation of membrane domains, in this case designated as detergent–resistant membrane domains (DRMs) (Sargiacomo *et al.*, 1993; Lisanti *et al.* 1994 a, b), resulted in preparations exhibiting the very low or zero agonist efficacy for stimulation of GDP/GTP exchange reaction of G proteins. This has been demonstrated first in stably transfected HEK293 cell lines stably expressing δ–OR–Gi1α (I^{351}–C^{351}) fusion protein (Bourova *et al.*, 2003). The same was truth when using the "alkaline–treatment" protocol based on sonication and extraction of the cell homogenate in highly alkaline solution of 0.5–1 M Na_2CO_3 (Song *et al.* 1996a, b).

According to experimental results collected over the years in our laboratory, the best of the so–far described methods/ protocols for preparation of membrane domains is that of Smart *et al.* (1995, 1999). The views what the term *membrane domains* actually means from methodological, structural and functional point of view were reviewed by Pike (2004). The sometimes controversial viewpoints about the size and physiological meaning of *membrane domains* were expressed by Pike (2006a, b) and Shaw (2006).

4.12. Biochemical methods for preparation of membrane domains

The disadvantage of the method of Smart *et al.* (1995, 1999) using the sequence of three types of density gradients is, however, the very low amount of protein recovered in the final preparation of pure "domains" – about 0.2–0.5% of the original amount present in the starting material, i.e. the cell homogenate. Therefore, when trying to find some compromise between purity and quantity of the final preparation, we have combined centrifugation in Percoll gradient followed by the "flotation" in sucrose density gradient. Plasma membrane enriched fraction was prepared from the rat brain cortex by centrifugation at 116,000xg for 35 min in Percoll^R gradient (Beckman Ti60 rotor), subsequently, the low–density membrane fragments (LPM) were separated from the bulk of plasma membranes (BPM) by flotation in a step–wise 15/20/25/30/35/40% w/v sucrose gradient (**Fig. 10**).

Fig. 10 Isolation of plasma membranes in Percoll gradient followed by separation of LPM (low–density PM fragments) and BPM (bulk of plasma membranes) by flotation in sucrose density gradient; *subcellular fractionation of rat brain cortex under detergent–free conditions* (Drastichova *et al.*, 2008)

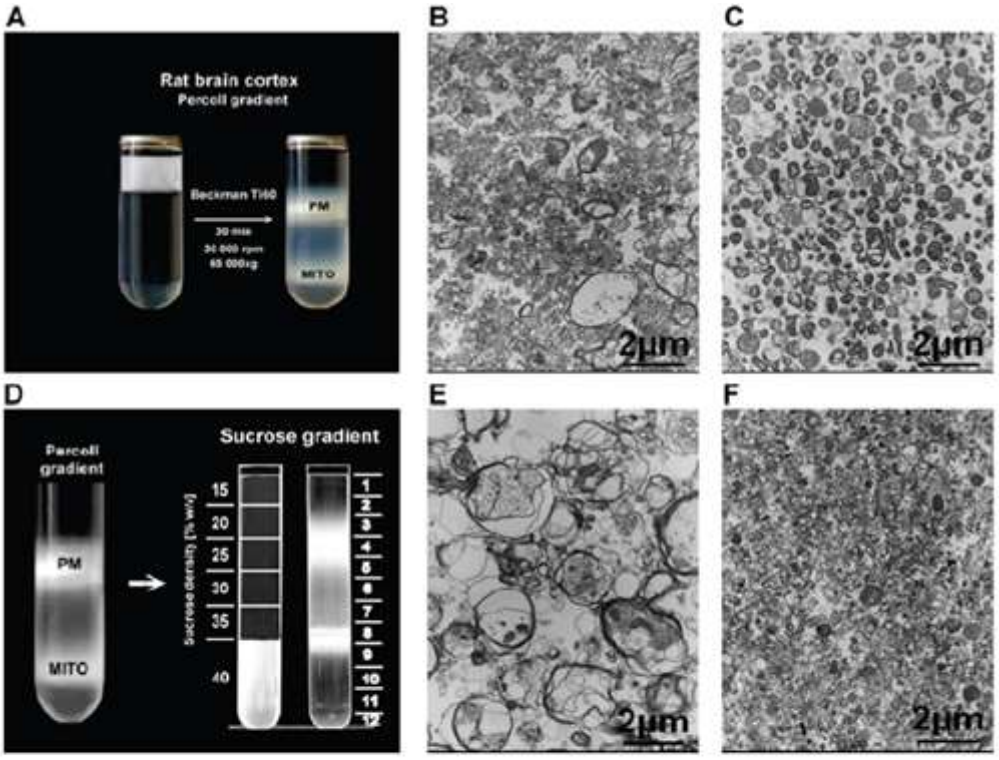

Subcellular fractionation of rat brain cortex. **A**, *Separation of plasma membrane and mitochondrial fractions in Percoll® gradient.* Post-nuclear supernatant was prepared from cerebral cortex of the rat and fractionated in Percoll® gradient. The upper layer of plasma membranes (PM) was separated from lower layer of mitochondria (MITO). **B**, plasma membrane fraction represented mixture of large and small vesicular structures together with sheets of myelin; **C**, in mitochondrial fraction, pure mitochondria were detected. **D**, *Flotation of plasma membrane fraction in sucrose gradient.* The upper layer collected from Percoll® gradient (PM) was fractionated by flotation in 15/20/25/30/35/40 % w/v sucrose gradient. Low-density plasma membrane (LPM), represented by hazy area in 15/20 % sucrose (fractions 3-5), were resolved from bulk of PM observed as distinct, optically dense band in 35 % sucrose or at 35/40 % sucrose interface (fractions 7-8). **E**, LPM were composed from large synaptosomal membrane particles and myelin; **F**, Bulk of plasma membrane (BPM) contained heterogeneous mixture of small vesicular structures (magnification 11700x).

Subsequently, we tried to prepare, from the frontal rat brain cortex, the detergent–resistant membrane domains which would exhibit the functional coupling between GPCRs and trimeric G proteins and compare the characteristics of neurotransmitter activation of $GABA_B$–R and other GPCRs in detergent–treated (DRMs) and detergent–untreated low–density PM fragments (LPM).

Figures **11–17**, accompanying text and the *comments* to these figures demonstrate how this goal was achieved.

Fig. 11 Subcellular fractionation of the rat brain cortex in the absence and presence of high (1% w/v) concentration of non/ionic detergent Triton X–100

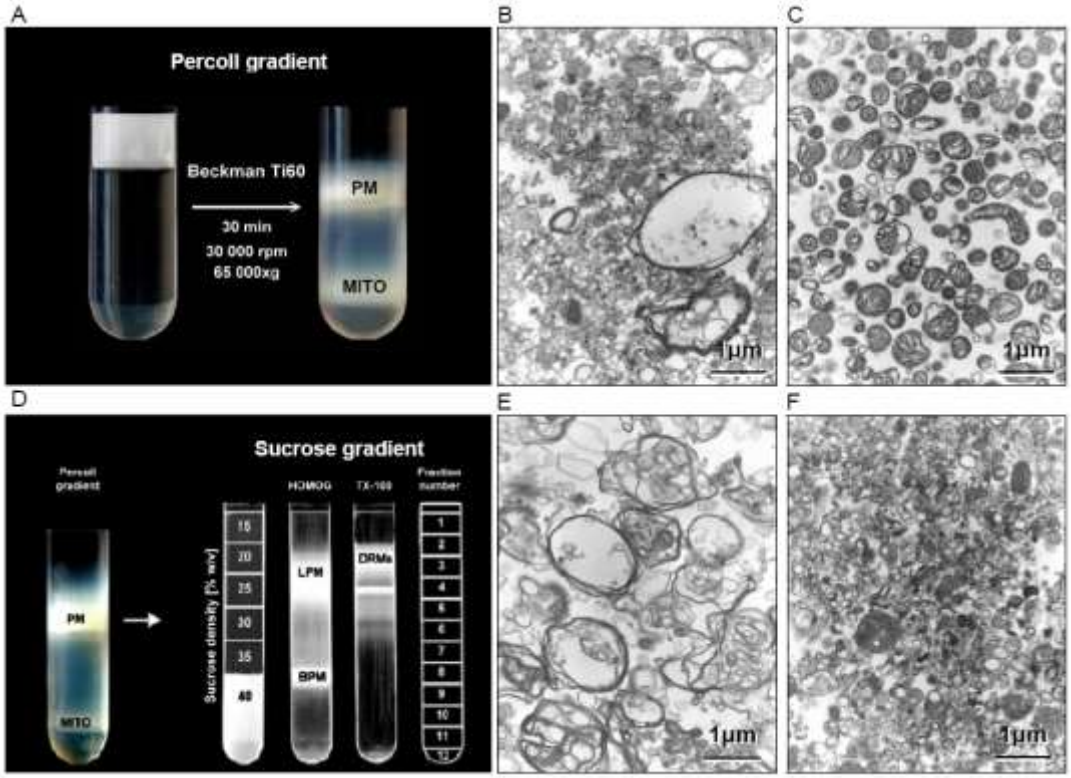

From PhD Thesis of Dr. Vladimír Rudajev, Charles University in Prague, Faculty of Natural Science, Department of Physiology, 2006

Legend to Fig. 11. A, separation of plasma membrane (PM) and mitochondrial (MITO) fractions in Percoll gradient; **B**, plasma membrane fractions represents a mixture of small and large (synaptomes) vesicles; **C**, mitochonrial fractions contains mitochondria; **D**, fractionation of PM by flotation in sucrose gradient; **E**, the low–density PM fragments (LPM) are enriched in synaptosomes; **F**, bulk of plasma membranes (BPM) contains the small vesicles.

As demonstrated in **Fig. 11**, the addition of 10% v/v Triton X–100 to Percoll–purified PM in the final concentration of 1% v/v and a subsequent resolution of TX–100 solubilized PM fragments by flotation in 15/20/25/30/35/40 % w/v sucrose density gradient for 24 hours at 118,000xg in Beckman SW41, results in flotation (of relatively small part when expressed as recovery of protein) **up**, i.e. to the low–density area of sucrose gradient. TX–100–resistant PM fragments exhibiting the low–density are localised in fractions 2–5. These fractions were collected from the top to the bottom of centrifuge tube, mixed together and represented the so–called detergent–resistant membrane domains, DRMs.

Unfortunately, as demonstrated in the following sequence of results presented in **Figs. 12–16**, DRMs prepared according to this protocol were not functional in the terms of functional coupling between $GABA_B$–R and G proteins of Gi/Go family. The ability of $GABA_B$–R agonist baclofen to stimulate G protein was diminished at the high detergent concentrations.

Fig. 12 Sucrose density gradient profile of plasma membrane marker Na^+/K^+–ATPase; *comparison of the detergent–untreated and TX–100–treated low–density membrane fragments (LDM)*

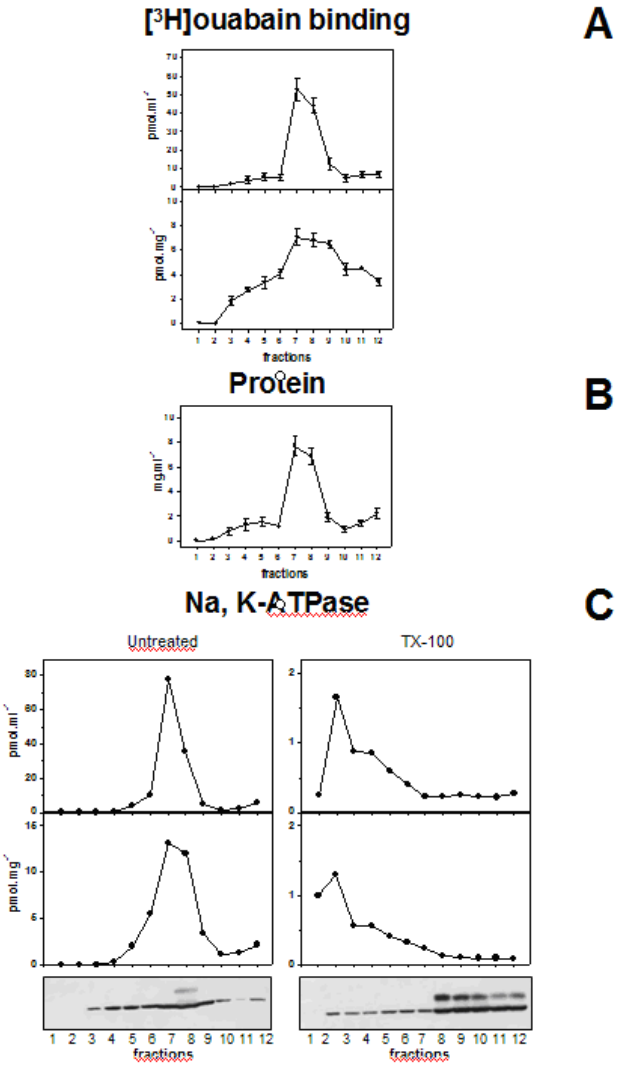

From PhD Thesis of Dr. Vladimír Rudajev, Charles University in Prague, Faculty of Natural Science, Department of Physiology, 2006

Legend to Fig. 12.

A) Distribution of prototypical plasma membrane marker Na^+/K^+–ATPase along the sucrose density gradient was determined by [^{3}H]ouabain binding assay. **B)** The protein

content in sucrose fractions 1–12 collected form the top to bottom of the centrifuge tube (Beckman SW 41) was determined by Lowry method. **C**) Distribution of Na^+/K^+–ATPase along the gradient was determined by imunoblot analysis with specific antibodies oriented against the alpha subunit of Na^+/K^+–ATPase and compared in detergent–untreated (**Untreated**) and Triton X–100 (0.5 %)–treated (**TX–100**) fractions. The results represent typical fractionation procedure.

Fig. 13 **Distribution of GPCR along sucrose density gradient**; detection by specific agonist and antagonist radioligand binding assays

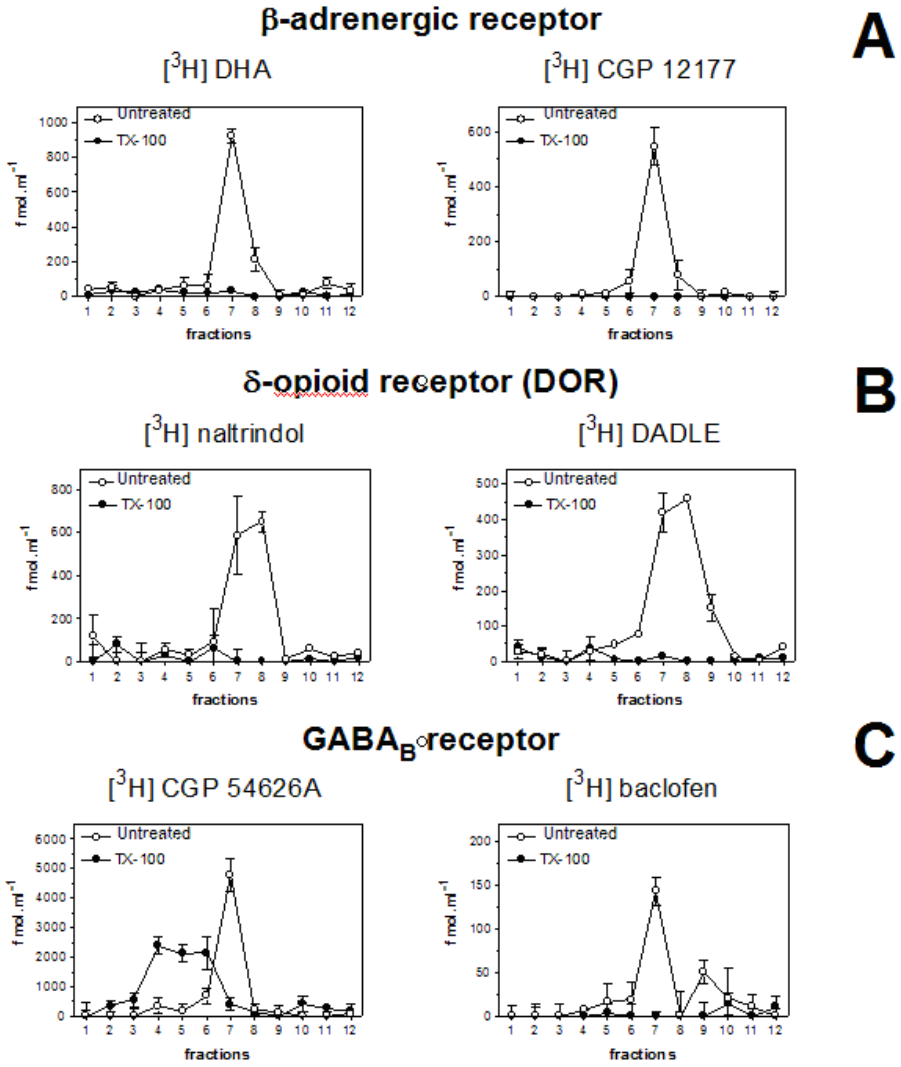

From PhD Thesis of Dr. Vladimír Rudajev, Charles University in Prague, Faculty of Natural Science, Department of Physiology, 2006

Legend to Fig. 13. Receptor content in sucrose fractions 1–12 (collected form the top to bottom of the centrifuge tube of Beckman SW 41) was determined by specific agonist and antagonist radioligand binding assays. In the contrary to β–AR and δ–OR, $GABA_B$–receptors were highly

enriched in TX–100–resistant membrane domains, DRMs.

Fig. 14 Distribution of GPCR along sucrose density gradient*; detection by immunoblot analysis with specific antibodies*

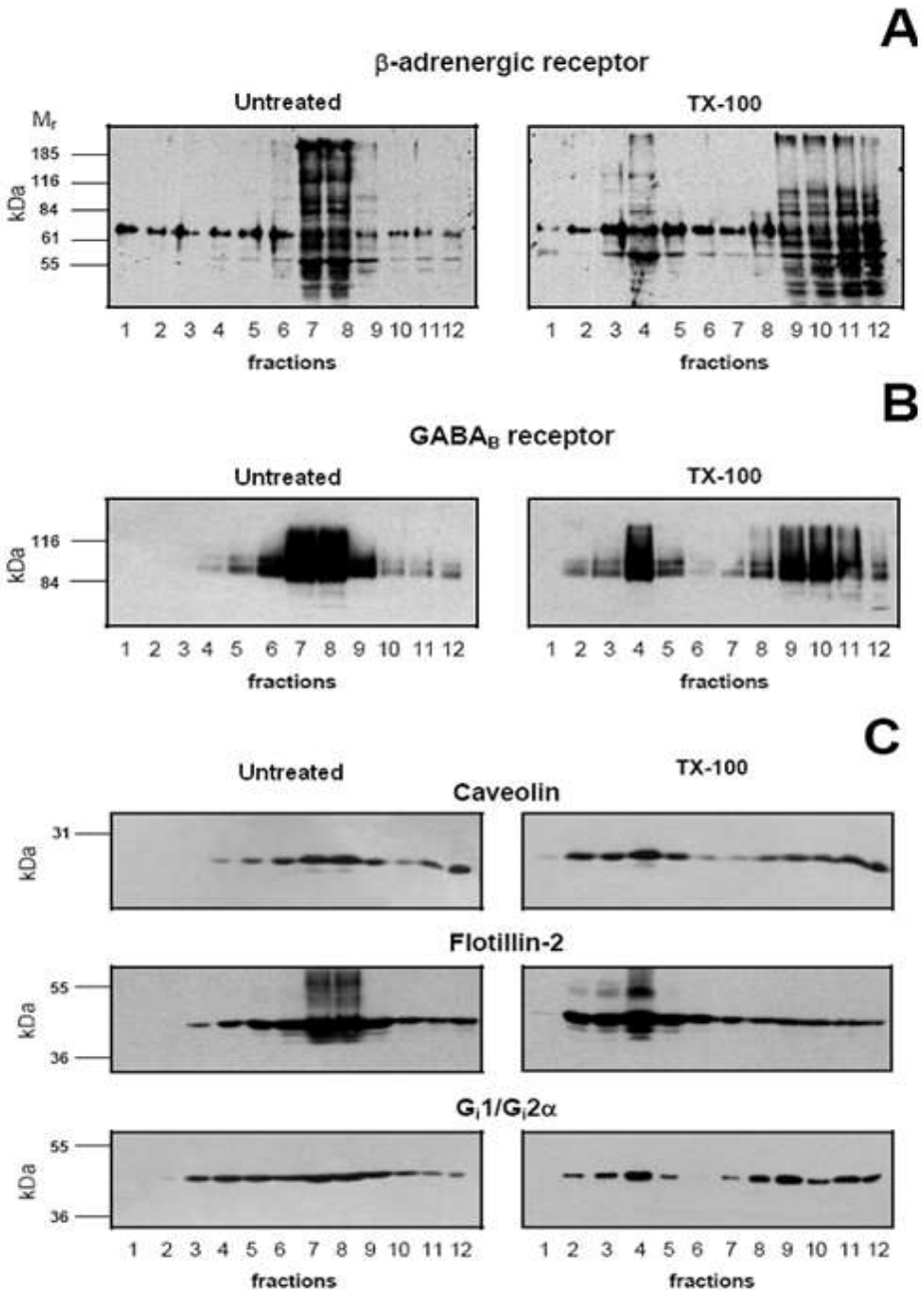

From PhD Thesis of Dr. Vladimír Rudajev, Charles University in Prague, Faculty of Natural Science, Department of Physiology, 2006

Legend to Fig. 14. Receptor content in sucrose fractions 1–12 collected form the top to bottom of the centrifuge tube (Beckman SW 41) was determined by specific agonist and antagonist radioligand binding assays. In the contrary to β–AR and δ–OR, $GABA_B$–receptors were highly enriched in TX–100–resistant membrane domains, DRMs.

Fig. 15 Deleterious effect of the high detergent concentration on functional activity of $GABA_B$–R

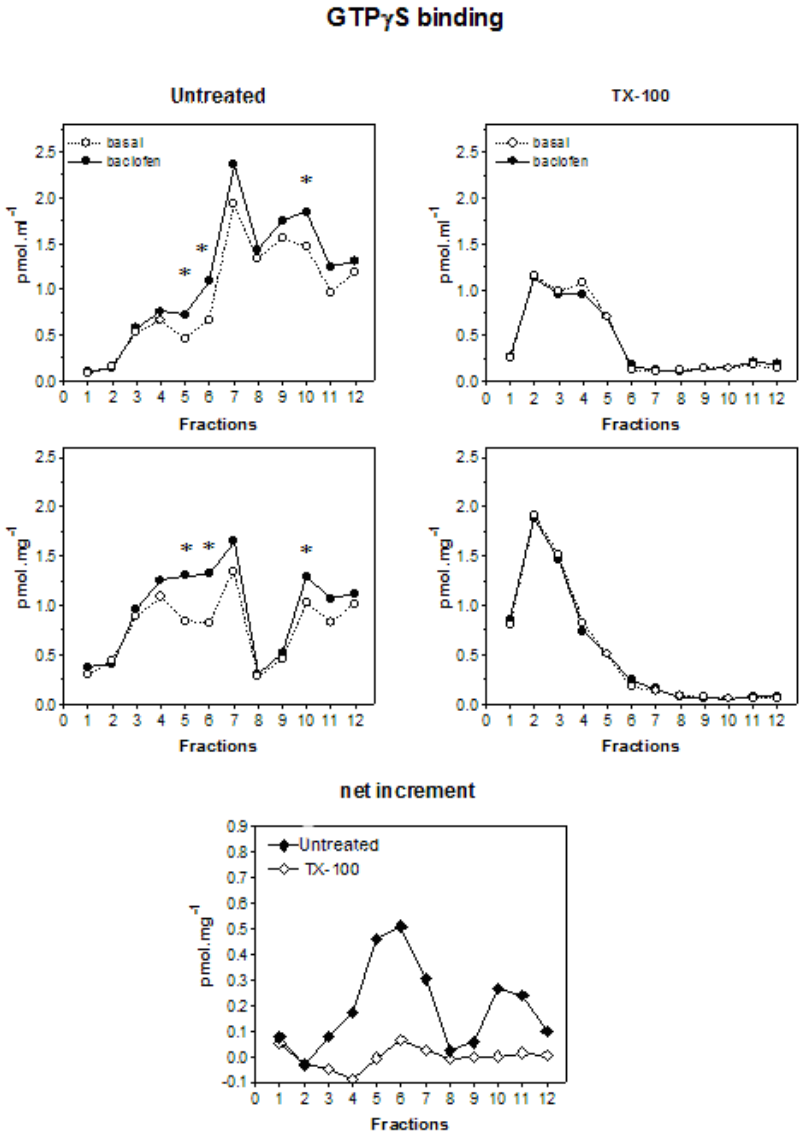

From PhD Thesis of Dr. Vladimír Rudajev, Charles University in Prague, Faculty of Natural Science, Department of Physiology, 2006

Legend to Fig. 15. Percoll purified plasma membranes were prepared from the brain cortex of adult rats and divided into two identical portions. The first portion was intensively mixed and represented the detergent–untreated PM sample; to the second portion, 10% v/v Triton–X100 was added to final concentration of 1 % w/v. Exactly 2 ml of these two PM preparations were mixed with 2 ml of 80% w/v sucrose and fractionated by flotation in 15/20/25/30/35/40 % w/v sucrose gradient (centrifugation for 24 hours at 116,000xg, Beckman SW41). The low–density fractions 1–5 (1 ml each) which were collected from the top of the centriguge tubes and combined together represented the detergent–untreated (LPM) and detergent–treated (TX–100) preparation of membrane domains.

Functional activity of G proteins was measured by high–affinity [^{35}S]GTPγS binding assay using the single concentration of baclofen (0.1 mM) as a stimulating agonist.

Fig. 16 Comparison of dose–response curves of baclofen–stimulated [^{35}S]GTPγS binding in detergent–untreated (LPM) and TX–100 (1 % v/v)–treated–plasma membranes; *agonist stimulation is diminished at high detergent concentration*

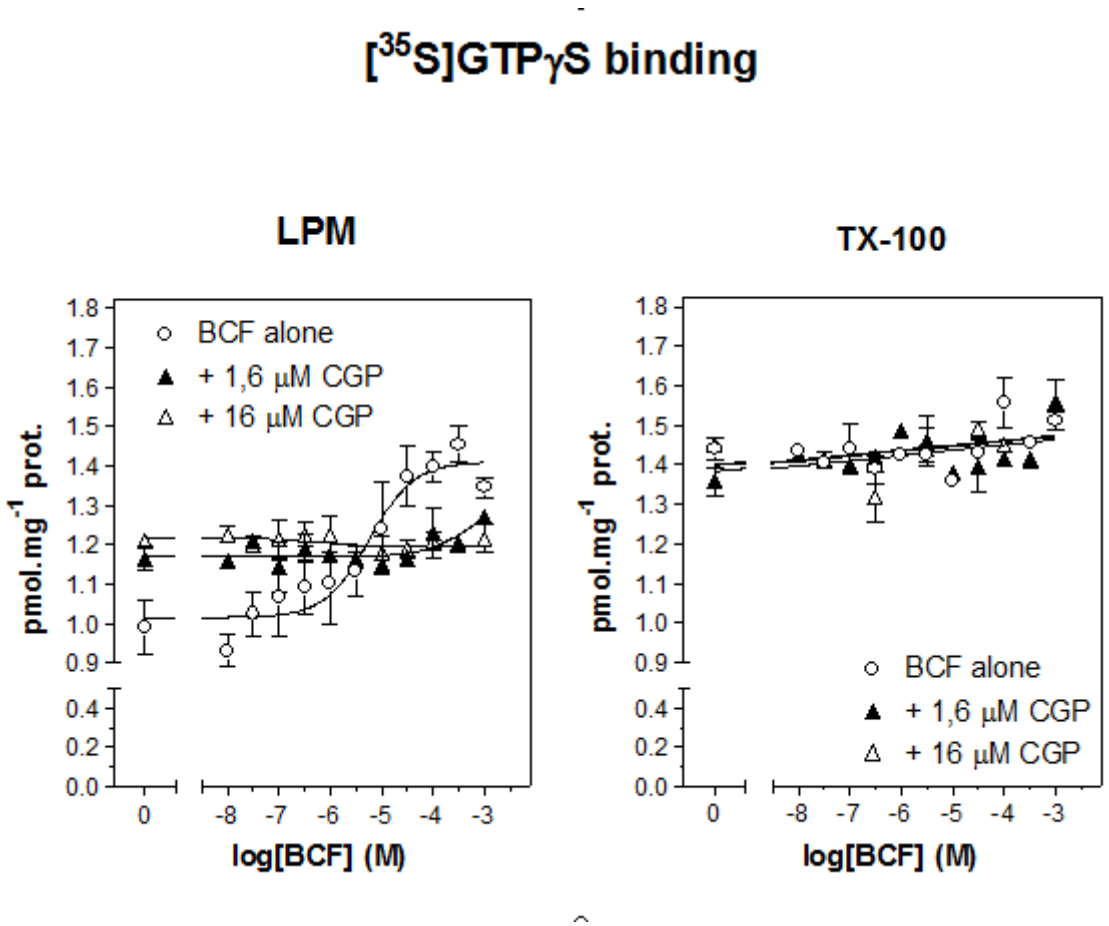

From PhD Thesis of Dr. Vladimír Rudajev, Charles University in Prague, Faculty of Natural Science, Department of Physiology, 2006

Legend to Fig. 16. The same legend as in Fig. 16. The functional activity of G proteins was measured by high–affinity GTPγS binding assay using the increasing concentrations of baclofen as a stimulating agonist (○), baclofen plus 1.6 µM CGP54626A (▲) or baclofen plus 16 µM CGP54626A (Δ).

Detergent–untreated membrane domains (LPM) exhibited the full responsiveness towards baclofen (BCF); contrarily, baclofen–stimulated [^{35}S]GTPγS binding was diminished in TX–100–resistant membrane domains prepared by addition of 10 % v/v Triton X–100 to

post–nuclear fraction to final concentration of 1 % v/v and subsequent flotation of detergent–treated PNS for 24 hours in 15/20/25/30/35/40 % w/v sucrose gradient.

With the aim to find a better procedure for preparation of DRMs, PM were exposed to increasing concentrations of non–ionic detergent Brij58 for 30 min at 0 ºC and assayed for baclofen–stimulated, high–affinity [^{33}S]GTPγS binding. Results presented in **Fig. 17** indicated that in relatively narrow range of detergent concentrations (0.01–0.1% w/v), the net–increment of baclofen–stimulated [^{33}S]GTPγS binding very high.

Fig. 17. The effect of increasing concentrations of Brij–58 on baclofen–stimulated, [^{33}S]GTPγS binding in Percoll–purified plasma membranes prepared from rat brain cortex.

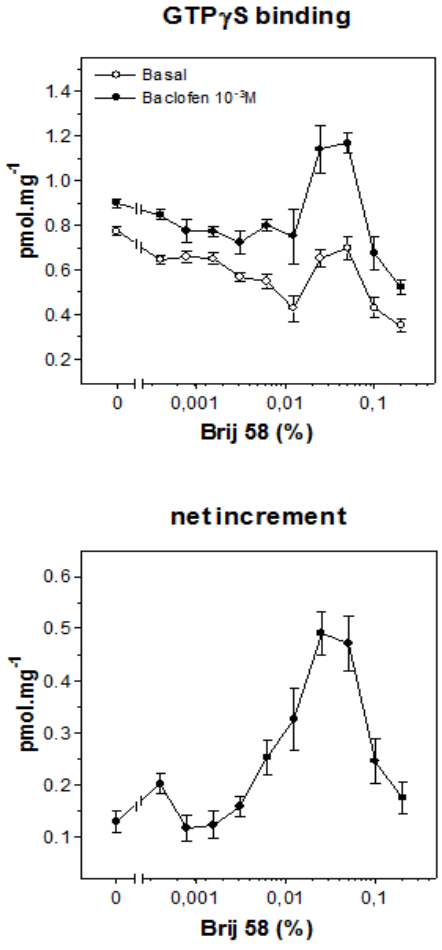

From PhD Thesis of Dr. Vladimír Rudajev, Charles University in Prague, Faculty of Natural Science, Department of Physiology, 2006

Based on this result, detergent–extraction of PM at 0 ºC was carried out in 0.025, 0.05% and 0.1% Brij58 and resulting PM fragments were separated by flotation in sucrose gradient

as described before. Distribution of Brij58–treated PM fragments was compared with distribution of detergent–untreated PM by measurement of the amount of protein in fractions 1–12 collected from the top to bottom of centrifuge tube (**Fig. 18**). We have also measured the distribution of membrane domain (caveolin and flotilin) and plasma membrane ($GABA_B$–R and Na^+/K^+–ATPase) markers in fractions 1–12 (**Fig. 19**) and compared distribution of Brij58–treated PM fragments with those formed by extraction of PM at the same concentrations of Triton X–100 (**Fig. 20**). Finally, baclofen–stimulated high–affinity [^{35}S]GTPase was measured in sucrose fractions 1–12 collected from Brij58–treated and Triton X–100–treated PM as an assay of baclofen–stimulated G protein activity (**Fig. 21**).

Fig. 18 Comparison of protein distribution in sucrose density gradients fractions prepared by flotation of *detergent–untreated (A) or Brij–58–treated (B) plasma membranes from rat brain cortex*

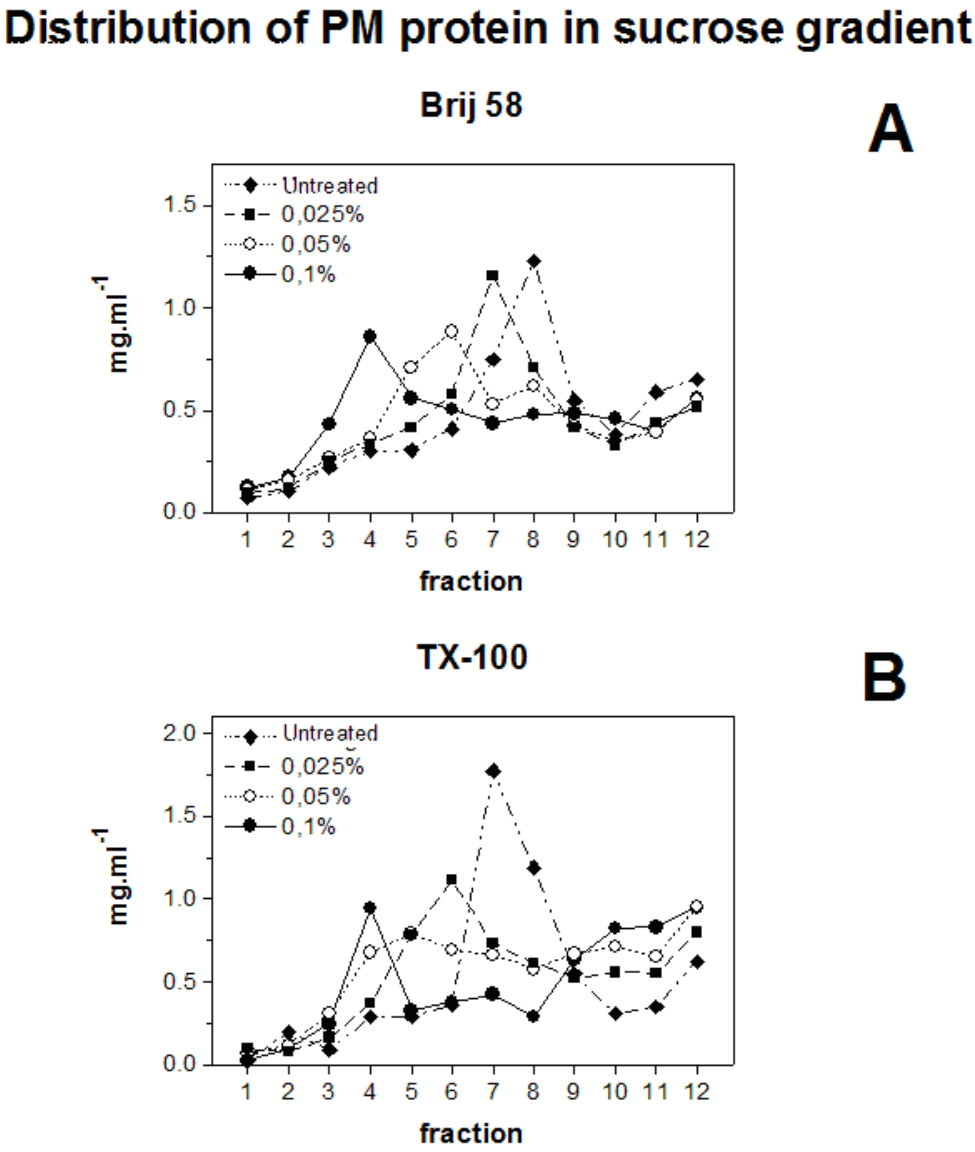

From PhD Thesis of Dr. Vladimír Rudajev, Charles University in Prague, Faculty of Natural Science, Department of Physiology, 2006

Legend to Fig. 18. Percoll–purified plasma membranes were prepared from brain cortex of adult rats and divided into four identical portions. The first portion was intensively mixed and represented the detergent–untreated PM sample (**Untreated**); to the second, third and fourth portion, the 10% w/v Brij58 was added to final concentration of 0.025, 0.05 and 0.1% w/v Brij–58. Exactly 2 ml of these four PM preparations were mixed with 2 ml of 80% w/v sucrose and fractionated by flotation in 15/20/25/30/35/40 % w/v sucrose gradient

(centrifugation for 24 hours at 116,000xg, Beckman SW41). The protein amount in fractions 1–12 collected from the top to the bottom of Beckman SW41 centrifuge tube was determined by Lowry method.

Fig. 19 Distribution of the membrane domain (caveolin–1, flotillin–2)– and plasma membrane (Na^+/K^+–ATPase and $GABA_B$–R) markers in sucrose density gradient; *the effect of increasing concentrations of Brij–58*

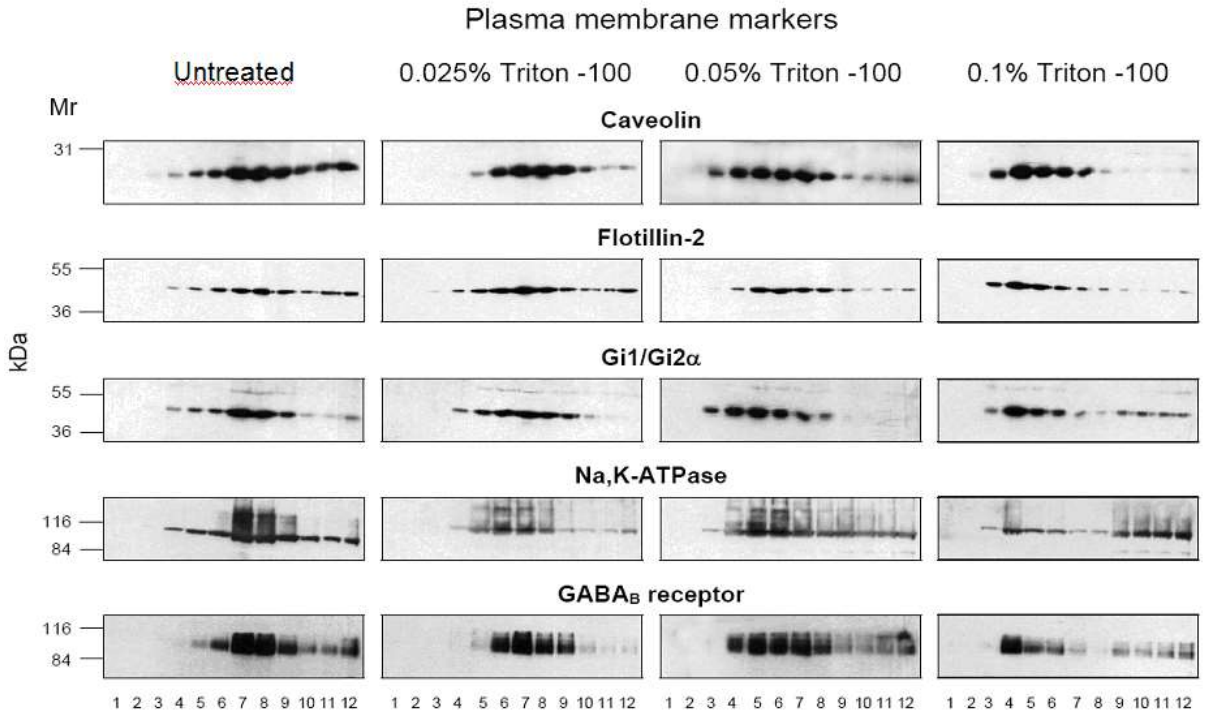

From PhD Thesis of Dr. Vladimír Rudajev, Charles University in Prague, Faculty of Natural Science, Department of Physiology, 2006

Legend to Fig. 19. Distribution of caveolin–1, flotillin–2, Gi1/Gi2α, α–subunit of Na^+/K^+–ATPase and $GABA_B$–R in sucrose density gradient was determined by TCA precipitation (6% TCA, 60 min on ice) of constant volume aliquots of fractions 1–12, SDS–PAGE and immunobloting with specific antibodies.

Fig. 20 Distribution of the membrane domain (caveolin–1, flotillin–2)– and plasma membrane (Na^+/K^+–ATPase and $GABA_B$–R) markers in sucrose density gradient; *the effect of increasing concentrations of Triton–X100.*

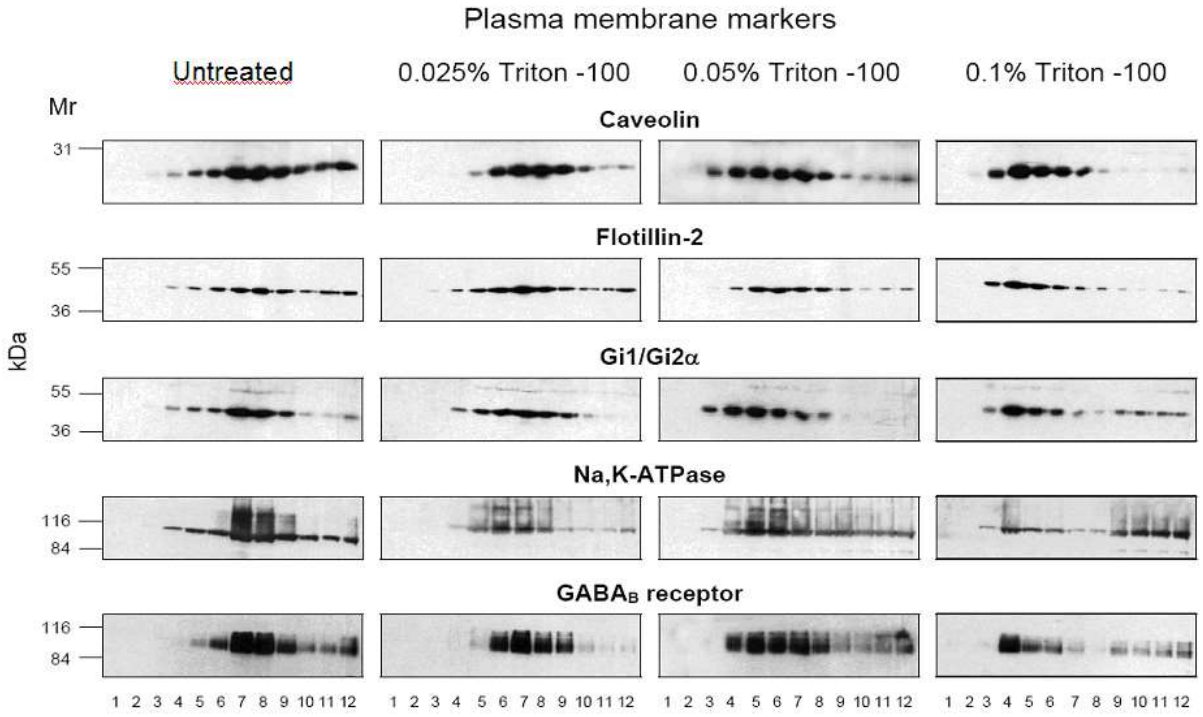

From PhD Thesis of Dr. Vladimír Rudajev, Charles University in Prague, Faculty of Natural Science, Department of Physiology, 2006

Legend to Fig. 20

Distribution of caveolin–1, flotillin–2, Gi1/Gi2α, α–subunit of Na^+/K^+–ATPase and $GABA_B$–R in sucrose density gradient was determined by TCA precipitation (6% TCA, 60 min on ice) of constant volume aliquots of fractions 1–12, SDS–PAGE and immunobloting with specific antibodies.

Fig. 21 Distribution of baclofen–stimulated, high–affinity[^{32}P]GTPase along the sucrose denisty gradient; *the effect of increasing concentrations of Brij–58 (A) and Triton X–100 (B)*

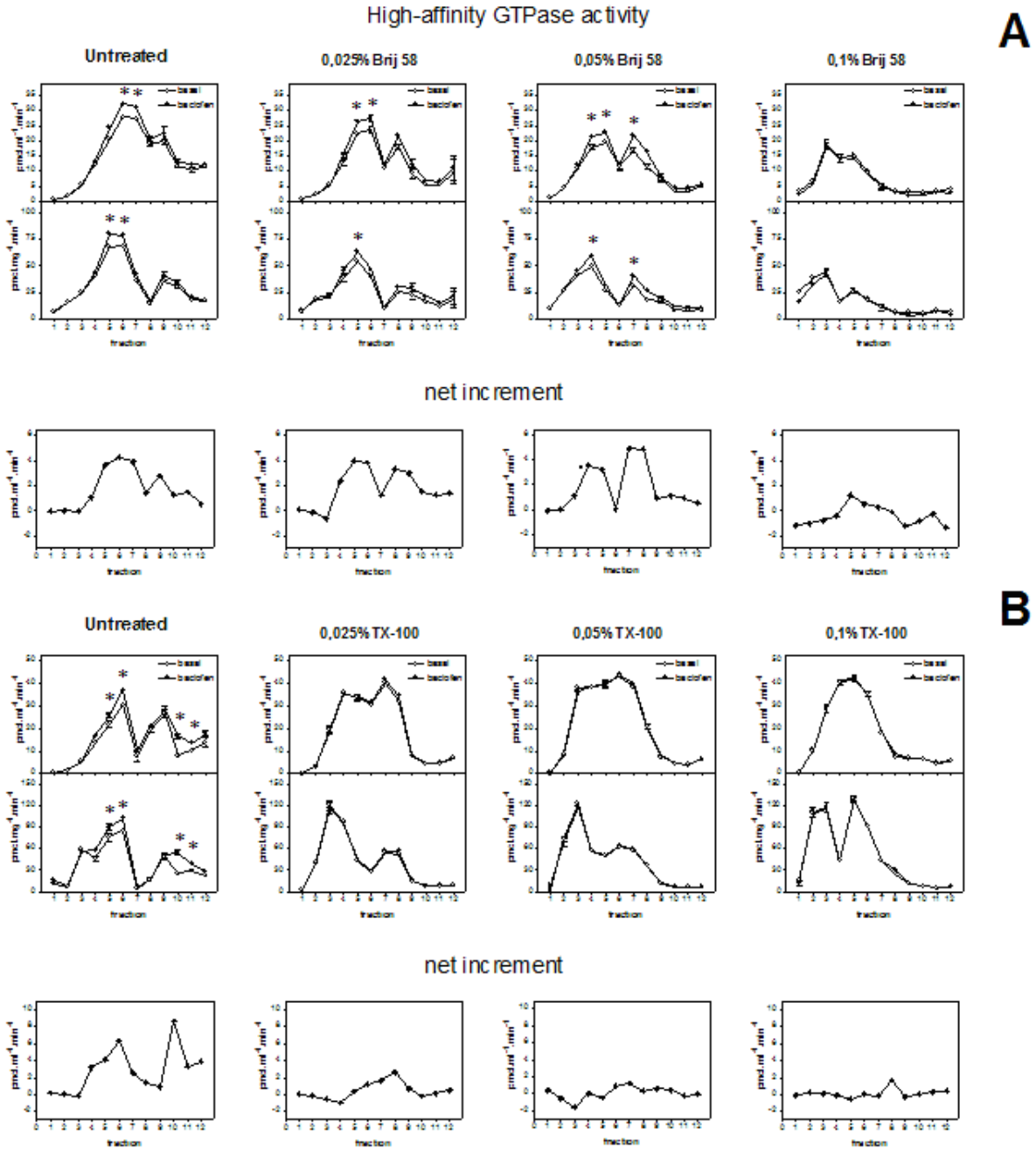

From PhD Thesis of Dr. Vladimír Rudajev, Charles University in Prague, Faculty of Natural Science, Department of Physiology, 2006

Legend to Fig. 21

Baclofen–stimulated high–affinity [^{35}S]GTPase was measured in sucrose fractions 1–12 collected from Brij58–treated– and Triton X–100–treated PM as an assay of baclofen–stimulated G protein activity.

Data presented in **Figs. 17–21** indicated, that the detergent–resistant membrane domains prepared in the presence of low concentrations of non–ionic detergent Brij58 exhibit baclofen–stimulated activity of G proteins. The optimum range of detergent concentrations was found to be in 0.025–0.05 % w/v range; at higher concentration, the agonist–stimulated component of G protein activity was attenuated due to the inhibitory action of the high detergent concentrations.

The reader might ask why the basal activity of G proteins is so high, much higher than of baclofen–stimulated component. The high basal, agonist–independent activity of G proteins is an inherent property PM prepared form natural tissues like brain or heart muscle. In natural tissues, the basal activity of G proteins is enhanced by RGS proteins which increase GTPase activity of Gα subunits and in this way increase the overall activity of G protein cycle (compare with **Fig. 4**). RGS proteins, under resting conditions residing in cytoplasmic space, are navigated to the inner side of plasma membrane by free Gβ subunits which appear on the inner side of plasma membrane shortly after agonist stimulation of receptor molecules.

4.13. Reactive oxygen species (ROS)

The earth began its life without free oxygen in its atmosphere (Dole, 1965). Oxygen accumulation is a consequence of the establishment and propagation of photosynthesizing archea and bacteria on this planet (Campbell and Reece, 2005).With the arrival of the world's first de facto pollutant (i.e., oxygen), approximately 3 billion years ago there evolved organisms that reductively metabolized oxygen to produce ATP in mitochondria (Rich, 2003) (i.e., aerobic respiration). Mitochondrial energymetabolism yields several reactive oxygen species (ROS) including oxygen ions (O_2^-, the primary ROS), free radicals, and peroxides (inorganic and organic). The presence of ROS produced profound consequences for life on earth, both beneficial and deleterious. For example, awealth of evidence suggests that high levels of ROS are intimately linked to the appearance of neuronal death in various neurological disorders. These include chronic diseases (Parkinson's disease or Alzheimer's disease) (Guglielmotto, 2009), acute injury of the brain (brain trauma and cerebral ischemia) (Chen et al, 2011; Valko et al, 2007), or psychiatric disorders (autism, attention deficit hyperactivity disorder, depression, and schizophrenia) (Michel et al, 2012). An increase in oxidative and nitro-oxidative stress and a decrease in the antioxidant capacity of the brain may be regarded as the important factors involved in the etiology of neuropsychiatric diseases.

An increase in oxidative and nitro–oxidative stress and a decrease in the antioxidant capacity of the brain are key factors involved in the etiology of neuropsychiatric diseases.

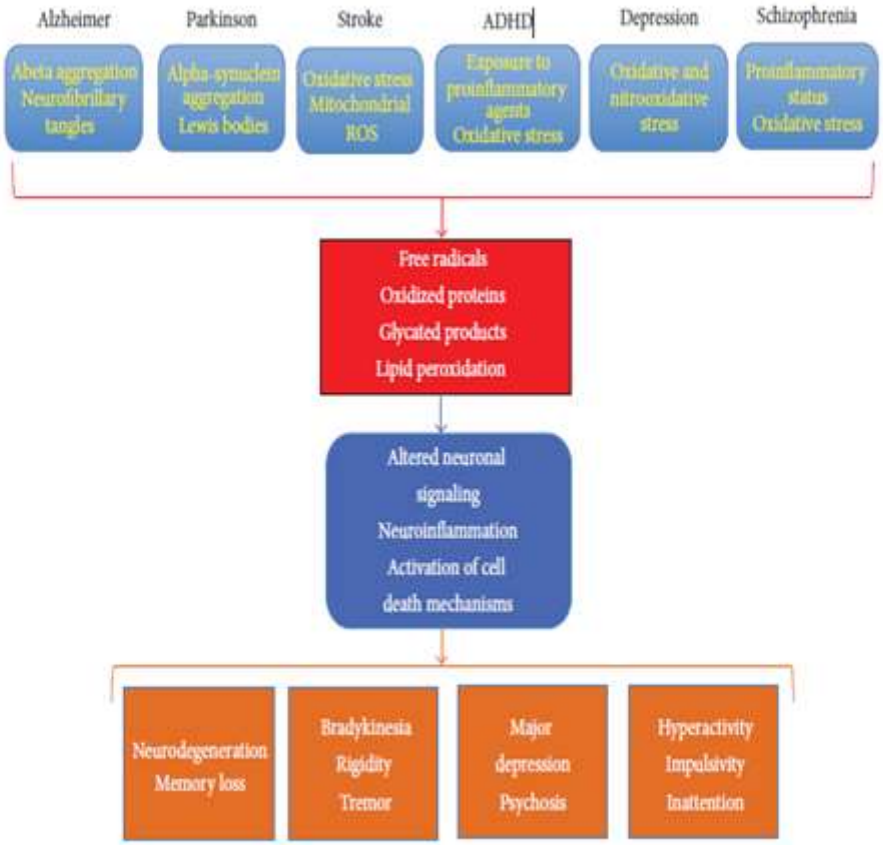

Schematic representation of oxidative stress-related mechanisms underlying disease development in Alzheimer's disease (AD), Parkinson disease (PD), stroke, attention deficit and hyperactivity disorders (ADHD), schizophrenia, and depression.

Besides the pathological states mentioned above, the generation of ROS may proceed largely shortly after the birth of mammals, as the newly born organism is suddenly exposed to much higher concentration of oxygen than in the mothers womb. Furthermore, in the brain of mammals (like the rat) which are born at relatively low level of maturation, the mitochondrial respiratory chain is not fully functional. Therefore, the possibility for the high production of ROS shortly after the birth of is high.

4.14. Lipofuscin–like pigments (LFP) as the end–products of free radical mediated membrane lipid oxidation

LFP are autofluorescent, liposoluble compounds which may be separated from cells or tissues by chloroform extraction. They represent the end–products of reactions involving free radical attack on biological molecules and can be formed, for example, in reactions between lipid peroxidation products, mainly unsaturated aldehydes, with compounds containing free

amino groups. Their characteristic emission maximum was found to be at 420–470 nm after being excited at 340–390 nm. The mechanism of their formation and chemical identity has been revealed in many in vitro studies, in which reactive aldehydes were incubated with amino group–containing molecules. Owing to their intrinsic fluorescent properties and molecular stability these products are easily measured by means of spectrofluorimetry and are used as **biomarkers of oxidative stress caused by various triggers**.

As relatively stable end–products of lipid peroxidation, LFP are good markers of free radical production and of consequent damage to lipids. Moreover, they are used not only as markers of lipid degradation but also to estimate amino acid and protein loss due to cross–linking. So far, LFP have been mostly used as robust markers of oxidative damage without defining the specific chemical identity of compounds representing these pigments. *In such cases, the fluorescent pigments are simply markers of free radical production under different circumstances.*

5. MATERIALS AND METHODS

5.1. Materials

$GABA_B$–receptor agonists baclofen (β–p–chlorophenyl–GABA), SKF97541 [3–aminopropyl (methyl) phosphinic acid] and antagonist [^{3}H]CGP54626A (41.5 Ci/mmol, cat. no. R1088) were purchased from Tocris. [^{35}S]GTPγS (1250 Ci/mmol) was from Perkin–Elmer (NEG030H). Complete protease inhibitor cocktail was from Roche Diagnostic (cat. no. 1697498). All other chemicals were of highest quality available.

All experiments were approved by Animal Care and Use Committee of the Institute of Physiology, Academy of Sciences of the Czech Republic to be in agreement with Animal Protection Law of the Czech Republic as well as European Community Council directives 86/609/EEC.

5.2. Isolation of plasma membrane–enriched fraction from rat brain cortex

The first goal of my work was to standardize the technique for preparation of Percoll–purified plasma membranes from the rat brain cortex. The first problem which I had to solve was to find an optimum compromise between the amount of protein applied per density gradient and quantity and purity of plasma membrane (PM) preparation. Application of the high amount of protein in post–nuclear fraction (PNS) resulted in PM preparation contaminated with mitochondria and lysosomes which are present in brain tissue in extraordinary high amounts. The final version of this procedure is out–lined in the following paragraph.

Rat brain cortex was minced with razor blade on pre–cooled plate and diluted in STEM medium containing 250 mM sucrose, 20 mM Tris–HCl, 3 mM $MgCl_2$, 1 mM EDTA, pH 7.6, fresh 1 mM PMSF plus protease inhibitor cocktail. It was then homogenized mildly in loosely–fitting Teflon–glass homogenizer for 5 min (2 g w.w. per 10 ml) and centrifuged for 5 min at 3500 rpm. Resulting post–nuclear supernatant (PNS) was filtered through Nylon nets of decreasing size (330, 110 and 75 mesh, Nitex) and applied on top of Percoll in Beckman Ti70 tubes (30 ml of 27.4 % Percoll in STE medium). Centrifugation for 60 min at 30000 rpm (65000 x g) resulted in the separation of two clearly visible layers (Bourova *et al.* 2009).

The upper layer represented plasma membrane fraction (PM); the lower layer contained mitochondria (MITO). The upper layer was removed, diluted 1:3 in STEM medium and centrifuged in Beckman Ti70 rotor for 90 min at 50000 rpm (175000 x g). Membrane sediment was removed from the compact, gel–like sediment of Percoll, re–homogenized by hand in a small volume of 50 mM Tris–HCl, 3 mM $MgCl_2$, 1 mM EDTA, pH 7.4 (TME medium), snap frozen in liquid nitrogen and stored at –80 °C.

5.3 Subcellular fractionation of rat brain cortex by flotation in sucrose density gradient; isolation of detergent–untreated and detergent–resistant membrane domains

The second goal of my work was to extend and test the reproducibility of the methods which were used previously in our laboratory for isolation of detergent–untreated and detergent–resistant membrane domains (DRMs). The usage of high detergent concentrations for preparation of membrane domains (Sargiacomo *et al.*, 1993; Lisanti *et al.* 1994 a, b) resulted in membrane fragments exhibiting the very low or zero agonist efficacy for stimulation of GDP/GTP exchange reaction of G proteins (Bourova *et al.*, 2003). Using other words, DRMs isolated in the presence of high detergent concentrations were inactive as far as stimulation of GPCR was involved. The same was truth when using the "alkaline–treatment" protocol based on sonication and extraction of the cell homogenate in highly alkaline solution of 0.5–1 M Na_2CO_3 (Song *et al.* 1996a, b).

According to experimental results collected over the years in our laboratory, the best of the so–far described methods/ protocols for preparation of membrane domains is that of Smart *et al.* (1995, 1999). The views what the term *membrane domains* actually means from methodological, structural and functional point of view were reviewed by Pike (2004). The sometimes controversial viewpoints about the size and physiological meaning of *membrane domains* were expressed by Pike (2006a, b) and Shaw (2006).

The disadvantage of the method of Smart *et al.* (1995, 1999) using the sequence of three types of density gradients is, however, the very low amount of protein recovered in the final preparation of pure "domains" – about 0.2–0.5% of the original amount present in the starting material, i.e. the cell homogenate. Therefore, when trying to find some compromise between purity and quantity of the final preparation, centrifugation in Percoll gradient was followed by the "flotation" in sucrose density gradient.

Plasma membrane enriched fraction was prepared from the rat brain cortex by

centrifugation at 116,000xg for 35 min in Percoll^{R} gradient (Beckman Ti60 rotor) as described in Methods (compare with **Figs. 10** and **11**) and subsequently, the low–density membrane fragments (LPM) were separated from the bulk of plasma membranes (BPM) by flotation in a step–wise 15/20/25/30/35/40% w/v sucrose gradient (Roubalova *et al.*, 2009). The protein profile of sucrose density gradient was clearly dependent on detergent concentration (**Fig. 23** and **24**): when increasing detergent concentration, the PM band recovered in the lower part of centrifugation tube (at zero concentration of the detergent) was transferred up, towards the low–density end of the gradient.

Measurement of functional activity of $GABA_B$–R as baclofen–stimulated, high–affinity [^{35}P]GTPase (**Fig. 20**) indicated the best results when using 0.025% or 0.05% w/v Brij58. At these concentrations, the baclofen–stimulated, high–affinity [^{35}P]GTPase in DRMs was comparable with that in detergent–untreated PM. Based on these results, the 5 main areas of the sucrose density gradient were distinguished: **area I**, the top of gradient containing no protein; **area II**, low–density PM fragments; **area III**, plasma membranes (PM); **area IV**. An intermediate area between PM band and gradient pellet; **area V**, gradient pellet containing PM fragments exhibiting the higher density than 40% w/v sucrose (**Fig. 23**). Reproducibility of the sucrose density gradient profiles obtained after flotation of detergent–untreated samples was satisfactory (**Fig. 24**).

Fig. 22 Preparation of detergent resistant membrane domains (DRMs) from rat brain cortex by extraction of Percoll–purified plasma membranes at low detergent concentrations; *dependence on detergent / protein ratio*

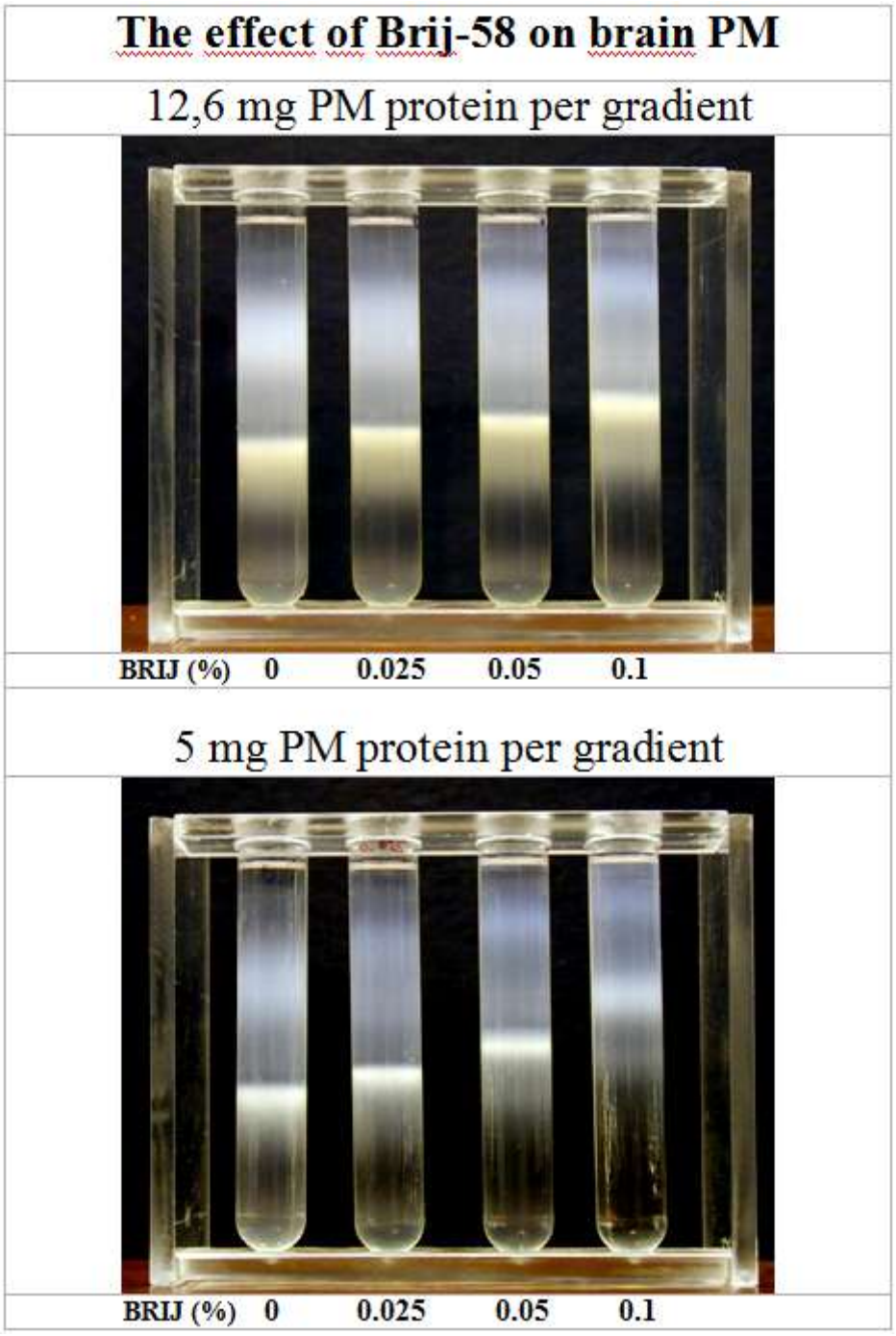

Fig. 23 **Preparation of functional DRMs from rat brain cortex by extraction of Percoll–purified plasma membranes at low detergent concentrations;** *the five main area sucrose density gradient*

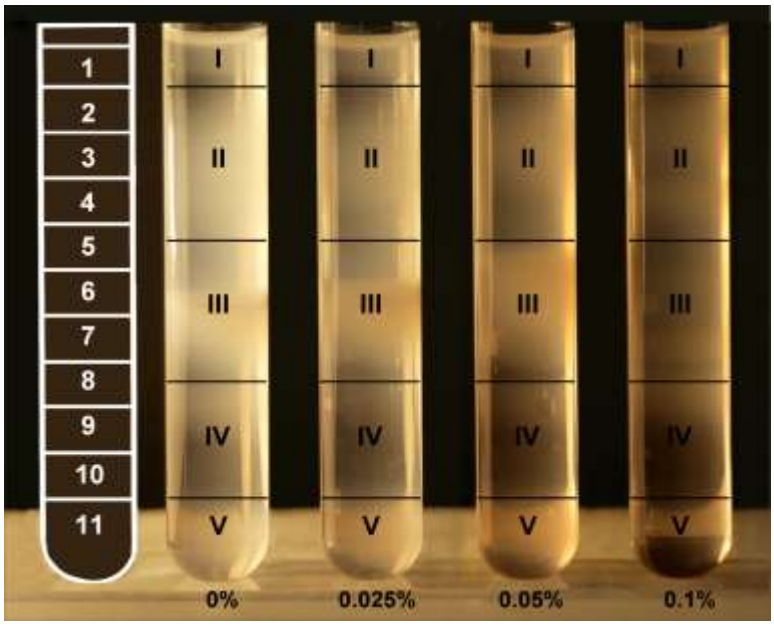

Fig. 24 **Reproducibility of sucrose density gradients profiles;** *fractionation of rat brain cortex under the detergent–free conditions*

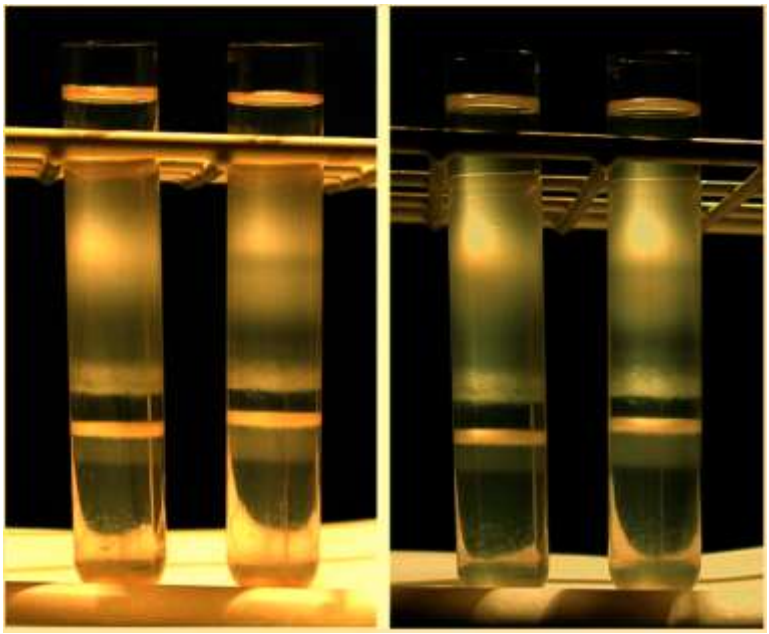

As demonstrated in **Fig. 25**, I have also tested the effect of the short–term ultrasound exposure (sonication) of 5s, 10s and 20s duration on distribution of PM fragments in flotation sucrose density. The short–term sonication resulted in an alteration of distribution of PM fragments: the broad distribution of PM fragments visualized as a wide band in the lower part of cuvette was transformed into the narrow, more restricted distribution pattern. To avoid this effect, I have not used sonication for subcellular fractionation of rat brain tissue and preparation of LDM and PM.

Fig. 25 Effect of the short–tem sonication on macroscopical profile of sucrose density gradient

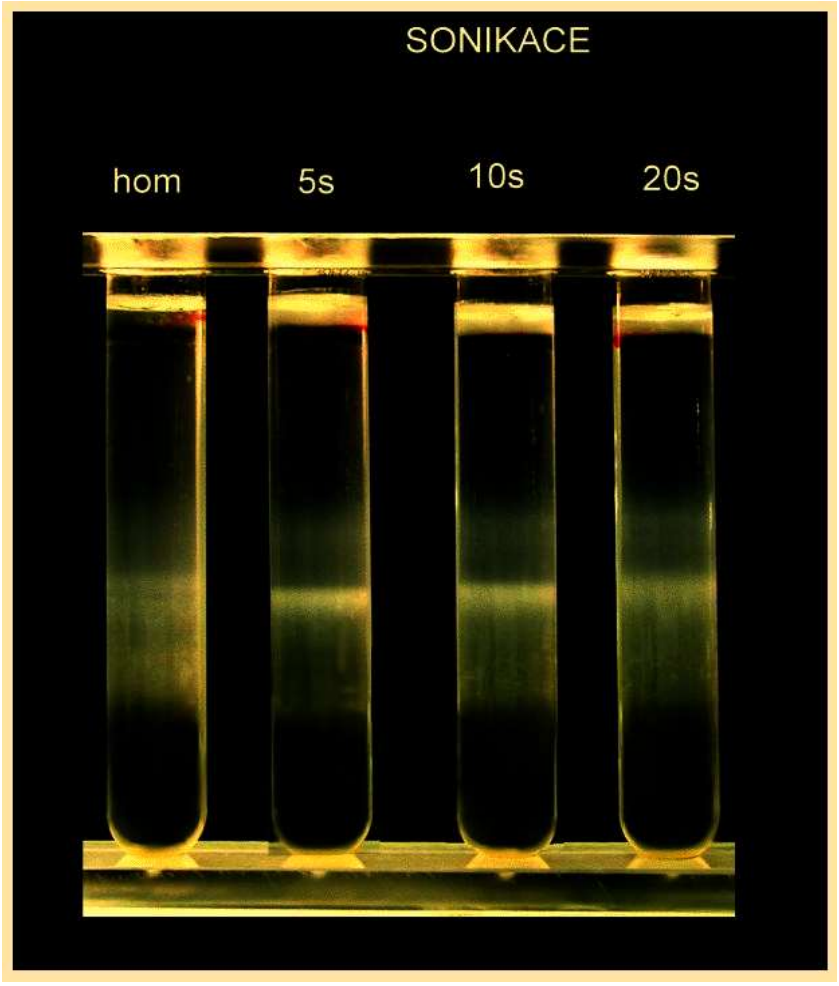

5.4. Agonist–stimulated [^{35}S]GTPγS binding; *dose–response curves*

Measurement of agonist–stimulated, high–affinity binding of non–hydrolysable analog of GTP, [^{35}S]GTPγS, represents a general and widely used method for determination of the effect of GPCR agonists on G protein activity. This method is based on agonist–induced exchange of GDP for GTP. The radioactive analog of GTP enters the ligand binding pocket within the short time–period when it is opened after interaction of G protein with agonist–bound, i.e. activated receptor. However, in natural tissues such as brain, the high basal level [^{35}S]GTPγS binding exists in the absence of GDP and this type of binding is not effected by agonist (**Fig. 27**). The strategy how to reveal the agonist–stimulated component of [^{35}S]GTPγS binding is to mimic the conditions in living cell most closely. That means to include GDP in reaction mix (i.e. in assay buffer) and, by means of increasing GDP concentration, to reveal the high–affinity component which responds to a given agonist. This component is otherwise hidden in the overall [^{35}S]GTPγS binding.

Fig. 26 Dependence of [^{35}S]GTPγS binding to the brain cortex PM on GDP concentration

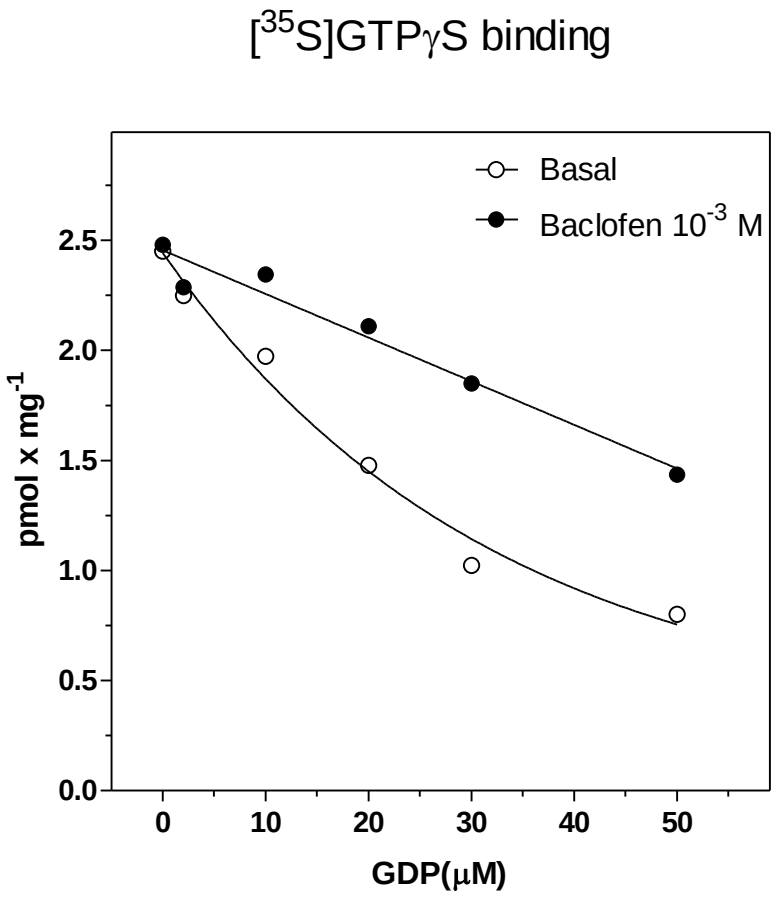

Based on results presented in **Fig. 26**, I have chosen the 20 μM concentration of GDP as that one, which will be included in [^{35}S]GTPγS binding assay mix in my studies of ontogenetic development of functional coupling between $GABA_B$–R and the cognate G proteins in rat brain cortex. At this GDP concentration, baclofen–stimulation of the basal level of [^{35}S]GTPγS binding was much higher than in previous studies of detergent–untreated PM (**Fig. 21**) which were performed in our laboratory. Therefore, the measurement of functional activity of $GABA_B$–R by determination of baclofen–stimulated, high–affinity [^{35}S]GTPγS binding, could be measured with higher accuracy.

Membranes prepared from 2–, 14– and 90–day–old rats of selected ages were incubated with (total binding, B_{total}) or without (basal binding, B_{basal}) increasing concentrations of $GABA_B$–R agonists baclofen and SKF97541 (10^{-10}–10^{-3} M) in final volume of 100 μl of reaction mix containing 20 mM HEPES, pH 7.4, 3 mM $MgCl_2$, 100 mM NaCl, 20 μM GDP, 0.2 mM ascorbate and [^{35}S]GTPγS (about 100–200,000 dpm per assay) for 30 min at 30 °C. The binding reaction was terminated by dilution with 3 ml of ice–cold 20 mM HEPES, pH 7.4, 3 mM $MgCl_2$ and filtration through Whatman GF/C filters on Brandel cell harvester. Radioactivity remaining on the filters was determined by liquid scintillation using Rotiszcint Eco Plus cocktail. Non–specific binding was determined in parallel assays containing 10 μM unlabelled GTPγS. Data were analyzed by GraphPad Prism 4 (GraphPad Software, San Diego, CA, USA) and B_{basal}, B_{max} and EC_{50}, values calculated according to the method of least–squares by fitting the data with sigmoidal dose–response curve.

5.5. Agonist–stimulated [^{35}S]GTPγS binding; one–point assay

With the aim to screen PM prepared from all age intervals under the same assay conditions, membranes (20 μg protein per assay) were incubated with ($B_{agonist}$) or without (B_{basal}) 1 mM baclofen or 100 μM SKF97541 in final volume of 100 μl of reaction mix containing 20 mM HEPES, pH 7.4, 3 mM $MgCl_2$, 20 μM GDP, 0.2 mM ascorbate and [^{35}S]GTPS (1–2 nM) for 30 min at 30 °C. The binding reaction was discontinued by dilution with 3 ml of ice–cold 2 mM HEPES, pH 7.4, 0.15 mM $MgCl_2$ and immediate filtration through Whatman GF/C filters on Brandel cell harvester. Radioactivity remaining on the filters was determined by liquid scintillation using Rotiszcint Eco Plus cocktail. Non–specific

GTPγS binding was determined in parallel assays containing 10 μM GTPγS. The binding data were analyzed by GraphPad Prism 4 and represent an average ± S.E.M. of 3 experiments.

5.6. [^{3}H]CGP54626A binding; saturation binding study

Membranes (100 μg protein per assay) were incubated with increasing concentrations of $GABA_B$–antagonist [^{3}H]CGP54626A (0.06–36.8 nM) in final volume of 100 μl of binding mix containing 50 mM Tris–HCl (pH 7.4) plus 2.5 mM $CaCl_2$ for 60 min at 30 °C. The bound and free radioactivity was separated by filtration through Whatman GF/B filters in Brandel cell harvestor. Filters were washed 3x with 3 ml of ice–cold incubation buffer and radioactivity remaining and placed in 5 ml of scintillation cocktail (Rotiszint Eco Plus). The non–specific binding was determined in the presence of 1 mM GABA in binding mix. Data were analyzed by GraphPad Prism 4 and K_d and B_{max} values calculated according to the method of the least–squares by fitting the data with rectangular hyperbola.

5.7. Na^+/K^+–ATPase; *[^{3}H]ouabain binding*

Sodium plus potassium–activated, oubain–dependent Na^+/K^+–ATPase (E.C. 3.6.1.3) was determined by "one–point" [^{3}H]ouabain binding assay according to Svoboda *et al.* (1988). Membranes (50 μg of protein) were incubated with 20 nM [^{3}H]ouabain in a total volume of 0.45 ml of 5 mM $NaHPO_4$, 5 mM $MgCl_2$, 50 mM Tris–HCl, pH 7.6 (Mg–Pi buffer) for 90 min at 30 ºC. The bound and free radioactivity was separated by filtration through Whatman GF/B filters in Brandel cell harvester. Filters were washed 3× with 3 ml of ice–cold incubation buffer and placed in 4 ml of scintillation cocktail (CytoScint, ICN). Radioactivity remaining on filters was determined after 10 h at room temperature by liquid scintillation. Non–specific binding was determined in the presence of 1 μM unlabelled ouabain.

5.8. Protein determination

The method of Lowry was used for determination of membrane protein (Lowry et al, 1951). Bovine serum albumin (Sigma, Fraction V) was used as standard. Data were calculated by fitting the data with calibration curve as quadratic equation.

5.9. Measurement of lipofuscin like pigments

The technique described by Goldstein and McDonagh (Goldstein and Mc Donagh, 1976), modified in (Wilhelm and Herget, 1999), was used for the analysis of LFP in brain

homogenates. Approximately 30 mg of frozen brain sample was weighed, chopped to fine pieces, and transferred into a glass–stoppered test tube containing 6 ml of chloroform–methanol mixture (2:1, v/v). After 1–h extraction on a motor–driven shaker, 2 ml of double distilled water was added, the sample was agitated, and the ensuing mixture was centrifuged (400 g, 10 min). After centrifugation, the lower chloroform phase was separated and used for measurement of fluorescence.

Fluorescence excitation and synchronous spectra were measured in Aminco–Bowman 2 spectrofluorometer. Recordings and analysis was performed by AB–2 computer program, which was also used for organization of the spectra into tridimensional spectral arrays. The *excitation spectra* were measured in the range of 250–400 nm for emission adjusted between 400 and 500 nm in steps of 10 nm. The quantitative estimation of LFP was based on excitation and emission maxima found in tridimensional spectral arrays. The three major fluorophores F325/380, F335/410, and F355/440 (excitation/emission, nm) were identified. The fluorometer was calibrated based on the standard No. 5 of the instrument manufacturer, and the LFP concentration was expressed in arbitrary units per mg tissue wet weight. The statistical evaluations were made using ANOVA with Scheffe post–hoc test, and the results are shown as means ± SEM. The synchronous *emission spectra* were measured in the range of 350–550 nm, with a constant difference of 50 nm between excitation and emission wavelengths. Their second derivatives were obtained using the AB–2 software.

5.10. HPLC analysis

Brain chloroform extracts were evaporated under the stream of nitrogen. The evaporated sample was dissolved in approximately 1 ml of running phase used in isocratic HPLC separation. A mixture of acetonitrile–methanol– water (50:10:40, v/v) was used for separation of LFP. A Jasco HPLC instrument equipped with fluorescence detector was set at the excitation and emission maxima of the three major fluorophores. A C18 column (4 x 250 mm) was used for the analysis. Isocratic elution gave optimum separation at 0.2 ml/min.

6. RESULTS

6.1. The ontogenetic development of $GABA_B$–receptor signaling cascade

6.1.1. Functional coupling of $GABA_B$–R with G proteins

The efficacy (maximum of G protein response) and potency (affinity of G protein response) of $GABA_B$–receptors in plasma membranes isolated from brain cortex of 2–, 14– and 90–days old rats was determined as baclofen– and SKF97541–stimulated, high–affinity [^{35}S]GTPγS binding in the presence of 20 μM GDP. The addition of 20 μM GDP into the assay mix was necessary to suppress the high basal level of binding of this non–hydrolysable analog of GTP with the aim to reveal the agonist–stimulated component of G protein activity (compare with **Fig. 26**). Dose–response curves were measured in 0.1 nM–1 mM range of baclofen or SKF97541 concentrations and the significance of difference among PM prepared from 2–(PD2), 14– (PD14) and 90–days (PD90) old rats was analyzed by one–way ANOVA followed by Bonferroni's *post–hoc* comparison test using GraphPad Prism 4 software.

Surprisingly, baclofen exhibited the significant ability to increase the basal level of [^{35}S]GTPγS binding measured in the absence of agonist (B_{basal}) already in 2–day–old animals (PD2). This ability was further increased in the course of the first two weeks of postnatal life (**Fig. 27**), but virtually unchanged when viewed over the whole period of brain development as the averaged dose–response curve measured in 2–days–old animals was not significantly different from that measured in adult rats (90–days old). The basal level of [^{35}S]GTPγS binding was also significantly increased between PD2 and PD14 and subsequently decreased to the adult level. The same result applied to the net–increment of agonist stimulation expressed as the difference between baclofen–stimulated and the basal level of [^{35}S]GTPγS (**Table 1**). The % of baclofen–stimulation over the basal level of binding was unchanged.

The developmental alteration of dose–response curves of SKF97541–stimulated [^{35}S]GTPγS binding, analyzed in an independent set of PM preparations, was similar to that of baclofen, however, a substantial difference between the two agonists was also noticed. SKF97541 exhibited the significant ability to increase the basal level of [^{35}S]GTPγS binding already in 2–day–old animals. The maximum response of SKF97541 was increased between PD2 (B_{max} = 1.13 pmol x mg^{-1}) and PD14 (B_{max} = 1.51 pmol x mg^{-1}) and further development was reflected in decrease of SKF97541–stimulated [^{35}S]GTPγS binding to the level in 90–days–old animals (B_{max} = 1.08 pmol x mg^{-1}), which was not significantly different from that in 2–days–old animals.

The significant difference, however, was observed when comparing the basal level of binding in 2–days–old (B_{basal} = 0.83 pmol x mg^{-1}), 14–days–old (B_{basal} = 1.02 pmol x mg^{-1}) and 90–days–old (B_{basal} = 0.66 pmol x mg^{-1}) animals: PD2 versus PD14, $p<0.01$, **; PD14 versus PD90, $p<0.01$,**; PD2 versus PD90, $p<0.01$,** (**Table 1).** The % of SKF97541–stimulation over the basal level was unchanged. Comparison of SKF97541– and baclofen–stimulated [^{35}S]GTPγS binding data indicated, that usage of different animals for preparation of PM was associated with the difference in the basal level of binding in the absence of agonist.

The potency (EC_{50} values) of G protein response to baclofen was not significantly different in membranes prepared from 2–, 14– and 90–day–old rats, but decreased from the birth to adulthood in the case of SKF97541 (**Table 1**). This finding was compatible with electrophysiological studies of brain maturation indicating an altered sensitivity to different $GABA_B$–R agonists in the course of brain development (Bernasconi *et al.* 1992, Hosford *et al.* 1992, Marescaux *et al.* 1992, Lin *et al.* 1993, Kubová *et al.* 1996, Mareš 2008).

Fig. 27 Dose–response curves of baclofen and SKF97541–stimulated [^{35}S]GTPγS binding in PM isolated from 2–, 14– and 90–day–old rats

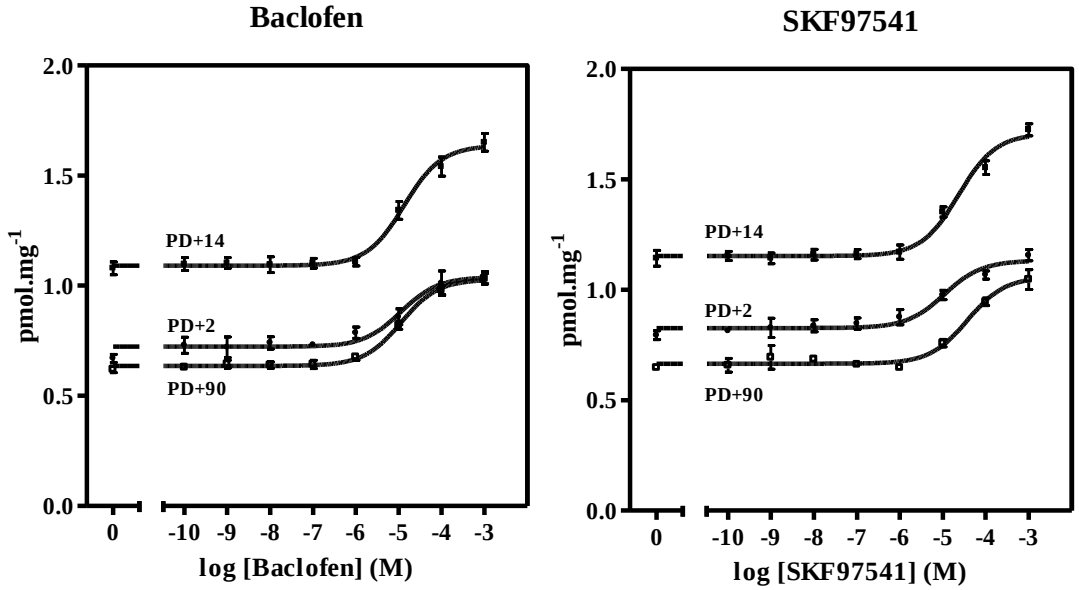

Legend to Fig. 27. PM were isolated in parallel from brain cortex of 2 (●)–, 14 (○)– and 90 (■)–days–old rats and the high–affinity [^{35}S]GTPγS binding was measured in the presence of

increasing concentrations of $GABA_B$–R agonists (–)–baclofen (left) or (–)–SKF97541 (right panel) in different age groups as described in Methods. The binding data were fitted by sigmoidal dose–response curves using GraphPad *Prism 4* and represent the average of three experiments ± S.E.M. Differences between the averaged dose–response curves corresponding to PM prepared from 2–(PD2), 14–(PD14) and 90–days (PD90) old rats were statistically analyzed by one–way ANOVA followed by Bonferroni's post–hoc comparison test. The results of this analysis are presented in **Table1.**

Table 1. Maximum response (B_{max}) and affinity (EC_{50}) of baclofen– and SKF97541–stimulated [^{35}S]GTPγS binding in PM isolated from 2–, 14– and 90–days old rats.

A(–)–baclofen	**2–days**	**14–days**	**90–days**
Bbasal	0.72 ± 0.01	1.09 ± 0.02	0.64 ± 0.01
Bmax	1.04 ± 0.03	1.64 ± 0.03	1.03 ± 0.01
Bmax – Bbasal	0.31	0.62	0.40
100 x Bmax / Bbasal	152 %	152 %	166 %
EC_{50} (μM)	9.00 (4.46–18.15)	13.35 (7.80–22.85)	13.26 (9.96–17.65)
B(–)–SKF97541			
Bbasal	0.83 ± 0.01	1.15 ± 0.01	0.66 ± 0.01
Bmax	1.13 ± 0.02	1.71 ± 0.02	1.08 ± 0.02
Bmax – Bbasal	0.30	0.49	0.42
100 x Bmax / Bbasal	142 %	152 %	168 %
EC_{50} (μM)	9.79 (5.30–18.10)	23.40 (14.31–38.25)	36.51 (21.87–60.95)

B_{basal} (pmol · mg^{-1}), binding in the absence of agonist; B_{max} (pmol · mg^{-1}), binding at saturating agonist concentration; = B_{max} – B_{basal}, net–increment of agonist stimulation; 100 x B_{max} / B_{basal}, % stimulation of the basal level by agonist. EC_{50} (μM), agonist concentration inducing half–maximum stimulation (95 % confidence

limit). B_{max}, B_{basal} and EC_{50} values were determined by analysis of the sigmoidal dose–response curves of baclofen– (**A**) and SKF97541– (**B**) stimulated [^{35}S]GTPγS binding presented in Figure 1 by GraphPad Prism 4 and represent the average of three experiments ± S.E.M. The significance of difference between B_{basal}, B_{max} and EC_{50} values in PM prepared from 2 (PD2)–, 14 (PD14)– and 90 (PD90)–days–old rats was determined by one–way ANOVA followed by Bonferroni's *post–hoc* comparison test.

The significance of difference between Bbasal, Bmax and EC50 values in PM prepared from 2 (PD2)–, 14 (PD14)– and 90 (PD90)–days–old rats was determined by one–way ANOVA followed by Bonferroni's post–hoc comparison test.

A (baclofen).

Bbasal (PD2 versus PD14, p<0.0001, ***; PD14 versus PD90, p<0.0001, ***; PD2 versus PD90, p>0.05, not significant. **Bmax** (PD2 versus PD14, p<0.001, ***; PD14 versus PD90, p<0.001, ***; PD2 versus PD90, p>0.05, not significant. **EC50** (PD2 versus PD14, p>0.05, NS; PD14 versus PD90, p>0.05, NS; PD2 versus PD90, p>0.05, NS.

B (SKF97541).

Bbasal (PD2 versus PD14, p<0.0001, ***; PD14 versus PD90, p<0.0001, ***; PD2 versus PD90, p=0.0022, **. **Bmax** (PD2 versus PD14, p<0.0001, ***; PD14 versus PD90, p<0.0001, ***; PD2 versus PD90, p>0.05, NS. **EC50** (PD2 versus PD14, p>0.05, NS; PD14 versus PD90, p>0.05, NS; PD2 versus PD90, p<0.01, **).

Determination of the dose–response curves of baclofen– and SKF9754–stimulated [^{35}S]GTPγS binding in 1–, 15– and 90–days old rats was followed by the detailed analysis of ontogenetic profile of agonist–stimulated G protein activity in fetuses (–1) and in PM prepared from 1–, 2–, 4–, 5–, 9–, 10–, 14–, 15–, 25–, 30–, 35–, 42–, 47– and 90–days old rats. Data presented in **Fig. 28** indicated clearly the existence of maximum of baclofen– and SKF97541–stimulated G protein activity at PD14 and PD15. Baclofen–stimulated, SKF9754–stimulated and the basal level of [^{35}S]GTPγS binding in adult animals were not significantly different from those detected in 2–days–old animals (PD2). Accordingly, the peak value of [^{3}H]GABA binding was detected at PD14 in rat brain cortical slices by quantitative autoradiography and this high level of [^{3}H]GABA binding subsequently declined to the adult level (Turgeon and Albin 1994).

Fig. 28 Baclofen– and SKF97541–stimulated [^{35}S]GTPγS binding; *one–point assay*

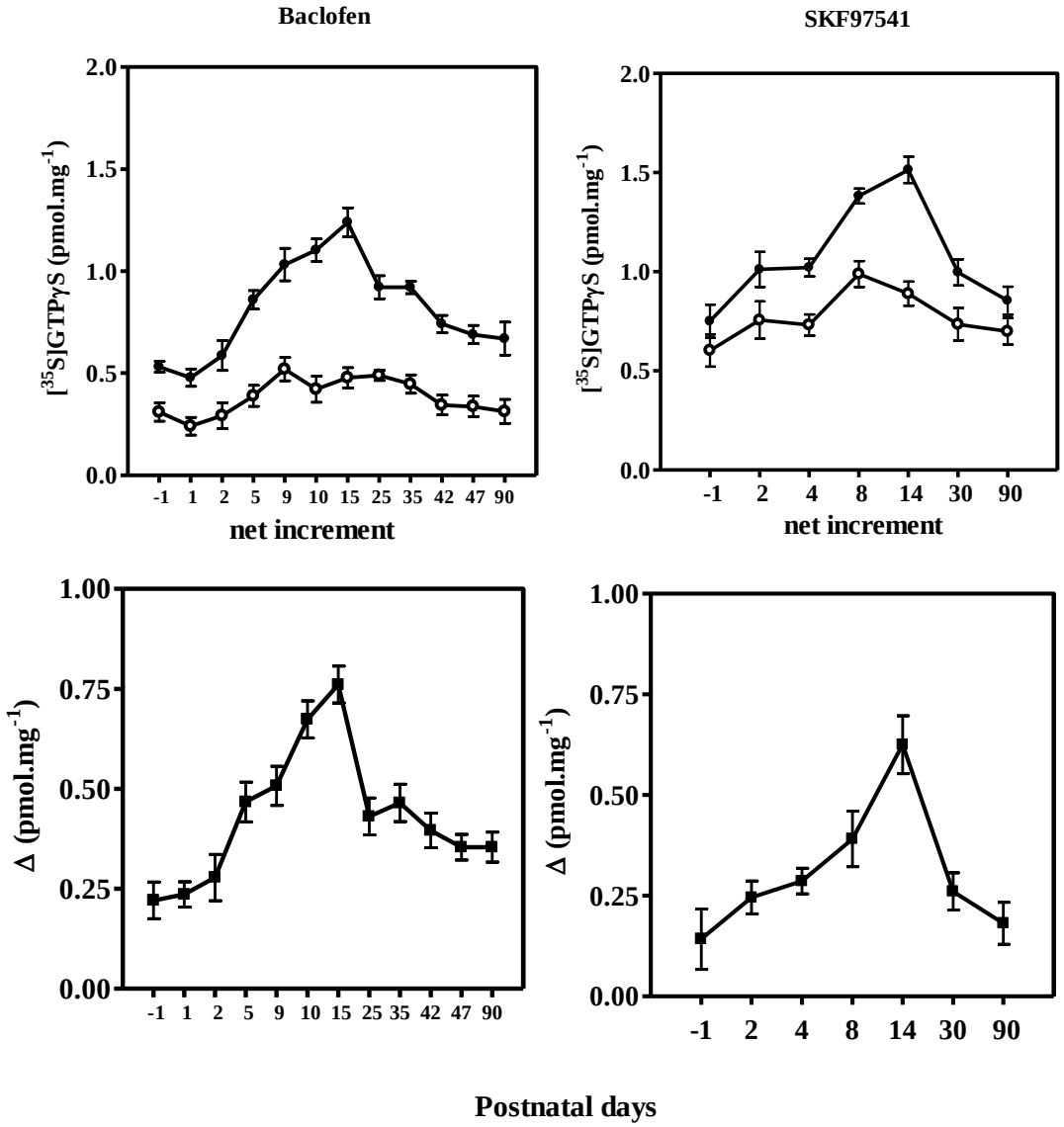

Legend to Fig. 28.

Upper panels. PM were isolated from fetuses (–1) and from 1–, 2–, 4–, 5–, 8–, 9–, 10–, 14–, 15–, 25–, 30–, 35–, 42–, 47– and 90–days old rats, frozen in liquid nitrogen and used only once. Baclofen– and SKF97541–stimulated [^{35}S]GTPγS binding was determined in different age groups as described in Methods in the presence (●, $B_{agonist}$) or absence (○, B_{basal}) of 1 mM baclofen (left) or 100 μM SKF97541 (right panel).

The significance of difference between the two sets of data ($B_{agonist}$ versus B_{basal}) at all age intervals was analyzed by Student s t–test using GraphPad Prism 4: baclofen, $p < 0.001$, ***; SKF97541, $p < 0.0022$, **. The same type of comparison ($B_{agonist}$ versus B_{basal}) was also performed at individual age intervals: **baclofen** [day –1 (*), PD2 (**), PD5(***), PD9(***),

$^{+}$10(***), PD15(**), PD25(***), PD35(****), PD42(***), PD47(**), PD90(***)]. **SKF97541** [day –1 (NS), PD2 (NS), PD4(*), PD8(*), PD14(**), PD30(NS), PD90(NS)].

Lower panels. Difference between agonist–stimulated ($B_{agonist}$) and basal ($B_{basal\ )}$ level of binding was expressed as the net–increment of agonist stimulation $\Delta = B_{agonist} - B_{basal}$. Data represent the average ± S.E.M. of three experiments.

The existence of the sharp maximum of $GABA_B$–R agonist–stimulated [^{35}S]GTPγS binding at PD15 and PD14 **(Fig. 28)** was fully consistent with our previous data indicating the striking maximum of basal, manganese–, fluoride– and forskoline–stimulated AC activity in 12–day–old rats (Ihnatovych *et al.* 2002). Thus, the increase of baclofen– and SKF97541–stimulated G protein activity during the first two weeks of postnatal life, its maximum in 14–15–day–old rats and the subsequent decrease is correlated in time with the maximum of AC activity. The question to what extend the maximum of AC activity observed at PD12 precedes the peak of activity of G proteins can not be decided at the present stage of our experimentation, as AC activity was determined at PD12 and PD18 only, i.e. not in the period between these two age intervals.

6.1.2 Number and affinity of $GABA_B$–R; *direct saturation binding study with antagonist [^{3}H]CGP54626A*

Plasma membrane density of $GABA_B$–R at different age intervals was determined by saturation binding study with specific antagonist [^{3}H]CGP54626A. Data presented in **Fig. 29** indicated clearly that the highest PM density of $GABA_B$–R, estimated as the maximum binding capacity (B_{max}) of [^{3}H]CGP54626A binding sites, was detected in PM samples prepared from 1–day–old rats (2.27±0.08 pmol · mg^{-1}). The further development was reflected in a marked decrease of [^{3}H]CGP54626A binding as the B_{max} values of 1.38±0.05 and 0.93±0.04 pmol · mg^{-1} were determined in PM isolated from 13– and 90–days old rats, respectively. The dissociation constant (K_d) was increased from 11.8 nM (PD1) to 15.3 nM (PD13) and 22.1 nM (PD90), indicating the decreased affinity and qualitative change of $GABA_B$–R binding sites towards this antagonist in the course of rat brain cortex maturation. The decrease in affinity of [^{3}H]CGP54626AA binding (expressed as 1 / K_d), observed together with the decrease in affinity of SKF97541–response of G proteins (**Fig. 27**), suggests a partial agonistic nature of [^{3}H]CGP54626AA interaction with $GABA_B$–R which would be altered in the course of brain cortex ontogenesis.

Fig. 29. Saturation of [^{3}H]CGP54626AA binding sites in PM isolated from 1–, 13– and 90–day–old rats

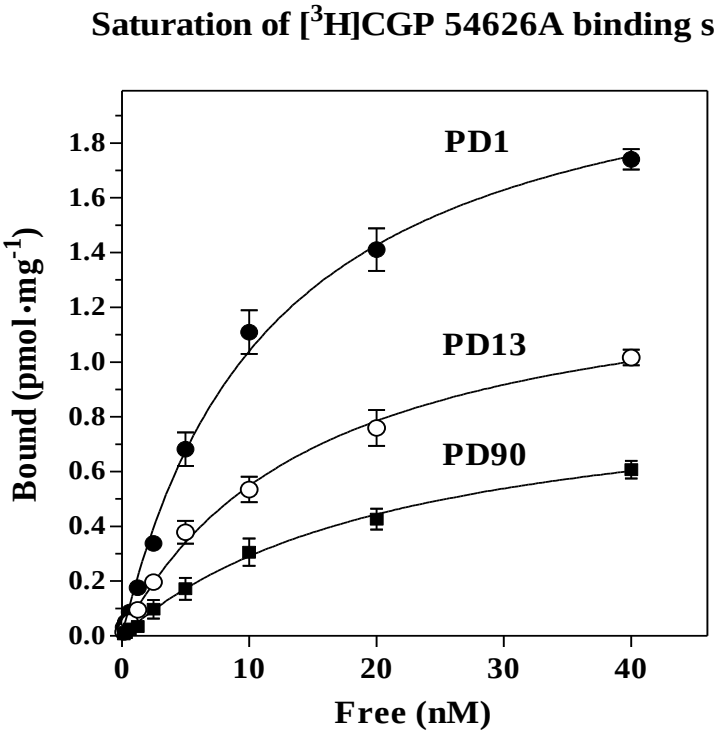

Legend to Fig. 29. Maximum number (B_{max}) and affinity (K_d) of specific [^{3}H]CGP54626AA binding sites was determined in PM isolated in parallel from brain cortex of 1 (●)–, 13 (○)– and 90 (■)–days old rats by direct saturation binding assay as described in Methods. B_{max} (maximum binding capacity) and K_d (dissociation constant) of specific [^{3}H]CGP54626AA binding sites were calculated by fitting the data by 1–site hyperbola by GraphPad *Prism 4* and represent the average ± S.E.M. of 3 experiments. One–way ANOVA followed by Bonferroni's post–hoc comparison test was used for statistical analysis of the difference between B_{max} or K_d values in PM prepared from rats of different ages. **B_{max}** : PD1 versus PD13, $p < 0.01$, **; PD13 versus PD90, $p < 0.001$, ***; PD13 versus PD90, $p < 0.05$, *. **K_d** : PD1 versus PD13, $p > 0.05$, NS; PD13 versus PD90, $p < 0.01$, **; PD13 versus PD90, $p < 0.05$, *.

6.1.3. Ontogenetic development of sodium plus potassium activated, ouabain dependent Na^+/K^+–ATPase (EC 3.6.1.3)

Postnatal development of $GABA_B$–R–G protein coupling and antagonist ligand binding to $GABA_B$–R was substantially different from maturation of the prototypical plasma membrane marker, Na^+/K^+–ATPase (**Fig. 30A, B**). Membrane density of Na, K–ATPase, determined by immunoblotting with specific antibodies oriented against the affinity purified α–subunit of this enzyme, was low around the at birth (PD–1, PD1 and PD2) and further development was reflected in a marked increase of this protein. The major increase occurred between the birth and PD25. Since this age interval, PM content of Na, K –ATPase was not significantly different in PM isolated from 35–, 42– and 90–day–old rats.

The intensity of average immunoblot signal in adult rats (PD90) was 3.5–times higher than around the birth, i.e. in PM samples prepared from foetuses 1–day before the birth or from 1– and 2–days–old animals (PD1 and PD2). This result indicated a marked increase of plasma membrane density of Na,K–ATPase molecules in the course of brain cortex development.

Virtually the same result was obtained when selective inhibitor [^{3}H]ouabain was used for determination of the number of Na^+/K^+–ATPase molecules in PM (**Fig. 30C**). The major increase of [^{3}H]ouabain binding in PM was noticed between the birth and PD25. Since PD25, the binding of this radioligand was not significantly different from the adult animals. [^{3}H]ouabain binding in 90–day–old rats (13.89 pmol.mg^{-1}) was 1.6x higher than in 15–day–old rats (8.64 pmol.mg^{-1}) and 2.6x higher than in fetuses 1 day before the birth (5.44 pmol.mg^{-1}).

Thus, the postnatal development of plasma membrane density of Na^+/K^+–ATPase molecules proceeded in completely different way when compared with maturation of $GABA_B$–R signaling cascade. The highest number of $GABA_B$–R was observed around the birth and further development was reflected in 2.4–fold decrease of $GABA_B$–receptor binding sites for specific antagonist [^{3}H]CGP54626AA while the amount of Na^+/K^+–ATPase molecules was increased ≈3–fold between the birth and adulthood (90–days old rats).

Fig. 30 Plasma membrane density of Na^+/K^+–ATPase determined by immunoblot analysis (A, B) and [^{3}H]ouabain binding (C)

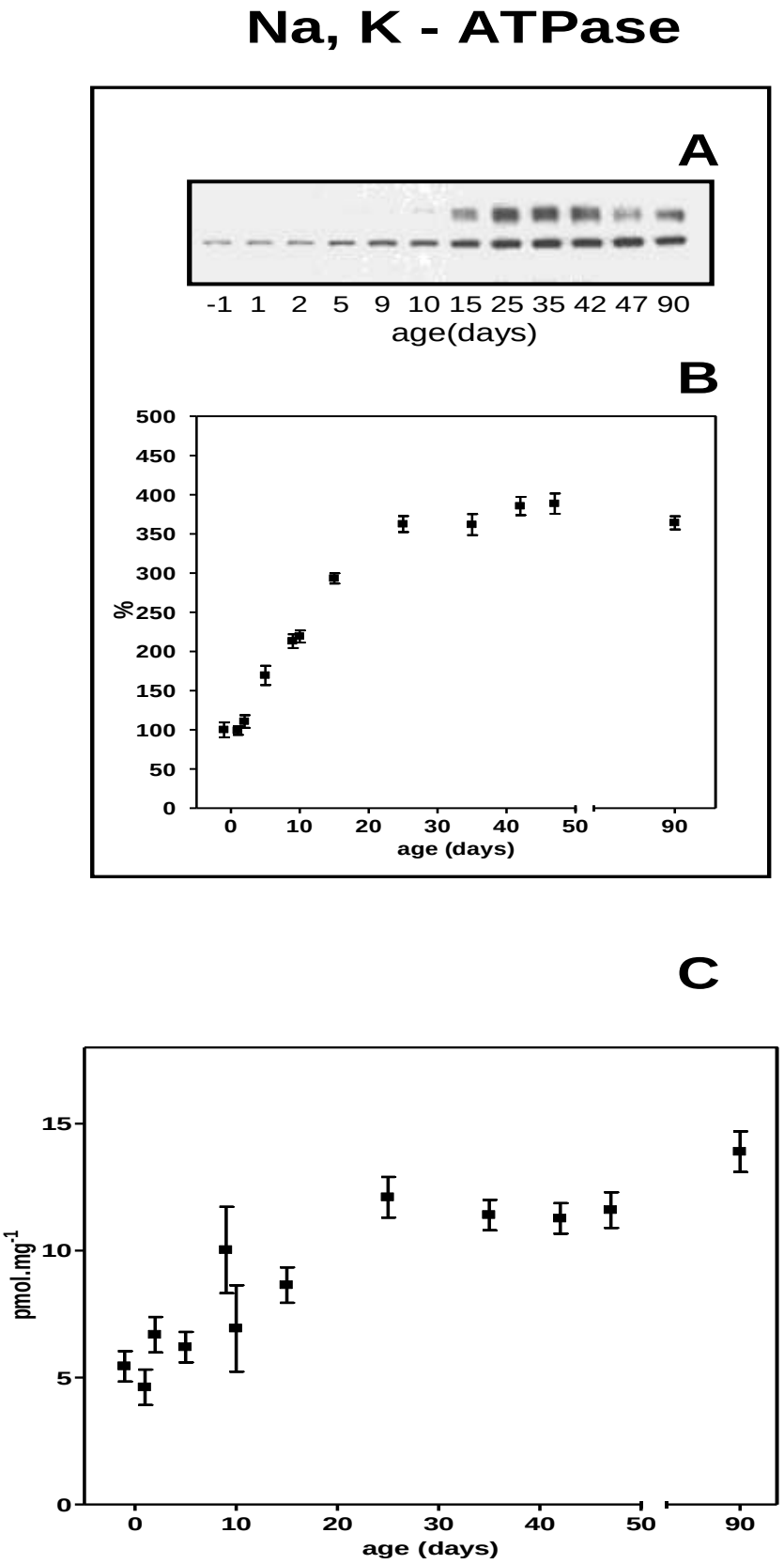

Immunoblot detection of α–subunit of Na^+/K^+–ATPase was performed by polyclonal Ab (Santa Cruz, sc–28800). **(A)** Typical immunoblot. **(B)** Average of 5 immunoblots. The significance of the difference between the immunoblot signal determined in fetuses 1–day before the birth (100%) and signals determined at different ages (PD1, PD2, PD5, PD9, PD10, PD15, PD25, PD35, PD42, PD47, PD90) was analyzed by one–way ANOVA followed by Bonferroni's test using GraphPad Prism 4. Since PD5, the increase of Na^+/K^+–ATPase was highly significant (**, $p < 0.01$). **(C)** [^{3}H]ouabain binding was measured as described in Methods. Data represent the average ± S.E.M. of three experiments performed in triplicates. Significance of the difference between the binding at different age intervals was analyzed by one–way ANOVA followed by Bonferroni's test: fetuses D–1 versus PD15 (*, $p<0.05$), D–1 versus PD25 (**, $p<0.01$), D–1 versus PD90 (**, $p<0.01$), PD15 versus PD25 (*, $p<0.05$), PD15 versus PD90 (**, $p<0.01$), PD25 versus PD90 (NS, $p>0.05$).

6.2. The ontogenetic development of oxidative damage of the brain; *generation of lipofuscin–like pigments (LFP)*

6.2.1. Study of lipofuscin–like pigments in brain tissue homogenates.

The aim of our first study of LFP production in rat brain (Wilhelm at al., 2011) was to get information about free oxygen radical damage proceeding in rat rain cortex before and shortly after the birth. We have also analyzed the whole postnatal period up to the postnatal–day–90 (PD90). Our studies were performed with the tissue homogenates prepared from animals of different ages: *group A*, 7 days before birth; *group B*, 1 day before birth; *group C*, postnatal day 1; *group D*, postnatal day 2; *group E*, postnatal day 5; *group F*, postnatal day 10; *group G*, postnatal day 15; *group H*, postnatal day 25; *group I*, postnatal day 35; *group J*, 90–days–old animals. For a detailed characterization of fluorescent properties of LFP, we used the fluorescence spectroscopy methods comprising the 3–dimensional spectral arrays with synchronous screening of the fluorescence spectra. Furthermore, the total LFP were resolved into several fractions by means of chloroform–metanol 3 : 1 extraction followed by HPLC with fluorescence detection.

We have shown that the brain LFP constitute a complex mixture of very many different chemical compounds (fluorophores) whose composition is changing in the course of brain development, **Figs. 31, 32 and 33).** Our results also indicated that the *highest*

accumulation of oxidative products in the forebrain, when tested by detection of LFP, occurred immediately after the birth, at PD2 and PD5 (**Fig. 32**). This result may be interpreted as indication of the high oxidative damage proceeding in rat brain shortly after the birth.

Fig. 31. Examples of 3D–fluorescence excitation spectra determined in brain chloroform extracts. (A) 7 days before birth, (D) 2 days after the birth, (J) 90 days after the birth

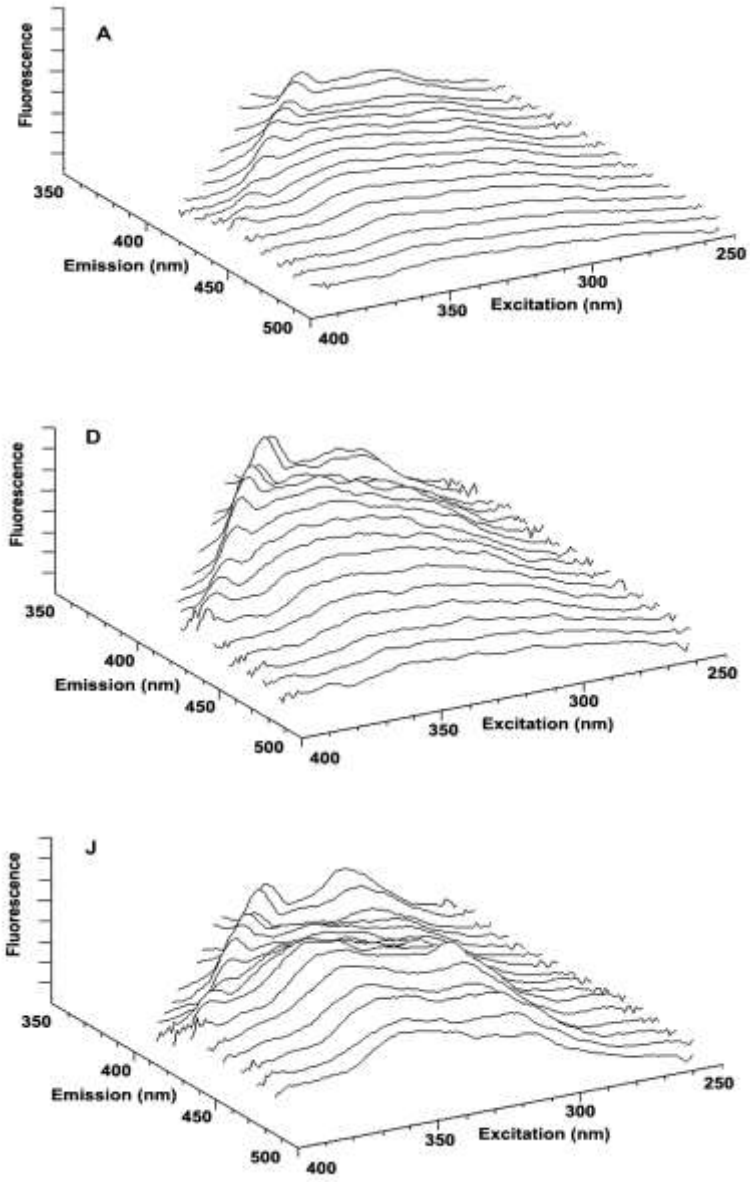

Legend to Fig. 31.

A total of 70 pregnant female Wistar rats were used throughout the experiments. They had free access to water and standard laboratory diet. The offspring's of both sexes were divided into 10 groups. Group **A** (110 fetuses) was sampled 7 days before birth, group **B** (110 fetuses) 1 day before birth, group **C** (50 animals) on postnatal day 1, group **D** (50 animals) on postnatal day 2, group **E** (50 animals) on postnatal day 5, group **F** (50 animals) on postnatal day 10, group **G** (50 animals) on postnatal day 15, group H (30 animals) on postnatal day 25, group **I** (30 animals) on postnatal day 35, and group **J** (20 animals) 3 months after birth.

Fig. 32. Quantitative determination of three major LFP fluorophores found in 3D spectra.

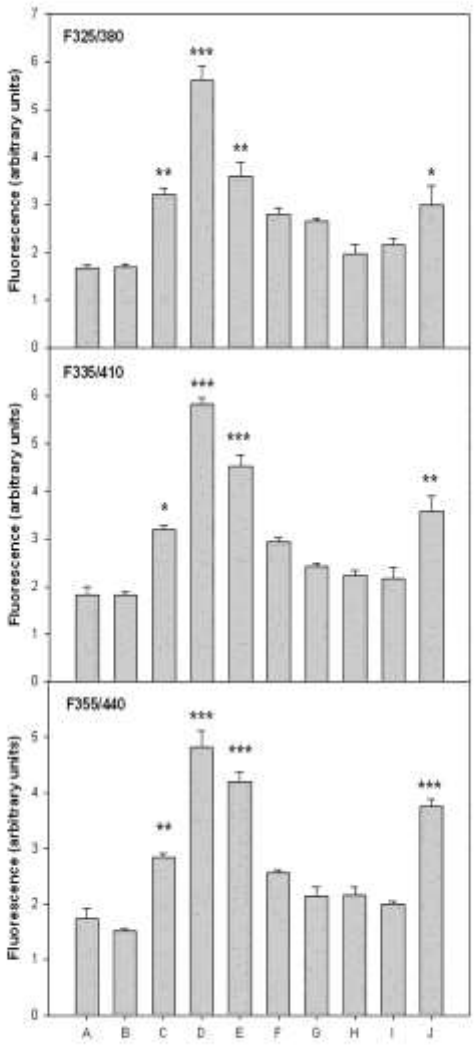

Legend to Fig. 32. Group **A**, 7 days before birth; group **B**, 1 day before birth; group **C**,

postnatal day 1; group **D**, postnatal day 2; group **E**, postnatal day 5; group **F**, postnatal day 10; group **G**, postnatal day 15; group **H**, postnatal day 25; group **I,** postnatal day 35; group **J**, 3 months old animals. Statistical significance was related to group A:

* P< 0.05, ** P<0.01, *** P< 0.001.

Fig. 33. Examples of synchronous fluorescence spectra (left–hand panels) and their 2nd derivatives (right–hand panels). (A) 7 days before the birth; (D) postnatal day 2; (E) postnatal day 5; (J) 3 month old animals.

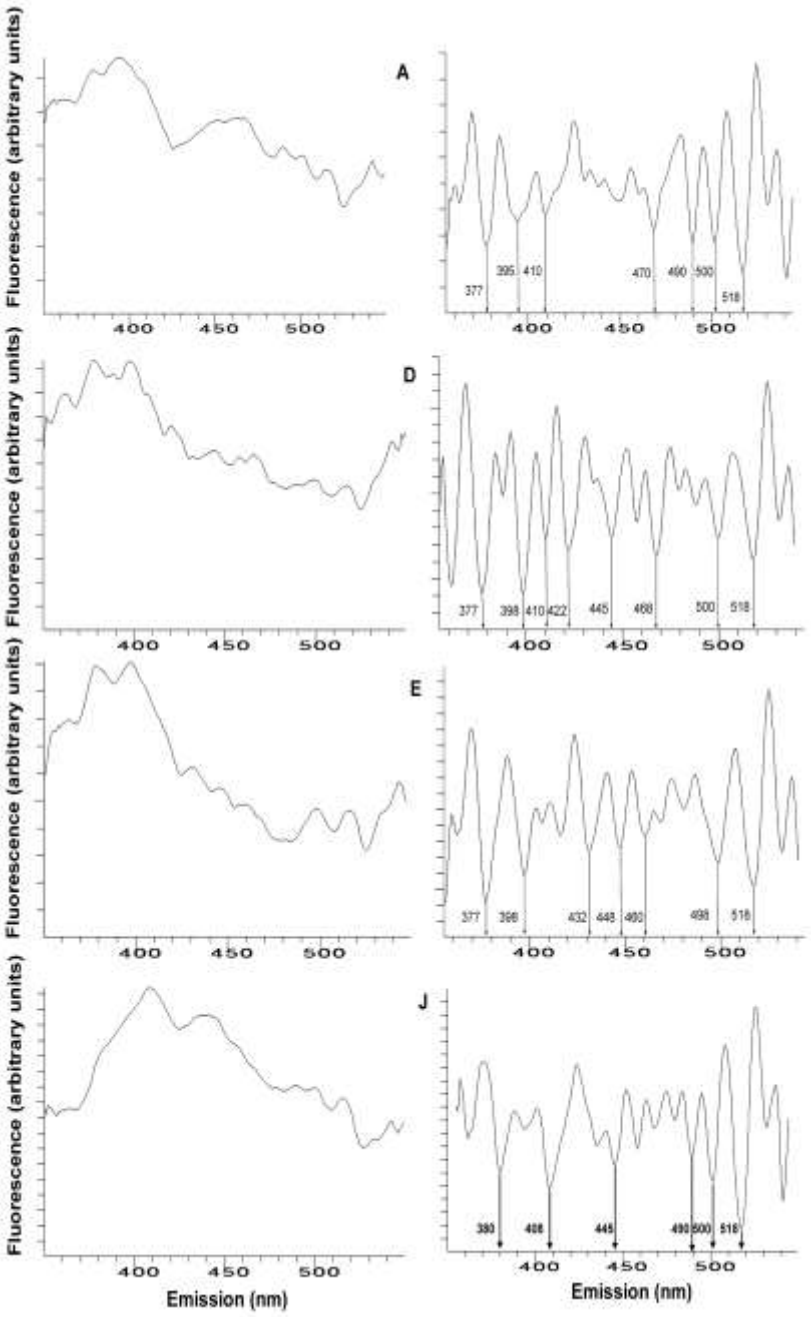

Legend to Fig. 33. Vertical arrows in the 2nd derivatives of the spectra indicate the emission

maxima of the resolved fluorophores.

Fig. 34. Examples of the HPLC tracings of fluorophore F355/410 in brain chloroform extracts prepared from of animals of different ages. A) 7 days before birth, D) postnatal day 2, E) postnatal day 5, J) 3 month old animals.

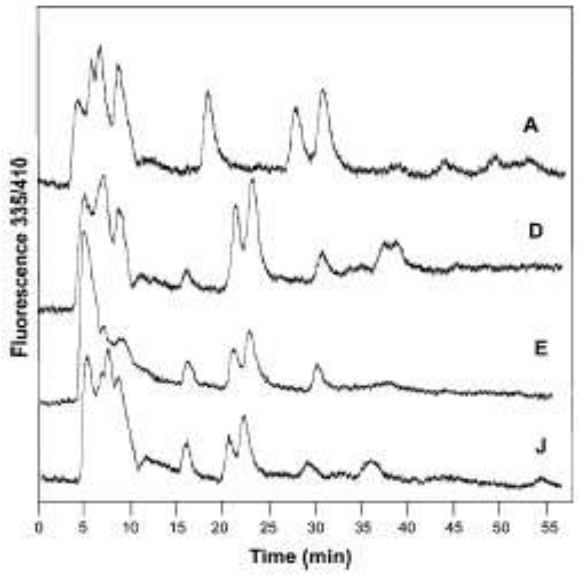

Legend to Fig. 34. Brain chloroform extracts were evaporated under the stream of nitrogen. The evaporated sample was dissolved in approximately 1 ml of running phase used in isocratic HPLC separation. A mixture of acetonitrile–methanol–water (50:10:40, v/v) was used for separation of LFP. A Jasco HPLC instrument equipped with fluorescence detector was set at the excitation and emission maxima of the three major fluorophores. A C18 column (4 x 250 mm) was used for the analysis. Isocratic elution gave optimum separation at 0.2 ml/ml.

6.2.2. Study of lipofuscin–like pigments in subcellular membrane fractions.

The aim of our second study of LFP in the brain (Wilhelm at al., 2014; manuscript in preparation) was to determine the ontogenetic development of LFP production in different subcellular membrane fractions (post–nuclear fraction, mitochondria, miscrosomes, crude plasma membranes, cytosol) and to compare the ontogenetic patterns observed in these membranes with data obtained by analysis of the whole tissue homogenates. The LFP level in fetuses was taken as a reference value corresponding to 100%. The LFP content in different membrane fractions collected at different time intervals of brain development were expressed

as percentage of this value. The results are presented in **Fig. 35**.

Fig. 35. LFP levels in brain homogenate and subcellular fractions during development. Foetal homogenate level was taken as 100%. Statistical significance: * P< 0.05, ** P< 0.01, *** P< 0.001

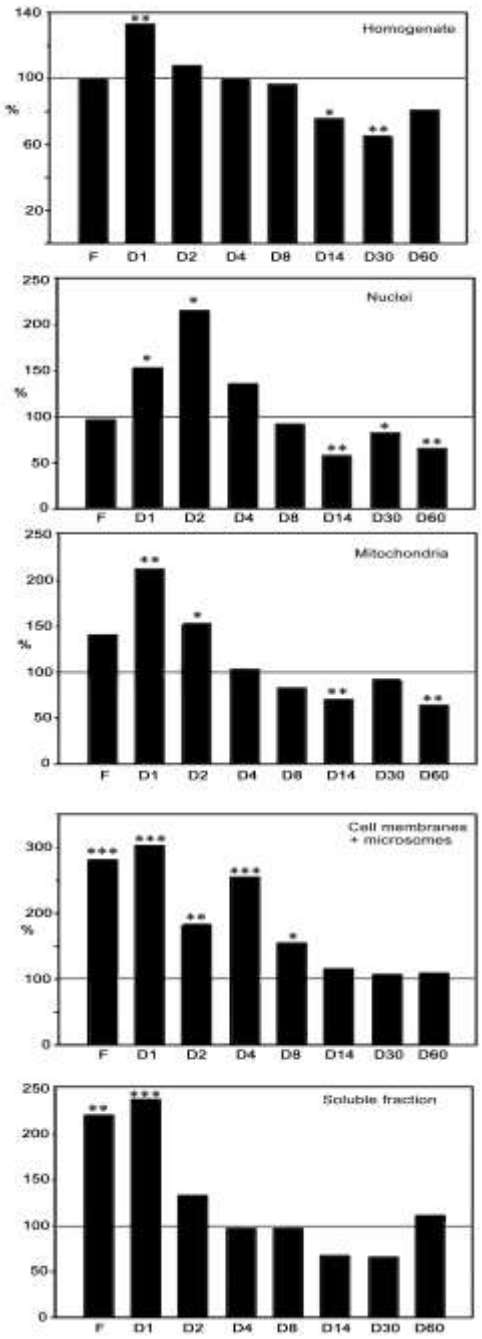

Judged from an overall point of view, the results were in full accordance with our

previous study of tissue homogenates (Wilhelm et. al. 2011). However, analysis of LFP in 5 subcellular fractions has also brought some unexpected observations. First, it was found that the high LFP levels were detected already in the foetal brain in ***soluble*** *fraction* (220%) and in ***crude*** *plasma membrane* fraction (CM) representing the mixture of vesicles derived from plasma membrane and microsomes (282%), whilst the LFP level in other fractions was not increased. The soluble fraction was still increased on PD1 (236%) and then returned to the control level and stayed unchanged throughout the whole time scale of experiment. *In the soluble fraction, we might expect lipoproteins containing the oxidized lipids with characteristics of LFP. Apparently, these lipoproteins are quickly decomposed after birth.*

In "crude plasma membranes" containing the small vesicular fragments derived from plasma membrane, endoplasmic reticulum and Golgi, the increased LFP level stayed until PD8. This was a unique observation when compared with other membrane types, as the LFP levels in other fractions were increased only up to PD2. Detection of this prolonged LFP increase in CM might indicate a change of this cell structure proceeding well beyond the birth.

LFPs in mitochondria were increased on PD1 (212%) and PD2 (152%). Afterwards, they returned to normal levels and were further decreased on PD14 (70%) and PD60 (64%). Thus, and as already noticed in our previous analysis of brain tissue homogenates (Wilhelm *et al.*, 2011), the increase of LFPs immediately after birth (PD1 and PD2) may be interpreted as an indication of an intensive aerobic metabolism accompanied by free radical production and consequent damage of membrane structures. The decrease of mitochondrial and nuclear LFP in samples collected from older rats (PD8–PD14) might be an indication of the high mitochondrial turnover proceeding in this period. The newly formed mitochondria, containing the low amount of LFP appear and dilute the concentration of these substances in the whole MITO fraction.

In nuclei, LFP was increased at PD1 (152%) and PD2 (215%). This increase was followed by decrease below the control value observed at PD14 (58%), PD30 (82%) and PD60 (65%). Nuclear membrane contains the electron transfer system analogical to that of endoplasmic reticulum which can be the source of free radicals and LFP. In similarity to mitochondria, the decrease of LFP level at PD8 and PD14 might be caused by an intensive cell proliferation, when the newly formed nuclei, containing less LFP, are merged into the overall pool detected in nuclear fraction.

7. DISCUSSION

7.1. The ontogenetic development of $GABA_B$–receptor signaling cascade

The highest maximum response (efficacy) of baclofen– and SKF97541–stimulated [^{35}S]GTPγS binding was measured at postnatal day 14 and 15 and afterward, the ability of these two $GABA_B$–R agonists to increase activity of G proteins decreased continuously towards the adult level (**Fig. 28**). Accordingly, the peak value of [^{3}H]GABA binding was detected at PD14 in rat brain cortical slices by quantitative autoradiography and this high level of [^{3}H]GABA binding subsequently declined to the adult level (Turgeon and Albin 1994).

The existence of the maximum of coupling efficacy between $GABA_B$–R and G proteins, which was observed in "opening of eyes period" at PD14 and PD15, may be interpreted as an overlap between the two opposite regulatory effects: the stimulation which is stronger at age intervals before this period and inhibition, which prevails in older rats.

Data presented in my work (**Figs 27 and 28**) indicated a noticeable extent of compatibility of our present results with experimental data obtained before by functional assays of adenylyl cyclase (AC) activity in the presence or absence of $GABA_B$–R agonists, (Ihnatovych *et al.* 2002 a,b). Maximum activation of baclofen– and SKF97541–stimulated [^{35}S]GTPγS binding at PD14 and PD15 coincided with the developmental profile of AC activity. The maximum of agonist–stimulated G protein activity (**Fig. 28**) as well as basal, fluoride–, GTP– and forskoline–stimulated AC was found in the same period of brain development, i.e. between PD10 and PD15. However, a marked difference between the two sets of data was noticed as well. Maturation of functional coupling of $GABA_B$–R with G proteins preceded maturation of AC system because AC activity was very low at birth while both baclofen and SKF97541 exhibited significant efficacy already at PD2 (**Fig. 27**).

The highest plasma membrane density of $GABA_B$–R determined by saturation binding study with specific antagonist [^{3}H]CGP54626A was observed shortly after the birth (at PD1) and subsequently decreased in 13– and 90–day–old rats (**Fig. 29**). It may be therefore suggested that the physiological significance of the high receptor number and significant efficacy of coupling of $GABA_B$–R with G proteins shortly after the birth (at PD1 and PD2) is related to some other effectors but AC–cAMP system. Ionic channels regulated by the free $G_o\alpha$ and Gβ subunits represent the primary candidates for such effectors (Newberry *et al.* 1984a,b, Gähwiler *et al.* 1985, Bormann 1988, Bowery *et al.* 1989).

Comparison of EC_{50} values of baclofen–stimulated [^{35}S]GTPγS binding indicated no

significant difference in PM samples isolated from 2–, 14– and 90–day–old rats. Contrarily, the EC_{50} values of G protein stimulation by SKF97541 were clearly increased from the birth to adulthood (**Table 2**). This result suggests a developmental decrease in affinity of $GABA_B$–R response for the latter agonist and it is compatible with electrophysiological studies of brain function indicating the differences in sensitivity of $GABA_B$–R to different agonists (Bernasconi *et al.* 1992, Hosford *et al.* 1992, Lin *et al.* 1992, Marescaux *et al.* 1992). Furthermore, epileptological studies of brain function indicated that anticonvulsant action of baclofen was unchanged during postnatal period (Kubová *et al.* 1996); simultaneously, the ontogenetic profile of anticonvulsant action of SKF97541 was not identical with that of baclofen (Mareš 2008). Thus, the time–span between PD12 and PD18 represented the most critical period from this point of view.

7.2. The ontogenetic development of Na^+/K^+–ATPase

The ontogenetic development of Na^+/K^+–ATPase[1] was completely different from that obtained in studies of $GABA_B$–R–signaling cascade (**Fig. 30**). Membrane density of Na^+/K^+–ATPase molecules, determined by immunodetection of the α–subunit of this enzyme, was increased 3.5–fold in PM isolated from adult, 90–days–old animals when compared with PM isolated from foetuses 1–day before the birth. The similar increase (2.6–fold) was detected in [^{3}H]ouabain binding studies. Thus, the overall maturation of the brain cortex, which was in our studies monitored by a developmental study of prototypical plasma membrane marker Na^+/K^+–ATPase, proceeds between the birth and the adulthood. *The increase of Na^+/K^+–ATPase molecules in PM proceeds in striking contrast to ontogenetic change of number of $GABA_B$–R which is in this period decreased 2.4–fold.*

1, Sodium plus potassium activated, magnesium dependent adenosinetriphosphatase (EC 3.6.1.3) represents a crucial enzyme for preservation of the continuous neuronal activity as it is catalyzing the active, ATP–dependent transport of sodium and potassium cations across plasma membrane. The 3 sodium cations are transported from the cell interior to the extracellular space in exchange of 2 potassium cations which pumped into the cell. The single cycle of Na^+/K^+–ATPase catalytical activity results in transfer of one positive charge out from the cell.

7.3. Postnatal ontogenesis of oxidative damage of the brain

LFP were used as a tool to assess the extent of ROS formation in brain cortex of rats during early postnatal development. The highest accumulation of these compounds was found immediately after birth and the level of these compounds was subsequently falling down to the three months of age, which is believed to represent a period when ageing starts in rats.. Although the increased free radical production shortly after the birth is to be expected because

of the rapid increase in oxygen concentration in the brain of new born animals and absence of fully functional mitochondria at this age interval, the detection of the final products of peroxidative damage (LFP) has not been analyzed before in the detailed manner, i.e. on the day by day basis.

When considering the up–to–date literature data from the broader scope of view, ROS–mediated oxidative damage of DNA was demonstrated in rat brain, liver, kidney and skin during the first few hours after the birth (Randerath *et al.* 1997). Lungs were not affected. The brain lesions were considered as substantial and were similar to or even greater than the lesions in senescent, 24–month old rats. The concept of oxidative stress generated after the normal birth was also supported by the finding of a pronounced neonatal decreases in the hepatic GSH/GSSG ratio in rats (Sastre *et al.* 1994, Pellardo *et al.* 1991). Also the product of membrane lipid peroxidation, malonaldehyde, exhibited a transient rise after the birth in rat liver and kidney (Gunther *et al.* 1993). The tissue specificity of manifestation of oxidative damage may be easily explained by differences in balance between the intensity of oxidative metabolism and antioxidant protection existing in a given tissue. *Up to now, no such studies were undertaken in the brain.*

Our results indicated a transient accumulation of LFP in neonatal rat brain: LFP, were increased on the day 1 after the birth (PD1), reached the maximum level on the day 2 (PD2) and decreased to the prenatal level already on postnatal day 5 (PD5) (**Fig. 35;** Wilhelm *et al.*, 2011). A new rise of LFP production was found in 3–month–old animals (PD90). As already mentioned, results presented in our work correlated with the demonstration of oxidative damage of DNA (Randerath *et al.* 1997). The fact that all fluorophores had similar ontogenetic pattern supported the physiological relevance of our results as this finding may be interpreted to mean that LFPs are generated by the same process or are localized in the same subcellular membrane compartment.

Wihelm and Ostadalova (2012) investigated the ontogenetic profile of generation of LFPs in neonatal rat heart and found that the observed changes were similar to those obtained in frontal brain cortex. Mitochondria are the first suspected source for ROS production when considering the brain. This interpretation is supported by the previously published data (Svoboda and Lodin 1972, 1973) indicating the low activity of α–glycerolphosphate and succinate dehydrogenases in immature brain: the activity of both enzymes was very low before and shortly after the birth. The temporary activation of α–GPDH (maximum at PD4–8) faded away before PD10. The major increase of these mitochondrial enzyme activities proceeded between PD10 and PD20 and was not completed before PD30. Thus, the presence

of immature respiratory chain of mitochondria in brain cortex of newborn animals may explain the increase of LFP immediately after the birth.

Besides mitochondria, the high LFP production in brain of new–born animals may be also interpreted as an indication for the presence of the high amount of microglia phagocytosing the apoptosed brain cells. In mice, the maximum phagocytosis associated with significant ROS production, occurred on postnatal day 3 (Marı´n–Teva *et al.* 2004). This time period corresponds well with the maximum of LFP production measured in our experiments: between PD1 and PD5. Thus, at least some part of the early production of LFP in the brain may be cell specific and functionally related to activity of microglia. Transition from hypoxia to normoxia and increase of oxygen partial pressure was also shown to increase production of free radicals (Wilhelm *et al.* 1999). It is therefore possible that the hypoxic/ normoxic transition proceeding in the newly born rats contributes to the process of LFP formation.

The pattern of 3D–spectral arrays, synchronous spectra and their derivatives (all together) indicate the presence of many fluorescent species belonging to the category of LFP. Each of these spectrally characterized species can be further resolved into several chromatographically distinct compounds (**Fig. 31, 32, 33**; Wilhelm *et al.*, 2011). Taken together, LFP may originate from hundreds, may be thousands, of unknown compounds which are functionally related to or produced by the brain oxidative damage after the birth. We assume that a formation of LFPs in 3–month–old animals, when aging starts in rats, is based primarily on ROS generated by mitochondria (Kann and Kovacs, 2007). Since that time, these products only accumulate (Brunk and Terman, 2002).

8. CONCLUSIONS

1) The significant intrinsic efficacy of $GABA_B$–receptors was detected in rat brain cortex already shortly after the birth: at postnatal day 1 and 2. Subsequently, both baclofen and SKF97541–stimulated G protein activity, measured as the high–affinity [^{35}S]GTPγS binding, was increased. The highest level of agonist–stimulated [^{35}S]GTPγS binding was detected at postnatal days 14 and 15. In older rats, the efficacy, i.e. the maximum response of baclofen– and SKF97541–stimulated [^{35}S]GTPγS binding was continuously decreased so, that the level in adult, 90–days old rats was not different from that in newborn animals. This profile of ontogenetic development of functional coupling between $GABA_B$–R and the cognate G proteins was similar to the maturation of adenylyl cyclase activity (Ihnatovych *et al.* 2002).

The existence of maximum of coupling efficacy between $GABA_B$–R and G proteins, observed in "opening of eyes period" at PD14 and PD15, may be interpreted as an overlap between the two opposing / counter–acting regulatory effects: stimulatory which is stronger at age intervals before this period and inhibitory effect, which prevails in older rats.

2) The potency of G protein response to baclofen stimulation, characterized by EC_{50} values, was also high at birth but unchanged by further development. The individual variance among different agonists was observed in this respect as the potency of SKF97541 response was decreased when compared in 2– and 90–days old rats.

3) Plasma membrane density of $GABA_B$–R, determined by saturation binding assay as maximum binding capacity (B_{max}) of specific antagonist [^{3}H]CGP54626A, was highest in 1–day old animals. The further maturation of rat brain cortex was reflected in decrease of PM density of $GABA_B$–R observed in 13– and 90–days old animals.

4) The ontogenetic development of Na^+/K^+–ATPase was completely different from that obtained in studies of $GABA_B$–R–signaling cascade. In contrast to the number of $GABA_B$–R, plasma membrane density of Na^+/K^+–ATPase molecules was increased ≈ 3–fold when compared in new born (1–day–old) and 90–days–old rats.

5) The high level of lipofuscin like pigments (LFP) was generated in rat brain cortex during the first 5 days of postnatal life. Maximum level of LFP was detected on the postnatal day 2. Starting from the postnatal day 10, LFP concentration returned down to the prenatal level. A new rise in LFP concentration was observed in 90–days old animals. This second increase of LFP may indicate the beginning of the aging process in rat brain cortex.

9. REFERENCES

AHNERT–HILGER, G., SCHAFER, T., SPICHER, K., GRUND, CH., SCHULZ, G. and WIEDENMANN, B. (1993) Detection of G protein heterotrimers on large dense core and small synaptic vesicles of neuroendocrine and neuronal cells. *Eur. J. Cell Biol. 65*, 26–38

ALLEN, J.A., HALVERSON–TAMBOLI, J.A. and RASENICK, M.M. (2007) Lipid raft microdomains and neutrotransmitter signalling. *Neuroscience 8*, 128–140ASANO, T. and OGASAWARA, N. (1986) Uncoupling of gamma–aminobutyric acid B receptors from GTP–binding proteins by N–ethylmaleimide: effect of N–ethylmaleimide on purified GTP–binding proteins. *Mol. Pharmacol. 29*, 244–249

ASANO, T., UI, M. and OGASAWARA, N. (1985) Prevention of the agonist binding to gamma–aminobutyric acid B receptors by guanine nucleotides and islet–activating protein, pertussis toxin, in bovine cerebral cortex. Possible coupling of the toxin–sensitive GTP–binding proteins to receptors. *J. Biol. Chem. 260*, 12653–12658

BABIYCHUK, E.R. and DRAEGER, A. (2006) Biochemical characterisation of detergent–resistant membranes: a systematic approach. *Biochem. J.*, 407–416

BARRAL, J., TORO, S., GALARRAGA, E. *et al.* (2000). GABAergic presynaptic inhibition of rat neostriatal afferents is mediated by Q–type Ca(2^+) channels. *Neuroscience Letters 283*, 33–36

BERNASCONI, R., LAUBER, J., MARESCAUX, C., VERGNES, M., MARTIN, P., RUBIO, V., LEONHARDT, T., REYMANN, N. and BITTIGER, H. (1992) Experimental absence seizures: potential role of gamma–hydroxybutyric acid and $GABA_B$ receptors. *J. Neural. Transm. 35*, 155–177

BIRNBAUMER, L. (1990) Transduction of receptor signal into modulation of effector activity by G proteins. *FASEB J. 4*, 3178–3188

BIRNBAUMER, L., ABRAMOWITZ, J., and BROWN, A.M. (1990) Receptor–effector coupling by G proteins. *Biochim. Biophys. Acta 1031*, 163–224

BLOCH–TARDY, M., ROLLAND, B. and GONNARD, P. (1971) Ontogenetic evolution of the molecular forms of 4–aminobutyrate 2–oxoglutarate aminotransferase in rat brain and liver. *J. of Neurochem. 18*, 1779–1781

BOCKAERT J. and PIN, J.P. (1999) Molecular tinkering of G protein–coupled receptors: an evolutionary success. *The EMBO Journal 18*, 1723–1729

BORMANN, J. (1988) Electrophysiology of $GABA_A$ and $GABA_B$ receptor subtypes. *Trends Neurosci. 11*, 112–116

BORMANN, J. and FEIGENSPAN, A. (1995) $GABA_C$ receptors. *TiNS 18*, 515–519

BOUROVA, L., KOSTRNOVA, A., HEJNOVA, L., MORAVCOVA, Z., MOON, H.E., NOVOTNY, J., MILLIGAN, G. and SVOBODA, P. (2003). Delta–opioid receptors exhibit high efficiency when activating trimeric G proteins in membrane domains. *J. Neurochem. 85*, 34–49

BOUROVA, L., STOHR, J., LISY, V., RUDAJEV, V., NOVOTNY, J. and SVOBODA, P. (2009) Isolation of plasma membrane compartments from rat brain cortex; detection of agonist–stimulated G protein activity. *Med. Sci. Monit. 15*, 111–122

BOUROVA, L., VOSAHLIKOVA, M., KAGAN, D., DLOUHA, K., NOVOTNY, J. and SVOBODA, P. (2010) Long–term adaptation to high doses of morphine causes desensitization of mu–OR– and delta–OR–stimulated G protein response in forebrain cortex but does not decrease the amount of G protein alpha subunits. *Med. Sci. Monit. 16 (8)*, 260–270

BOWERY, N. G., HILL, D. R. and HUDSON, A. L. (1983) Characterization of $GABA_B$ receptor binding sites on rat whole brain synaptosomes. *Br. J. Pharmacol.* 78, 191–206

BOWERY, N. G., PRICE, G. W., HUDSON, A. L., HILL, D. R. and WILKIN, G. P., TURNBULL, M. J. (1984) GABA receptor multiplicity. *Neuropharmacology 23*, 219–231, 1984

BOWERY, N. G., HILL, D. R. and HUDSON, A. L. (1985) [^{3}H](–)Baclofen: an improved ligand for $GABA_B$ sites. *Neuropharmacology 24*, 207–210

BOWERY, N. G., HUDSON, A. L. and PRICE, G. W. (1987) $GABA_A$ and $GABA_B$ receptor site distribution in the rat central nervous system. *Neuroscience 20*, 365–383

BOWERY, N. G. (1989) $GABA_B$ receptors and their significance in mammalian pharmacology. *TiPS 10*, 401–407

BOWERY, N.G., MAGUIRE, J.J. and PRATT, G.D. (1991) Aspects of molecular pharmacology of GABA receptors. *Semin. Neurosci. 3*, 241–249

BOWERY, N. G. (1993) $GABA_B$ receptor pharmacology. *Ann. Rev. Pharmacol. Toxicol. 33*, 109–147

BROWN, D.A. and LONDON, E. (2000) Structure and function of sphingolipid– and cholesterol–rich membrane rafts. *J. Biol. Chem. 275*, 17221–17224

BRUNK, U.T. and TERMAN, A. (2002) Lipofuscin: mechanisms of age–related accumulation and influence on cell function. *Free Radic Biol Med 33*, 611–619

BUSSIERES, N. and EL MANIRA, A. (1999) $GABA_B$ receptor activation inhibits N–and P/Q–type calcium channels in cultured lamprey sensory neurons. *Brain Research 847*, 175–185

CAMPBELL, N. A. and REECE, J. B. (2005) *Biology*, Pearson–Benjamin Cummings, 7th edition

CHANCE, B., SIES., H., CHEN, G., and van den POL, A. N. (1998). Presynaptic GABAB autoreceptor modulation of P/Qtype calcium channels and GABA release in rat suprachiasmatic nucleus neurons. *Journal of Neuroscience 18,* 1913–1922

CHEN, S. D., YANG, D. I., LIN, T. K., SHAW, F. Z., LIOU, C. W. and CHUANG, Y. C. (2011) Roles of oxidative stress, apoptosis, PGC–1 and mitochondrial biogenesis in cerebral ischemia. *Int. J. of Mol. Sci. 12 (10),* 7199–7215

COUVE, A., THOMAS, P., CALVER, A. R. , HIRST, W. D., PANGALOS , M. N., WALSH, F. S., SMART , T. G. and MOSS, S. J. (2002) Cyclic AMP–dependent protein kinase phosphorylation facilitates GABA(B) receptor–effector coupling. *Nat. Neurosci. 5,* 415–424

DAVLETOV, B. A., MEUNIER, F. A., ASHTON, A. C., MATSUSHITA, H., HIRST, W. D. *et al.* (1998) Vesicle exocytosis stimulated by alpha–latrotoxin is mediated by latrophilin and requires both external and stored Ca^{2+}. *EMBO J. 17 (14),* 3909–3920

DE PIERRE, J.W. and KARNOVSKY, M.L. (1973) Plasma membranes from mammalian cells. A review of methods fro their characterisation and isolation. *J. Cell Biol. 56,* 275–303

DE ROBERTIS, E., DE IRALDI, A.P., DE LORES ARNAIZ, G.R. and SALGANICOFF, L. (1962a) Isolation and subcellular distribution of acetylcholine and acetylcholine esterase. *J. Neurochem. 9,* 23–35

DE ROBERTIS, E., DE LORES ARNAIZ, G.R. and DE IRALDI, A.P. (1962b) Isolation of synaptic vesicles from the rat brain. *Nature (Lond.) 194*, 794–795

DLOUHA, K., KAGAN, D., ROUBALOVA, L., UJCIKOVA, H. and SVOBODA, P. (2013) Plasma membrane density of GABA(B)–R1a, GABA(B)–R1b, GABA–R2 and trimeric G proteins in the course of postnatal development of rat brain cortex. *Physiol. Res. 62 (5),* 547–559

DOLE, M. (1965) Thenatural history of oxygen. *Journal of General Physiology 49 (1),* 5–27

DOLPHIN, A.C. (1990) G protein modulation of calcium currents in neurons. *Ann. Rev. Physiol. 52*, 243–255

DOLPHIN, A.C. (1991) Regulation of calcium channel activity by GTP binding proteins and secondary messengers. *Biochim. Biophys. Acta 1091,* 68–80

DUNKLEY, P. R., JARVIE, P. E., HEATH, J. W., KIDD, G. J. and ROSTAS, J. A.

(1986) A rapid method for isolation of synaptosomes on Percoll gradients. *Brain Res. 372*, 115–129

FERNANDEZ–ALACID, L., AGUADO, C., CIRUELA, F. *et al.* (2009). Subcellular compartment–specific molecular diversity of pre–and post–synaptic GABA–activated GIRK channels in Purkinje cells. *Journal of Neurochemistry 110*, 1363–1376.

FISHER, T.E., TUCHEK, J.M. and JOHNSON, D.D. (1986) A comparison of methods for removal of endogenous GABA from brain membranes prepared for binding assays. *Neurochem. Res. 11*, 1–8

GÄHWILER B. H. and BROWN, D.A. (1985) $GABA_B$–receptor–activated K^+ current in voltage–clamped CA3 pyramidal cells in hippocampal cultures. *Proc. Natl. Acad. Sci. U S A 82*, 1558–1562

GILMAN, A.G. (1987) G proteins: transducers of receptor–generated signals. *Ann. Rev. Biochem. 56*, 615–649

GOLDSTEIN, B.D. and MCDONAGH, E.M. (1976) Spectrofluorescent detec–tion of in vivo red cell lipid peroxidation in patients treated with diaminodiphenylsulfone. *J. Clin. Investig. 57*, 1302–1307

GRAHAM, J. (2002) Fractionation of Golgi, endoplasmic reticulum, and plasma membrane from cultured cells in a preformed continuous iodixanol gradient. *The Sci World 2*, 1435–1439

GRAHAM, J. (2002) Homogenization of mammalian cultured cells. *The Sci. World 2*, 1630–1633

GRAHAM, J. (2002) OptiPrep^{tm} density gradient solutions for mammalian organelles. *The Sci. World 2*, 1440–1443

GRAHAM, J. (2002) Peparation of preformed iodixanol gradients. *The Sci. World 2*, 1351–1355

GRAHAM, J. (2002) Preparation of crude subcellular fractions by differential centrifugation. *The Sci. World 2*, 1638–1642

GRAHAM, J. (2002) Purification of lipid rafts from cultured cells. *The Sci. World 2*, 1662–1666

GRAHAM, J. (2002) Rapid purification of nuclei from animal and plant tissues and cultured cells. *The Sci. World 2*, 1551–1554

GRAHAM, J. (2002) Separation of membrane vesicles and cytosol from cultured cells and bacteria in a preformed discontinuous gradient. *The Sci. World 2*, 1555–1559

GRAVE, G. D., KENNEDY, C. and SOKOLOFF, L. (1971) Impairment of growth and

development of the rat brain by xypoxia at atmospheric pressure. *J. of Neurochem. 19*, 187–194

GROSSFIELD, R.M and SHOOTER, E. M. (1971) A study of the changes in protein composition of mouse brain during ontogenetic development. *J. of Neurochem. 18*, 2265–2277

GUGLIELMOTTO, M., TAMAGNO, E. and DANNI, O. (2009) Oxidative stress and hypoxia contribute to Alzheimer's disease pathogenesis: two sides of the same coin. *The Scientific World Journal 9 (1)*, 781–791

GUNTHER, T., HOLLRIEGL, V. and VORMANN, J. (1993) Perinatal development of iron and antioxidant defense systems. *J. Trace Elem. Electrolytes Health Dis*. *7*, 47–52

GUROFF, G. and Brodsky, M. (1971) Enzymes of nucleic acid metabolism in the brains of young and andult rats. *J. of Neorochem. 18*, 2077–2084

HELMREICH, J. M. and HOFMANN, K.– P. (1996) Structure and function of proteins in G protein coupled signal transfer. *Biochim. Biophys. Acta 1286*, 285–322

HILL, D. R. (1985) $GABA_B$ receptor modulation of adenylate cyclase activity in brain slices. *Br. J. Pharmacol. 84*, 249–257

HILL, D. R. and BOWERY, N. G. (1981) ^3H–Baclofen and ^3H–GABA bind to bicuculine–insensitive $GABA_B$ sites in rat brain. *Nature 290*, 149–152

HILL, D. R., BOWERY, N. G. and HUDSON, A. L. (1984) Inhibition of $GABA_B$ receptor binding by guanyl nucleotides. *J. Neurochem. 42*, 652–657

HOLLINGSWORTH, E.B., MCNEAL, E.T., BURTON, J.L., WILLIAMS, R.J., DALY, J.W. and CREVELING, C.R. (1985) Biochemical characterization of a filtered synaptoneurosome preparation from guinea pig cerebral cortex: cyclic adenosine 3':5'–monophosphate–generating systems, receptors and enzymes. *J. Neurosci. 5*, 2240–2253

HOLTER H. and MOLTER K. M. (1958) A substance for aqueous density gradients. *Exp. Cell Res. 15*, 631–632

HOLTER, H. and MOLTER, K. M. (1958) A substance for aqueous density gradients. *Exp. Cell Res. 15*, 631–632

HOSFORD, D. A., CLARK, S., CAO, Z., WILSON, W. A. jr, LIN, F. H., MORRISETT, R. A. and HUIN, A. (1992) The role of $GABA_B$ receptor activation in absence seizures of lethargic (lh/lh) mice. *Science 257*, 398–401

IHNATOVYCH, I., NOVOTNY, J., HAUGVICOVA, R., BOUROVA, L., MARES, P. and SVOBODA, P. (2002a) Opposing changes of trimeric G proteins during ontogenetic development of rat brain. Developmental Brain Res., 133, 57-67

IHNATOVYCH, I., NOVOTNY, J., HAUGVICOVA, R., BOUROVA, L., MARES, P. and

SVOBODA, P. (2002b) Ontogenetic development of the G-protein mediated adenylylcyclase signaling in rat brain. Developmental Brain. Res., 69-75

JACOBSON K. and DIETRICH, C. (1999) Looking at lipid rafts? *Cell biology 9*, 87–91

JAHANGEER, S. and RODBELL, M. (1993) The disaggregation theory of signal transmission revisited: further evidence that G proteins are multimeric and disaggregate to monomers when activated. *Proc. Nat. Acad. Sci. U S A 90*, 8782–8786

JAHANGEER, S. and RODBELL, M. (1993) The disaggregation theory of signal transmission revisited: further evidence that G proteins are multimeric and disaggregate to monomers when activated. *Proc. Nat. Acad. Sci. U S A 90*, 8782–8786

KAGAN, D., DLOUHA, K., ROUBALOVA, L. and SVOBODA, P. (2012) Ontogenetic development of GABA(B)–receptor signaling cascade in plasma membranes isolated from rat brain cortex; the number of GABA(B)–receptors is high already shortly after the birth. *Physiol. Res. 61 (6)*, 629–635

KANN, O. and KOVA´CS, R. (2007) Mitochondria and neuronal activity. *Am. J. Physiol. Cell Physiol 292*, C641–C657

KATADA, T. and UI, M. (1982a) ADP ribosylation of the specific membrane protein of C6 cells by islet–activating protein associated with modification of adenylate cyclase activity. *J. Biol. Chem. 257*, 7210–7216

KATADA, T. and UI, M. (1982b) Direct modification of the membrane adenylate cyclase system by islet–activating protein due to ADP–ribosylation of a membrane protein. *Proc Natl Acad Sci U S A 79*, 3129–3133

KAZIRO, Y., YTOH, H., KOZASA, M., NAKAFUKU, M. and SATOH, T. (1991) Structure and function of signal–transducing GTP–binding proteins. *Ann. Rev. Biochem. 60*, 349–400

KAZIRO, Y., YTOH, H., KOZASA, M., NAKAFUKU, M. and SATOH, T. (1991) Structure and function of signal–transducing GTP–binding proteins. *Ann. Rev. Biochem. 60*, 349–400

KERR, D. I. B. and ONG J. (1995) $GABA_B$ receptors. *Pharmac. Ther. 67*, 187–246

KRASNOPEROV, V. G., BITTNER, M. A., BEAVIS, R., KUANG, Y., SALNIKOW, K. V. *et al.* (1997) α–Latrotoxin stimulates exocytosis by the interaction with a neuronal G protein–coupled receptor. *Neuron 18 (6)*, 925–937

KUBOVÁ, H., HAUGVICOVÁ, R. and MAREŠ, P. (1996) Moderate anticonvulsant action of baclofen does not change during development. *Biol. Neonate 69*, 405–412

LADERA, C., DEL CARMEN GODINO, M., JOSE CABANERO, M. *et al.* (2008). Pre–

synaptic GABA receptors inhibit glutamate release through GIRK channels in rat cerebral cortex. *Journal of Neurochemistry 107*, 1506–1517

LADURON, P.M. (1984) Axonal transport of receptors: coexistence with neurotransmitter and recycling. *Biochemical Pharmacology 33*, 897–903

LI L, WRIGHT S.J., KRYSTOFOVA S., PARK G. and BORKOVICH K.A. (2007) Heterotrimeric G protein signalling in filamentous fungi. *Annual Rev. Microbiol. 61*, 423–452

LIN, F. H., CAO, Z., and HOSFORD, D. A. (1993) Increased number of $GABA_B$ receptors in lethargic (lh/lh) mouse model of absence epilepsy. *Brain Res. 608*, 101–106

LISANTI, M.P., SCHERER, P.E., TANG, Z. and SARGIACOMO, M., (1994) Caveolae, caveolin and caveolin–rich membrane domains: a signalling hypothesis. *Trends. Cell. Biol. 4*, 231–235

LISANTI, M.P., SCHERER, P.E., VIDUGIRIENE, J., TANG, Z.L., VOSATKA, A.H., TU, Y.–H., COOK, R.F. and SARGIACOMO, M. (1994b) Characterisation of caveolin–rich membrane domains isolated from an endothelial rich source: implications for human disease. *J. Cell. Biol. 126*, 111–126

LISY, V., KOVARU, H., FALTIN, J. and LODIN, Z. (1971) Activity of succinate dehydrogenase and acetylcholine esterase in synaptic endings isolated from neuropil and cerebral cortex. *Phys. Res. 20*, 229–234

LOWRY, O.H., ROSEBROUGH, N.J., FARR, A.L. and RANDALL, R.J. (1951). Protein measurement with the Folin phenol reagent. J Biol Chem 193 (1), 265–275

LUABEYA, M. K., VANISBERG M.A., JEANJEAN A.P., BAUDHUIN, P., LADURON, P.M. and MALOTEAUX, J.M. (1997) Fractionation of human brain by differential and isopycnic equilibration techniques. *Brain Res. Protocols 1*, 83–90

LUSCHER, C., JAN, L. Y., STOFFEL, M. *et al.* (1997). G protein–coupled inwardly rectifying K^+ channels (GIRKs) mediate postsynaptic but not presynaptic transmitter actions in hippocampal neurons. *Neuron 19*, 687–695

MALOTEAUX, J.M., LUABEYA, M.K., VANISBERG, M.A., JEANJEAN, A.P., BAUNHUIN, P., SCHERMAN, D. and LADURON, P.M. (1995) Subcellular distribution of receptor sites in human brain: differentiation between heavy and light structures of high and low density. *Brain Res. 687*, 155–166

MAREŠ, P (2008) Anticonvulsant action of $GABA–_B$ receptor agonist SKF97541 differs from that of baclofen. *Physiol. Res. 57*, 789–792

MARESCAUX, C., VERGNES, M., BERNASCONI, R. (1992) $GABA_B$ receptor antagonists: potential new anti–absence drugs. *J. Neural. Transm. Suppl. 35*, 179–188

MARI´N–TEVA, J.L., DUSART, I., COLLIN, C. et al (2004) Microglia promote the death of developing Purkinje cells. *Neuron 41*, 535–547

MATEYKO G. M. and KOPAC, M. J. (1959) Isopycnic cushioning for density gradient centrifugation. *Exp. Cell Res. 17*, 524–526

MICHEL, T. M., PÜLSCHEN, D. and THOME, J. (2012) The role of oxidative stress in depressive disorders. *Current Pharmaceutical Design 18 (36),* 5890–5899

MORAVCOVÁ, Z., RUDAJEV, V., NOVOTNÝ, J., ČERNÝ, J., MATOUŠEK, P., PARENTI, M., MILLIGAN, G. and SVOBODA, P. (2004) Long–term agonist stimulation of IP prostanoid receptor depletes the cognate $G_s\alpha$ protein from membrane domains but does not affect the receptor level. *Biochem. Biophys. Acta*, 1691, 51–65

NEUBIG, R. R. (1994) Membrane organisation in G protein mechanism. *FASEB J. 8*, 939–946

NEW, D. C., AN, H., IP, N. Y. and WONG, Y. H. (2006) GABAB heterodimeric receptors promote $Ca2^{+}$ influx via store–operated channels in rat cortical neurons and transfected Chinese hamster ovary cells. *Neuroscience 137*, 1347–1358

NEWBERRY, N. R. and NICOLL, R. A. (1984a) Direct hyperpolarizing action of baclofen on hippocampal pyramidal cells. *Nature 308*, 450–452

NEWBERRY, N. R. and NICOLL, R. A. (1984b) A bicuculline–resistant inhibitory post–synaptic potential in rat hippocampal pyramidal cells in vitro. *J. Physiol., 348*, 239–254

OLIANAS, M.C. and ONALI, P. (1999) GABA(B) receptor–mediated stimulation of adenylyl cyclase activity in membranes of rat olfactory bulb. Br J Pharmacol. 126, 657–664

OLSEN, R.W. and VENTER, C.J. (eds): Benzodiazepine/GABA Receptors and Chloride Channels: Structural and Functional Properties. Alan R. Liss, New York (1986)

PADGETT, C.L. and SLESINGER P. A. (2010) $GABA_B$ receptor coupling to G proteins and Ion channels. *Advances in Pharmacology 58*, 123–147

PELLARDO, F.V., SASTRE, J., ASENSI, M. et al (1991) Physiological changes in glutathione metabolism in fetal and newborn liver. *Biochem J. 274*, 891–893

PÉREZ–GARCI, E., GASSMANN, M., BETTLER, B. *et al.* (2006). The GABAB1b isoform mediates long–lasting inhibition of dendritic Ca^{2+} spikes in layer 5 somatosensory pyramidal neurons. *Neuron 50*, 603–616

PERTOFT, H. (1966) Gradient centrifugation in colloidal silica–polysaccharide media. *BBA 126*, 594–596

PERTOFT, H. (2000) Fractionation of cells and subcellular particles with Percoll. *J. Biochem. Biophys. Methods 44*, 1–30

PIKE, L. J. (2004) Lipid rafts: heterogeneity on the high seas. *Biochem. J. 378*, 281–292

PIKE, L. J. (2006) Rafts defined: a report on the Keystone symposium on lipid rafts and cell function. *J. Lipid Res. 47*, 1597–1598

PINARD, A., SEDDIK, R. and BETTLER, B. (2010) $GABA_B$ receptors: Physiological functions and mechanism of diversity. *Advances in Pharmacology 58*, 231–255

RANDERATH, E., ZHOU, G. D. and RANDERATH, K. (1997) Organ–specific oxidative DNA damage associated with normal birth in rats. *Carcinogenesis 18*, 859–866

RAYCHAUDHURI , C. and DESAI, I. D. (1972) Regulation of lysosomal enzymes. IV. Changes in enzyme activities of liver, kidney, and brain during development. *Int. J. of Biochem. 3 (15)*, 309–314

REN, X. and MODY, I. (2003) Gamma–hydroxybutyrate reduces mitogen–activated protein kinase phosphorylation via $GABA_B$ receptor activation in mouse frontal cortex and hippocampus. *J. Biol. Chem. 278*, 42006–42011

RICH, P.R. (2003) The molecular machinery of Keilin's respiratory chain. Biochem. *Soc. Transactions 31 (6)*, 1095–1105

RICKWOOD, D. (1984) Centrifugation, a practical approach. Oxford, IRL Press

RIOBO, N. A. and MANNING, D. R. (2005) Receptors coupled to heterotrimeric G proteins of G_{12}/G_{13} family. *Trends Phrmacol. Sci. 26 (3)*, 146–154

RODBELL, M. (1980) The role of hormone receptors and GTP–regulatory proteins in membrane transduction. *Nature 284*, 17–22

RUDAJEV, V., NOVOTNY, J., HEJNOVA, L., MILLIGAN, G. and SVOBODA, P. (2005) Thyrotropin–releasing hormone receptor is excluded from lipid domains. Detergent–resistant and detergent–sensitive pools of TRH receptor and $G_q\alpha/G_{11}\alpha$ protein. J. *Biochemistry (Jap) 138*, 111–125

SAKABA, T., and NEHER, E. (2003). Direct modulation of synaptic vesicle priming by GABA(B) receptor activation at a glutamatergic synapse. *Nature 424*, 775–778

SARGIACOMO, M., SUDOL, M., TANG, Z. and LISANTI, M.P. (1993) Signal transducing molecules and glycosyl–phosphatidylinositol–linked proteins form a caveolin–rich insoluble complex in MDCK cells. *J. Cell. Biol. 122*, 789–807

SASTRE, J., ASENSI, M., RODRIGO, F. et al (1994) Antioxidant admin–istration to the mother prevents oxidative stress associated with birth in the neonatal rat. *Life Sci 54*, 2055–2059

SCHWARK, W. S., SINGHAL, R. L. and LING, G. M. (1971) Glyceraldehyde–3–

phosphate dehydrogenase activity in developing brain during experimental cretinism. *BBA 273*, 308–317

SHAW, A.S. (2006) Lipid rafts: now you see them, now you don't. *Nature Immunology 7 (11)*, 1139–1142

SIMONDS, W.F. (1999) G protein regulation of adenylate cyclase. *Trends Pharmacol. Sci. 20*, 66–73

SIMONS, K. and Toomre, K. (2000) Lipid rafts and signal transduction. *Nature Reviews 1*, 31–39

SMART, E. J., GRAF, G. A., MCNIVEN, M. A., SESSA, W. C., ENGELMAN, J. A., SCHERER, P. E., OKAMATO, T. and LISANTI, M. P. (1999) Caveolins, liquid–ordered domains and signal transduction. *Mol. Cell. Biol. 19*, 7289–7304

SMART, E. J., GRAF, G. A., MCNIVEN, M. A., SESSA, W. C., ENGELMAN, J. A., SCHERER, P. E., OKAMATO, T. and LISANTI, M. P. (1999) Caveolins, liquid–ordered domains and signal transduction. *Mol. Cell. Biol. 19*, 7289–7304

SMART, E.J., YING, Y.–S., MINEO, CH. and ANDERSON, R.G.W. (1995) A detergent–free method for purifiying caveolae membrane from culture cells. *Proc. Nat. Acad. Sci. U S A 92*, 10104–10108

SONG, K.S., . SCHERER, P.E, TANG, Z., OKAMOTO, T., LI, S. , CHAFEL, M. , CHU, C. , KOHTZ, D.S. and LISANTI, M.P. (1996b) Expression of caveolin–3 in skeletal, cardiac, and smooth muscle cells. Caveolin–3 is a component of the sarcolemma and co–fractionates with dystrophin and dystrophin–associated glycoproteins, *J. Biol. Chem. 271*, 15160–15165

SONG, K.S., LI, S., OKAMOTO, T., QUILLIAM, L. A., SARGIACOMO, M. and LISANTI, M. P. (1996a) Co–purification and direct interaction of Ras with caveolin, an integral membrane protein of caveolae microdomains. Detergent–free purification of caveolae microdomains. *J. Biol. Chem. 271*, 9690–9697

STEIGER, J. L., BANDYOPADHYAY, S., FARB, D. H. and RUSSEK, S. J. (2004) cAMP response element–binding protein, activating transcription factor–4, and upstream stimulatory factor differentially control hippocampal GABABR1a and GABABR1b subunit gene expression through alternative promoters. *J. Neurosci. 24*, 6115–6126

SUNAHARA, R. and TAUSSIG, R. (2002) Isoforms of mammalian adenylyl cyclase: multiplicities of signaling. *Mol. Interv. 2*, 168–184.

SVOBODA, P. and LODIN, Z. (1972) Postnatal development of some mitochondrial enzyme activities of cortical neurons and glial cells. *Physiol. Bohemoslov. 21*, 457–465

SVOBODA, P. and LODIN, Z. (1973) Ontogenic development of oxidative capacity of the brain. *Physiol. Bohemoslov. 23*, 434

SVOBODA, P., TEISINGER, J., NOVOTNÝ, J., BOUŘOVÁ, L., DRMOTA, T., HEJNOVÁ, L., MORAVCOVÁ, Z., LISÝ, V., RUDAJEV, V., STOHR, J., VOKURKOVÁ, A., ŠVANDOVÁ, I. and DURCHÁNKOVÁ, D. (2004) Biochemistry of transmembrane signalling mediated by trimeric G proteins. *Physiol. Res. 53 (Suppl. 1),* S141–S152

SWEENEY, M.I. and Dolphin, A.C. (1992) 1, 4–Dihydropyrines modulate GTPhydrolysis by Go in neuronal membranes. *FEBS Lett. 310*, 66–70

UJCIKOVA, H., DLOUHA, K., ROUBALOVA, L., VOSAHLIKOVA, M., KAGAN, D. and SVOBODA, P. (2011) Up–regulation of adenylylcyclases I and II induced by long–term adaptation of rats to morphine fades away 20 days after morphine withdrawal. *BBA 1810 (12),* 1220–1229

UJCIKOVA, H., BREJCHOVA, J., VOSAHLIKOVA, M., KAGAN, D. et al (2014) Opioid–receptor (OR) signaling cascades in rat cerebral cortex and model cell lines: the role of plasma membrane structure. *Phys. Res. 63 (Suppl. 1),* 165–176

VALKO, M., LEIBFRITZ, D., MONCOL, J., CRONIN, M. T. D., MAZUR, M. and TELSER, J. (2007) Free radicals and antioxidants in normal physiological functions and human disease. *Int. J. of Biochem. And Cell Bio. 39 (1)*, 44–84

VICINI, S. (1991) Pharmacologic significance of the structural heterogeneity of the GAB_A receptor – chloride ion channel complex. *Neuropsychopharmacology 4,* 9–15

VOGEL, S.S., CHIN, G.J., SCHWARTZ, J.H. and REESE, T.S. (1991) Pertussis toxin–sensitive G proteins are transported toward synaptic terminals by fast axonal transport. *Proc. Nat. Acad. Sci. U S A 88*, 1775–1778

WAGNER, P. G., and DEKIN, M. S. (1993). GABAb receptors are coupled to a barium–insensitive outward rectifying potassium conductance in premotor respiratory neurons. *Journal of Neurophysiology 69,* 286–289

WHITTACKER, V.P. (1984) The structure and function of cholinergic synaptic vesicles *Biochemical Society Transactions (Lond.) 12*, 561–575

WHITTACKER, V.P., MICHAELSON, I.A. and KIRKLAND, R.J.A. (1964) The separation of synaptic vesicles from nerve ending particles (synaptosomes). *Biochem. J. 90,* 293–303

WILHELM, J. and HERGET, J. (1999) Hypoxia induces free radical damage to rat erythrocytes and spleen: analysis of the fluorescent end–products of lipid peroxidation. *Int. J. Biochem. Cell Biol. 31,* 671–681

WILHELM, J., IVICA, J., KAGAN, D. and SVOBODA, P. (2011) Early postnatal development of rat brain is accompanied by generation of lipofuscin–like pigments. *Mol. Cell. Biochem. 347*, 157–162

WILHELM, J. and OSTADALOVA, I. (2012) Ontogenetic changes of lipofuscin–like pigments in the rat heart. *Phys. Res. 61*, 173–179

XU, J. and WOJCIK, W.J. (1986) Gamma aminobutyric acid B receptor–mediated inhibition of adenylate cyclase in cultured cerebellar granule cells: blockade by islet activating protein. *J. Pharmacol. Exp. Therapeutics 239*, 568–573